THE SQUARE KILOMETRE ARRAY
DESIGN REFERENCE MISSION: SKA PHASE 1

Document number SCI-020.010.020-DRM-002
Revision 2.0
Author ..... SKA Science Working Group
Date 2011-09-23
Status ..... Draft

Name	Designation	Affiliation	Date	Signature
Submitted by:				
J Lazio (On behalf of Science Working Group)	SKA Project Scientist	SPDO	2011-09-23	
Approved by:				

DOCUMENT HISTORY

Revision	Date Of Issue	Engineering Change Number	Comments
2.0	2011-09-23	-	This revision of the SKA1 DRM is the next release of the document following the release utilised as baseline during the system dCoDR (which was v1.3)

DOCUMENT SOFTWARE

	Package	Version	Filename
Wordprocessor	MsWord	Word 2007	SCI-020.010.020-DRM-002-2.0_SKA1DesRefMission

ORGANISATION DETAILS

Name	SKA Program Development Office
Physical/Postal Address	Jodrell Bank Centre for Astrophysics Alan Turing Building The University of Manchester Oxford Road Manchester, UK M13 9PL
Fax.	+44 (0)161 275 4049
Website	www.skatelescope.org

Table of Contents

1. Introduction

The Square Kilometre Array (SKA) will be one of a suite of new, large telescopes for the 21st century probing fundamental physics, the origin and evolution of the Universe, the structure of the Milky Way Galaxy, the formation and distribution of planets, and astrobiology.

Like many existing radio telescopes, the SKA will be a sparse aperture instrument, with its collecting area distributed over a large geographical area (at least 3000 km). One of the key aspects of an interferometer is that it can begin conducting scientifically useful observations well before it reaches its full capabilities. Using the Very Large Array as an example, early observations began when the array had only 1/3 of its full complement of antennas (e.g., Goldstein & Wade 1977; Fomalont & Bridle 1978). Similarly, the construction of the SKA is envisioned to occur in "phases." The first phase, SKA Phase 1, represents crudely when the SKA has reached approximately 10% of its full capability (Garrett et al. 2010). However, the full scientific capability of the SKA will be achieved only with Phase 3. The current focus of the SKA Program is on Phase 2, as Phase 3 is to be informed by results from the EVLA and ALMA.

Though only the first phase of the SKA Program, SKA Phase 1 will be in its own right a powerful scientific instrument. The Design Reference Mission for the SKA Phase 1 describes a key set of observations and scientific requirements required to obtain the science goals for Phase 1. Further, as the SKA moves into a more intensive design phase, the impact of technical choices needs to be able to be traced back to the science requirements derived from the science case.

1.1. The SKA Phase 1 Science Case and Science Goals

The SKA Science Case is highlighted by Key Science Projects (KSPs), which represent unanswered questions in fundamental physics, astrophysics, and astrobiology. Each of these projects has been selected using the criterion that it represents science that is either unique to the SKA or is a topic which is complementary to multiwavelength data but in which the SKA plays a key role (Carilli & Rawlings 2004; Gaensler 2004).

Two aspects of the larger SKA Science Case have been selected as the focus for SKA Phase 1 (Garrett et al. 2010).

- Understanding the history and role of neutral hydrogen in the Universe from the Dark Ages to the present-day. This portion of the Phase 1 science case incorporates aspects of the full SKA Science Case "Probing the Dark Ages and the Epoch of Reionization" and "Galaxy Evolution, Cosmology, and Dark Energy."
- Detecting and timing binary pulsars and spin-stable millisecond pulsars in order to test theories of gravity (including General Relativity and quantum gravity), to discover gravitational waves from cosmological sources, and to determine the equation of state of nuclear matter. This portion of the Phase 1 science case incorporates aspects of the full SKA Science Case "Strong Field Tests of Gravity Using Pulsars and Black Holes."

1.2. The Design Reference Mission and Science Traceability

The Science Case sets out goals for the telescope. However, in all cases, fully realizing the science goals will require multiple, different kinds of observations. The Design Reference Mission is intended to establish a set of observations that define an "envelope" of requirements for the telescope. Specifically, if SKA Phase 1 meets the set of requirements described herein, it should be possible for the SKA Phase 1 to conduct a much broader set of science observations, potentially including even observations not yet recognized (Chapter 9).

Further, if additional technical design choices must be made during the next phase of the SKA design (Schilizzi et al., 2007), the Design Reference Mission establishes "traceability" from the science goals to science requirements to technical requirements (Table 11-1). That is, if one of the design requirements

cannot be met, at least one key science goal will be able to be identified quickly as being impacted. It is intended to be analogous to similar documents for other large projects, including the "Science Goals and Technical Requirements" in the EVLA Project Book, the ALMA Reference Science Plan, the JWST Design Reference Mission, the LSST Science Requirements Document, the Pan-STARRS PS1 Design Reference Mission, or general NASA science traceability matrices.

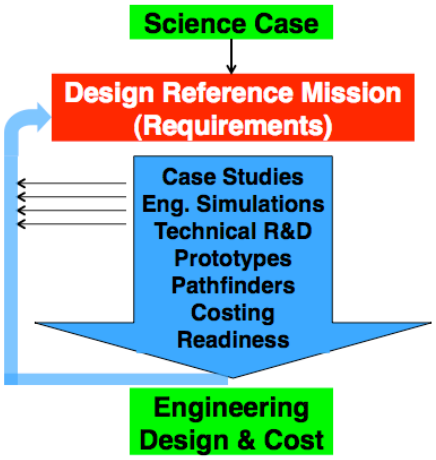

Figure 1-1. An illustration of how the Science Case, Design Reference Mission, and Engineering Design & Cost interact for the design of the SKA.

1.3. Scope of this Document

The following chapters present the initial Design Reference Mission as a series of science components or "use cases." Each chapter presents a summary of the motivation, an illustration of how the observation or summary might be conducted, a series of scientific requirements for that observation, and a series of technical requirements derived from the scientific requirements. While the division between "scientific" and "technical" requirements is not always clear, generally scientific requirements are taken to be an astronomical or physical quantity that we wish to determine (e.g., the amplitude of the gravitational strain produced by inspiraling supermassive black holes or the H I optical depth through a galaxy). Conversely, technical requirements are taken to be aspects of the telescope design, particularly those aspects that are likely to influence the cost (e.g., total collecting area or frequency range). No priority should be inferred from the order of presentation of the science components or of the ordering of scientific or technical requirements within each component.

An important consideration for this document is that the "boundary conditions" for SKA Phase 1 have been set, at least in part, by decisions taken by the SKA Science & Engineering Committee (SSEC). Garrett et al. (2010) provide a high-level concept description of SKA Phase 1, including a summary of key science goals. In developing this Design Reference Mission, these key science goals and the likely implementation were considered as guidance.

As Figure 1-1 suggests, during the design phase of the SKA, it is likely that there will be iteration between the requirements and the various design activities (engineering simulations, technology development...). Indeed, this process could be viewed as having started already in the Phase 1 concept definition. Further, in many cases, requirements are connected to other aspects of the observation (e.g., the thermal noise limit in an image depends upon the telescope sensitivity, observing bandwidth, and total integration time). Thus, while requirements are specified in the various components, the Design Reference Mission also contains motivation for the requirements as well as illustrations of how various requirements are coupled (e.g., Figure 3-1).

For each requirement, both scientific and technical, a concise statement of the requirement is presented, in the form of, "The SKA Phase 1 shall …." These statements are italicized and should be taken as the requirement. Additional text in each section presents explanatory material or discussion of scientific or technical considerations that lead to the requirement.

1.4. Assumptions

While the SKA Phase 1 and Phase 2 often are colloquially described in terms of their sensitivities or survey speeds, a more useful metric is observing time. Experience has shown that the operational cost of ground-based facilities, over their lifetime, often exceeds the capital costs, potentially by a significant factor. Thus, while there is in principle a tradeoff that can be conducted between sensitivity or survey speed and observing time, the integrated costs from operations may limit substantially the extent to which longer observing programs can be tolerated. Further, longer observing programs and a longer operational lifetime, may have implications for component reliability (e.g., mean time between failures) which can affect capital costs directly. For this reason, the SKA Program has adopted observing time as a metric by which to assess costs. In order to provide definiteness, two specific assumptions (§§1.4.1 and 1.4.2) are adopted for the SKA Phase 1 Design Reference Mission. Two further assumptions are adopted (§§1.4.3 and 1.4.4) based on guidance from the SKA Science and Engineering Committee (SSEC).

Table 1-1. SKA Phase 1 Assumptions

Parameter	Assumed Value
Survey "On-Sky" Time	2 years
Deep Field Integration Time	1000 hours
Sensitivity and Frequency Range	Up to 2000 $m^2 K^{-1}$ at frequencies between 70 and 450 MHz Up to 1000 $m^2 K^{-1}$ at frequencies between 0.45 and 3 GHz
Maximum Baseline	100 km

1.4.1. Survey "On-Sky" Time and Survey Speed

SCI-A-0010: The SKA Phase 1 can complete a major survey in 2 years of "on-sky" observation time, with nearly uniform, thermal noise-limited performance being obtained for a substantial majority of the pointings.

The assumed time for surveys bears on scientific, operational, and sociological aspects of the telescope. The time allotted for a survey can be used to set technical requirement on the systematics within the system, but it also relates to sociological aspects, such as the amount of time that funding and personnel for a project can be sustained. Table 1-2 specifies the maximum allotted time for surveys. These specified limits do not attempt to take into account any required calibration observations nor other aspects of the telescope operation (e.g., maintenance) that might be required. Finally, even in designing a survey, it is likely that there will be "inefficiencies." As an example, the frequency range for SKA Phase 1 means that ionospheric phase errors may be an important part of calibration. One method of mitigating ionospheric phase errors is to observe only at night. Consequently, the resulting duty cycle of observations might be less than 50%, meaning that the actual time to complete the survey ("wall-clock time") would be a factor of 2 larger than what is listed. Major surveys (e.g., SDSS, ALFALFA) typically take 5–7 years to complete. Allowing for calibration and other "inefficiencies," it is likely that the time to complete a survey that is allocated 2 yr will approach 5 yr.

As indicative values for measure of the performance, we specify that 90% of the pointings obtained have a noise level within a factor of 2 of thermal.

The time to complete a survey leads naturally to a "survey speed figure of merit" (SSFoM, Cordes 2007). Typically the SSFoM is defined as

$$\mathrm{SSFoM} \equiv \Omega \, (A_{\mathrm{eff}}/T_{\mathrm{sys}})^2$$

where A_{eff}/T_{sys} is the standard measure of the system sensitivity, related to the minimum flux density that can be obtained by the radiometer equation, and Ω is the field of view. The field of view is taken to be the area on the sky that can be accessed with essentially constant sensitivity; historically the field of view is taken to be the 3 dB (half-power) level of the power pattern of the receptor. In practice, a more appropriate definition would be

$$\mathrm{SSFoM} \equiv \Omega\,(A_{eff}/T_{sys})^2\,\Delta\nu$$

as the bandwidth $\Delta\nu$ also impacts how quickly a survey can be conducted—for a spectral-line survey, the bandwidth determines the range of redshift space that is covered, and, if insufficient redshift space is covered, the survey might require two or more observations of the every point on the sky; for a continuum survey, the bandwidth determines the sensitivity, and, if the bandwidth is too small, the limiting flux density of the survey will be impacted. For the current purposes of this document, the processed bandwidth is described by SCI-SYSR-0010 (§1.5.1), however, should that requirement be relaxed or modified, the survey speed required may have to be re-assessed.

1.4.2. Deep Field Integration Time

SCI-A-0020: The SKA Phase 1 can produce thermal noise-limited images even after 1000 hr of integration time.

Much like the case for surveys, the amount of time devoted to a "deep field(s)" has scientific, operational, and sociological aspects. The specified deep field integration time is the "on sky" integration time, and, similar to the case for surveys, the total time to acquire the observations may be longer. The specified time is comparable to the longest observations that have been conducted by radio telescopes to date. More generally, the amount of time (~ 3 Ms) is comparable to the longest observations conducted by other major facilities (e.g., *Hubble*, *Chandra*). Longer integrations times are being proposed (e.g., with ASKAP), and the outcome of those may justify increasing this requirement by a factor of 3 or more.

1.4.3. Sensitivity and Frequency Range

SCI-A-0030: The SKA Phase 1 has a sensitivity of up to 2000 $m^2\ K^{-1}$ at frequencies between 70 and 450 MHz.

SCI-A-0040: The SKA Phase 1 has a sensitivity of up to 1000 $m^2\ K^{-1}$ at frequencies between 0.45 and 3 GHz.

These are discussed together, based on a possible implementation using technologies identified by the SSEC for the SKA Phase 1. The specified values are taken from Garrett et al. (2010). To the extent possible, implementations that allow a larger frequency range, higher sensitivity, or both while maintaining the assumed cost cap would be scientifically valuable.

1.4.4. Maximum Baseline

SCI-A-0050: The SKA Phase 1 will have a maximum baseline of 100 km.

The specified value are taken from Garrett et al. (2010). To the extent possible, a configuration and implementation that allow a larger maximum baseline while maintaining the assumed cost cap would be scientifically valuable.

1.5. System-Level Design Specifications

During the course of the development of the Phase 2 Design Reference Mission, it was recognized that several of the design parameters transcend specific science cases. These parameters are considered to be "system-level" specifications, which is also consistent with the system-level approach recommended by the SKA International Engineering Advisory Committee (IEAC) and the design approach adopted under

the aegis of PrepSKA. This approach has been continued for Phase 1, and Table 1-2 summarizes these. Discussion of each specification follows.

Table 1-2. SKA Phase 1 System-Level Design Specifications

Parameter	Value
Fractional Instantaneous Bandwidth	~ 1
Spectral Baseline	Sufficiently flat to enable spectral line and polarization observations
Correlator Integration Time	Sufficient to mitigate time-average smearing
Spectral Resolution	Sufficient to mitigate bandwidth smearing
Operational Availability	At least 85%
Polarization Capabilities	Capable of receiving the full polarization information carried by the incident electric field

1.5.1. Fractional Instantaneous Bandwidth

SCI-SYSR-0010: The SKA Phase 1 shall be designed so that the fractional instantaneous bandwidth is comparable to the observing frequency, with the minimum acceptable value being a value that is 50% of the central frequency of the observing bandwidth.

Current telescopes (e.g., EVLA, ATCA, GBT) deliver instantaneous bandwidths comparable to the observing frequency, for observing frequencies below about 10 GHz. As the SKA Phase 1 should therefore perform at least as well as the current systems, the requirement on the fractional instantaneous bandwidth is $\Delta\nu/\nu \sim 1$. This requirement applies most directly to continuum observations (including pulsar observations), but also has a bearing on spectral line observations: If a large instantaneous bandwidth can be accessed for spectral line observations, more efficient searches for lines are enabled.

1.5.2. Spectral Baseline

SCI-SYSR-0020: The SKA Phase 1 shall be designed so that at least the central 90% of the bandpass in total intensity does not show ripples or other systematic fluctuations on scales smaller than a frequency corresponding to 300 km s^{-1} that are larger than would be achieved by twice the thermal noise level after an integration of 1000 hr.

SCI-SYSR-0025: The SKA Phase 1 shall be designed so that at least the central 90% of the bandpasses in both total intensity and individual senses of cross-polarization do not show ripples or other systematic variations with an amplitude that exceeds twice the thermal noise level after an integration of 1000 hr on frequency scales larger than the equivalent of 1 radian of Faraday rotation for a rotation measure of ±500 rad m^{-2}.

The error budget for the spectral baseline will likely include many factors, including contributions from the instrument and from the processing. It is acceptable if these requirements are met in post-calibration processing. Strictly, the second requirement is derived from requirements on extensibility toward SKA Phase 2 (Chapter 10), but it may also be important for various SKA Phase 1 observations and is therefore considered a system requirement.

1.5.3. Correlator Integration Time

SCI-SYSR-0030: The SKA Phase 1 shall be designed so that the integration time provided in the signal processing chain does not result in the time-average smearing at the edge of the field of view exceeding 2%.

Increasing the correlator integration time can reduce the data rate generated by the telescope, but at the cost of generating time-average smearing in images. Time-average smearing has the effect of reducing the peak brightness of sources in images, potentially rendering faint sources undetectable (i.e., below a predefined false-alarm threshold). Alternately, longer integration times will be required to obtain the same effective flux density threshold over the entire field of view. For a 2% reduction in peak brightness sensitivity, a 4% increase in integration time is required; smaller increases may be acceptable, depending upon the observations, because time-average smearing is not uniform across the field of view. As an illustration, a deep field of 1000 hr with time-average smearing would be equivalent to a deep field of 960 hr without time-average smearing. This small difference is considered acceptable.

1.5.4. Spectral Resolution

SCI-SYSR-0040: The SKA Phase 1 shall be designed so that the spectral resolution provided in the signal processing chain does not result in the bandwidth smearing at the edge of the field of view being larger than 2%.

Making the spectral resolution coarser can reduce the data rate generated by the telescope, but at the cost of generating bandwidth smearing in images. Bandwidth smearing has the effect of reducing the peak brightness of sources in images, potentially rendering faint sources undetectable (below a predefined false-alarm threshold). Alternately, longer integration times will be required to obtain the same effective flux density threshold over the entire field of view. For a 2% reduction in peak brightness sensitivity, a 4% increase in integration time is required; smaller increases may be acceptable, depending upon the observations, because bandwidth smearing is not uniform across the field of view. As an illustration, a deep field of 1000 hr with bandwidth smearing would be equivalent to a deep field of 960 hr without bandwidth smearing. This small difference is considered acceptable.

The spectral resolution required to enable identification and excision of radio frequency interference (RFI) may be higher, and it may be site dependent. Therefore, we do not consider RFI considerations in the remainder of this document.

1.5.5. Operational Availability

SCI-SYSR-0050: The SKA Phase 1 shall be designed so that its average operational availability is at least 85%.

The operational availability is a measure of the fraction of the time that the SKA Phase 1 would be available for science operations. A larger availability generally produces additional science output, but also places more stringent requirements on the design as it requires more robust equipment with longer mean times between failure. Moreover, as Tan (2001) discusses, defining the operational availability of an interferometer is complex. Interferometers degrade gracefully, so the loss of a single receptor, or even a small number of receptor, may not be result in significant impact to the science program. Further, because the receptors will be distributed widely and unable to be moved, it is possible that some science programs will not be able to use all of the receptors (e.g., more distant receptors might result in sources being "resolved out").

Tan (2001) presents a definition of operational availability, based on practice for at the NRAO, and assessment of a small number of interferometers, with the aim of determining a requirement for ALMA. Adopting his definition, the SKA operational availability is defined as

$$A = 100*(t_{tot\_ant\_obs} - \Sigma t_{and\_down})/t_{tot\_ant\_obs}$$

where $t_{tot\_ant\_obs}$ is the total time that all antennas could possibly be observing and t_{and_down} is the any loss of time due to one or more antennas. The sum is taken over all losses suffered in some sufficiently long interval. In general, for an N element array, the total time that all antennas could possibly be observing each day is $t_{tot\_ant\_obs} = 24N$ hours, while the loss of time t_{and_down} depends upon the cause and the number

of antennas affected. For ALMA, Tan (2001) adopts a nominal goal of 85%. In part this goal is motivated by the fact that current systems achieve values of A that equal or exceed 85%. (For the VLA, A ~ 95%.) At centimeter wavelengths, values of A approaching or exceeding 90% should be possible, based on current experience. We specify a slightly lower value because there may be times when the ionosphere is sufficiently disturbed that low frequency observations are not possible.

1.5.6. Polarization Capabilities

SCI-SYSR-0060: The SKA Phase 1 shall be designed so that it is capable of receiving the full polarization information carried by the incident electric field.

The study of Cosmic Magnetism is formally a Key Science Project for SKA Phase 2, although there may be aspects of calibration for multiple SKA Phase 1 science goals (e.g., Chapters 2 and 6) that require obtaining the complete polarization information. Traditionally, in radio astronomy, polarization is characterized by the Stokes parameters (I, Q, U, and V), though other descriptions are acceptable if they can be converted to the Stokes parameter standard.

1.6. Data Products

The initial focus of the international SKA effort has been in describing the hardware components of the telescope. Considerably less attention has been paid, until recently, to the data product(s) expected of the SKA Phase 1. As the SKA design efforts have matured, it is increasingly recognized that identifying and describing the processing aspects of the telescope are important. Throughout the document, an initial effort is made to determine what data products are generally expected for the various observations described.

1.6.1. Processing Capability

SCI-D-0010: The SKA Phase 1 shall be capable of conducting imaging and non-imaging processing simultaneously.

SCI-D-0020: The SKA Phase 1 shall be capable of conducting observations from different receptor types simultaneously.

There are various SKA Phase 1 observations that could be conducted simultaneously. The experiences of the SKA Precursors and pathfinders will provide additional guidance on this topic, but initial experiences already illustrate that some kinds of H I and pulsar observations can be conducted simultaneously. Traditionally, imaging (e.g., H I images of galaxies) and non-imaging (e.g., pulsar timing) observations require different approaches to processing the received signals. While it may not always be possible for the same set of signals to be used for multiple science programs, conducting observations simultaneously can provide a higher science return by using the same data for multiple science goals.

In a similar fashion, the current SKA Phase 1 concept involves two distinct types of receptors (dipoles and parabolic dishes), arranged in spatially disjoint locations. A larger science return will be obtained by being able to observe with these two sets of receptors simultaneously.

1.6.2. Meta-Data

For all science processing, certain meta-data either will be required as part of obtaining the science data products or will be required in order to make sense of the science data products. Common examples of the kinds of meta-data include

- Direction that the telescope is pointing;
- Central frequency;
- Bandwidth, and spectral resolution if relevant;
- Antenna locations; and

- Time-stamped system temperature information.

This list should be seen as illustrative and common, but may not be comprehensive.

Acknowledgements: In addition to members of the SKA Science Working Group, a large number of additional people have contributed to this document including P. Alexander, W. Brisken, P. Caselli, C. De Breuck, A. Deller, R. Ekers, J. Geisbüsch, L. Godfrey, M. Haynes, T. Henning, N. Kanekar, P. Lah, W. Lane Peters, T. Maccarone, E. Murphy, T. Oosterloo, H. Rottgering, R. Smits, I. Stairs, J. Stil, R. Taylor, W. Vlemmings, and R. Windhorst.

Bibliography

Carilli, C. L., & Rawlings, S. 2004, *Science with the Square Kilometer Array*, New Astron. Rev. (Elsevier: Amsterdam)

Cordes, J. M. 2007, "The SKA as a Radio Synoptic Survey Telescope: Widefield Surveys for Transients, Pulsars and ETI," SKA Memorandum #97; http://www.skatelescope.org/PDF/memos/97_Memo_Cordes_REVISED.pdf

Fomalont, E. B., & Bridle, A. H. 1978, "The Radio Source near NGC 2823," Mon. Not. R. Astron. Soc., 182, P1

Gaensler, B.M. 2004, "Key Science Projects for the SKA" SKA Memorandum #44; http://www.skatelescope.org/documents/Gaensler_key_science_projects_0402.pdf

Garrett, M. A., et al. 2010, "Concept Design for SKA Phase 1 (SKA_1)," SKA Memorandum #125; http://www.skatelescope.org/PDF/memos/125_Memo_Garrett.pdf

Goldstein, S. J., Jr., & Wade, C. M. 1977, "Radio Sources near the Globular Clusters M13 and M53," Astron. J., 82, 972

Schilizzi, R. T., et al. 2007, "Preliminary Specifications for the Square Kilometre Array," SKA Memorandum #100; http://www.skatelescope.org/PDF/memos/100MemoSchilizzi.pdf

Tan, G. H. 2001, "A Comparison of Availability of Major Radio Interferometers," ALMA Memorandum #370; http://www.alma.nrao.edu/memos/html-memos/abstracts/abs370.html

2. Probing the Neutral Intergalactic Medium During the Epoch of Reionization

Principal Authors: B. Ciardi, F. Briggs, C. Carilli, G. de Bruyn, L. Greenhill, C. Lonsdale, L. Koopmans, J. Pritchard, M. Santos

This Design Reference Mission component is motivated primarily by the Key Science Project "Probing the Dark Ages" (Carilli et al., 2004) and has the specific goal of tracking the transition of the intergalactic medium (IGM) from a neutral to an ionized state during the Epoch of Reionization (EoR).

This chapter is part of the Design Reference Mission because it provides requirements on the frequency range and sensitivity.

2.1. Motivation

The EoR sets a fundamental benchmark in cosmic structure formation, corresponding to the formation of the first luminous objects that act to ionize the neutral IGM. Observations at near-IR wavelengths of absorption by the IGM in the spectra of the highest redshift quasars (Becker et al. 2001; Djorgovski et al. 2001; Fan et al. 2006) and at radio wavelengths of the electron scattering optical depth for the cosmic microwave background (CMB, Spergel et al. 2007; Hinshaw et al. 2008) imply that we are finally probing into this key epoch of galaxy formation at $z > 6$.

Theoretical modeling based on the above existing observational constraints give the impression conveyed in Figure 2.1 of an IGM that becomes filled with growing ionized bubbles on a range of size scales. With the passage of time, the bubbles punch through the walls separating each other, to leave behind a fully ionized IGM, which remains ionized to the present. The SKA, and the pathfinder telescopes that will precede it, will provide critical insight into the EoR in a number of ways. The ability of these telescopes to perform a tomographic study of the neutral IGM in (redshifted) 21 cm emission will be a unique probe of the process of reionization, and is recognized as the next necessary and fundamental step in our study of the evolution of large-scale structure and cosmic reionization. The application of radio technologies to probing the EoR forms the basis for several chapters in the SKA Science Case (Carilli & Rawlings, 2004) and are also well described in the review articles by Furlanetto et al. (2006) and Morales & Whythe (2010).

The Phase 1 SKA can probe the EoR through statistical means, such as power spectrum analysis, or direct imaging. Initially, SKA Phase 1 EoR studies would apply a power spectrum analysis, since that requires less sensitivity, but this would be informed through the SKA pathfinders such as MWA, PAPER, and LOFAR. Imaging the history of reionization requires a significant collecting area and will not be feasible by the pathfinders. This is because the signal expected is a few μJy beam^{-1} in a 2' beam at 100 MHz; Figure 2-2 shows a theoretical prediction for brightness temperature images. IGM tomography offers an invaluable tool to discriminate between different ionization sources and to follow the spatial and temporal evolution of the reionization process (e.g., Loeb & Barkana 2001; Fan et al. 2006; Furlanetto et al. 2006).

2.2. Observational Summary

In order to minimize the contribution of the Galactic nonthermal emission to the system temperature, the observations would be conducted at high Galactic latitudes, but the exact specification of a field is likely to depend upon future observations and must also include selection against strongly polarized foregrounds, which can couple to the intrinsic instrumental polarization of SKA. In fact, high Galactic latitudes near the south Galactic pole are an area of generally low Galactic nonthermal background (Haslam et al., 1982), thus minimizing this contribution to the system temperature. Second, the southern Galactic pole is at a declination near −30º, meaning that it is at a high elevation from both candidate Southern Hemisphere sites, which again is likely to minimize the system temperature.

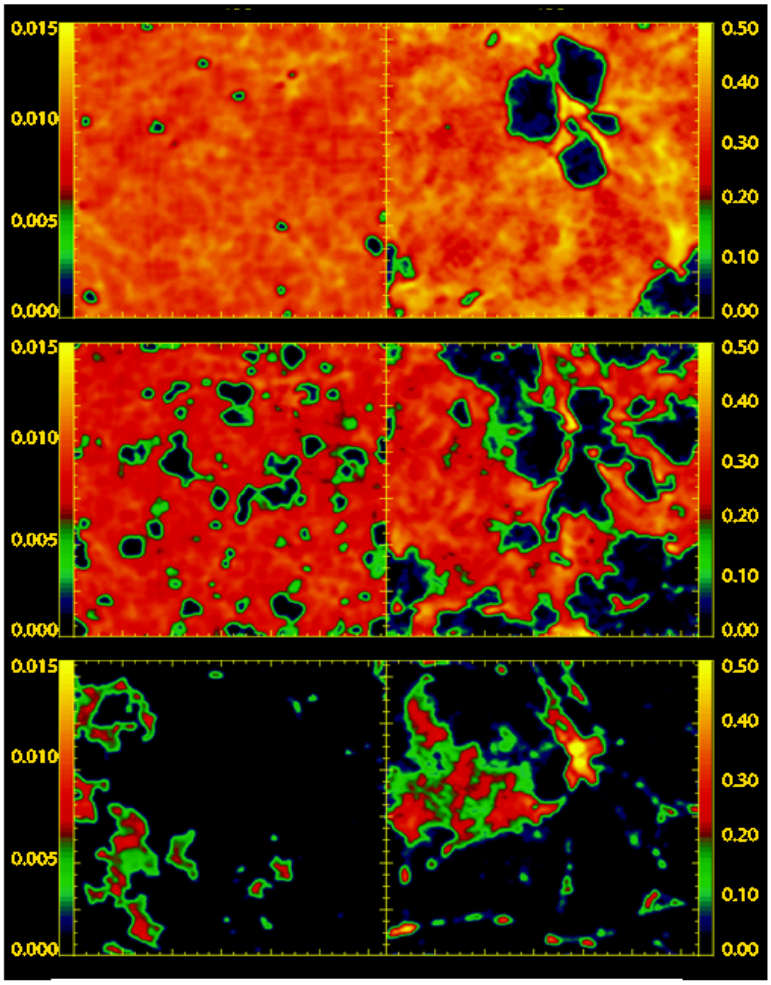

Figure 2-1. Reionization images showing the redshift evolution of the number density of neutral hydrogen in the field ($L = 20h^{-1}$ Mpc comoving box; left panels) and in a protocluster environment ($L = 10h^{-1}$ Mpc comoving box; right panels). From top to bottom, the redshift of the simulations is 15.5, 12, and 9 (Ciardi et al. 2003).

The diffuse Galactic foreground is dominated (> 99%) by synchrotron emission, which is intrinsically highly polarized and has a brightness temperature of about 5 orders of magnitude above the level of the expected H I fluctuations on the largest angular scales. This emission is spectrally smooth and has power of order several Kelvin (Bernardi et al. 2009, 2010) on a few arcminute angular scales in Stokes I. Similarly, there is considerable power on small angular scales in linear polarization due to the action of internal and foreground Faraday screens (Bernardi et al. 2009, 2010), with typically few K polarization levels observed at 150 MHz (Bernardi et al. 2010). If instrumental polarization across the field of view cannot be calibrated to better than 0.1%, the resulting residuals would be a few mK, comparable to the EoR signal. To make matters worse, these would be frequency dependent on a scale of a few MHz. The EoR observations should therefore target one, possible several, windows of low (polarized) Galactic foreground emission, the choice of which will be guided by the pathfinders.

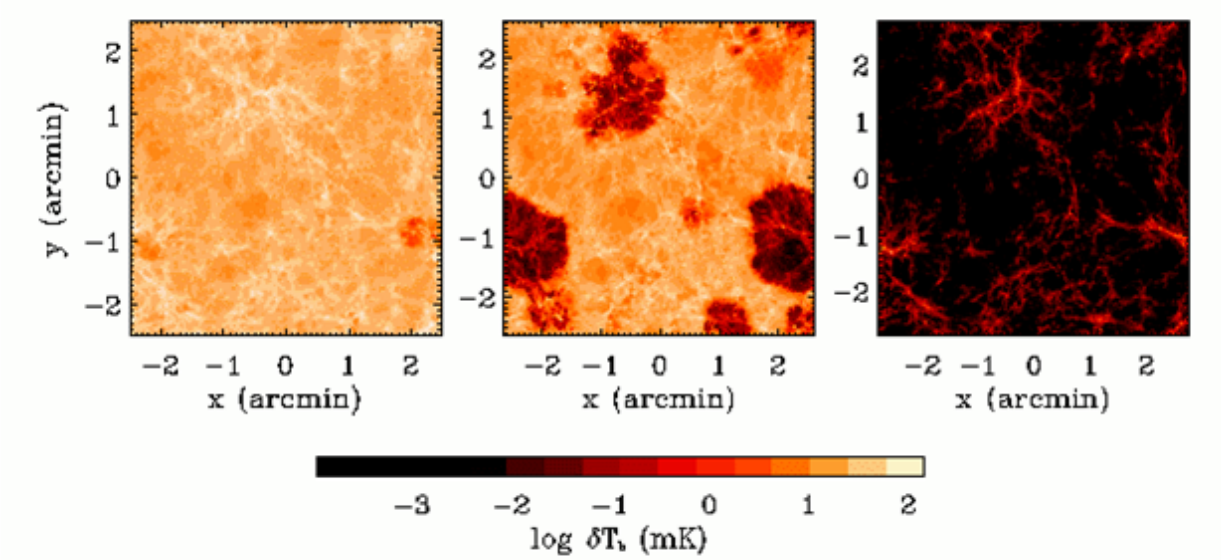

Figure 2-2. The brightness temperature of the (redshifted) 21 cm transition at several redshifts, as predicted by the "late reionization" simulation analyzed in Furlanetto et al. (2004). Each panel corresponds to the same slice of the simulation box (with width $10h^{-1}$comoving Mpc and depth $\Delta\nu$= 0.1 MHz), at z= 12.1, 9.2, and 7.6, from left to right. The three epochs shown correspond to the early, middle, and late stages of reionization in this simulation.

2.3. Scientific Requirements

Table 2.2-1 summarizes the scientific requirements. Motivation for and discussion of each scientific requirement follows.

Table 2.2-1. Scientific Requirements

Parameter	Value
Redshift	6 – 19 (6 – 30 goal)
Brightness temperature noise level	1 mK
Angular resolution	1'
Radial resolution	2 Mpc
Field of View	sufficient to mitigate cosmic variance

2.3.1. Redshift

SCI-S-REQ-0010: The SKA Phase 1 shall be able to observe the H I line over at least the redshift range of 6–19, with the goal of observing over the redshift range of 6–30.

The redshift range (6–19, with an upper redshift limit of 30 as a goal) is set by the cosmic epoch over which the reionization process takes place (e.g., Pritchard & Loeb 2010). The lower limit is set by the end of reionization, which is currently given by high-redshift QSO spectra (Fan et al. 2006). The upper limit is suggested theoretical modeling of the impact of the first stars on the neutral IGM. Lyman-α emission from the first stars couples the 21-cm spin temperature to the gas temperature via the Wouthysen-Field effect, inducing a strong absorption feature in the global H I signal, while X-ray emission from star-forming processes (or the first quasars) heats the gas. The redshift of the absorption

feature in the global H I signal induced by Ly-α photons depends on various heating scenarios but it may be as early as $z \sim 30$ (e.g., Pritchard & Loeb 2010).

2.3.2. Brightness Temperature Noise Level

SCI-S-REQ-0020: The SKA Phase 1 shall provide a brightness temperature noise level, typically taken as the root-mean-square value, of 1 mK on arcminute angular scales.

Current theoretical models for the differential brightness temperature predict a peak value of ~10 mK over arcminute scales in the redshift regime discussed above (e.g., Ciardi & Madau 2003; Furlanetto et al. 2006; Pritchard & Loeb 2010). In order to obtain a sufficient signal-to-noise ratio, we specify 1 mK as the brightness temperature noise level requirement, on arcminute scales. The exact value of the peak differential brightness temperature and redshift of occurrence depends on the reionization model and the angular scales assumed. Away from the peak (e.g., different redshifts or larger angular scales) the differential brightness temperature may be below 1 mK, but this region of parameter space will have to wait for the full SKA as it is too faint for SKA Phase 1, or can partly be accessed by smoothing the image (low-pass filtering of *u-v* space; see below).

2.3.3. Angular Resolution

SCI-S-REQ-0030: The SKA Phase 1 shall provide an angular resolution at least as high as 1'.

The observations need to resolve co-moving structures of a small enough size such that the differential brightness temperatures are of the order of 10 mK. The required angular resolution is about 1'–2' (e.g., Ciardi & Madau 2003), corresponding to a co-moving size scale in the range of 0.15–0.3 Mpc over the frequency range 50–240 MHz. At a lower angular resolution of 5', the differential sky brightness temperature is about 3 times less than that seen with a 1'–2' beam.

2.3.4. Radial Resolution

SCI-S-REQ-0040: The SKA Phase 1 shall provide a radial resolution over the required frequency range for these observations of 0.1 Mpc.

The objective of imaging tomography is to track the evolution of structures in the Universe as a function of redshift. Analogous to the angular resolution requirement is therefore a radial resolution requirement describing the size of the structures along the line of sight. As reference, the frequency scale corresponding to 1' on the sky is 0.10–0.17 Mpc over the frequency range of 50–240 MHz. Hence, a frequency resolution of at least 0.1 MHz is required to match spatial scales both along the line of sight and transverse to it.

2.3.5. Field of View

SCI-S-REQ-0050: The SKA Phase 1 shall provide a field of view large enough to mitigate cosmic variance.

The field of view must be large enough to obtain a signal-to-noise ratio of at least 3 for power spectrum analysis and to limit the effects of cosmic variance. These requirements imply a field of view sufficient to sample at least 1 Gpc^3 (co-moving), equivalent to an angular diameter greater than 5°. No coherent spatial structures exceeding this scale are expected.

2.4. Technical Requirements

Table 2.2-2 summarizes the technical requirements derived from the scientific requirements. Discussion of each technical requirement follows. The requirements for imaging tomography and power spectrum analysis remain largely the same, but differ for maximum baseline and sensitivity, as described below.

Table 2.2-2. Technical Requirements

Parameter	Value	Requirement
Frequency range	70–200 MHz (50–200 MHz goal)	Redshift coverage
Frequency resolution	100 kHz	Radial resolution
Maximum baseline	b_{max} = 5 km core (~50 km outer baselines)	Angular resolution (calibration, foreground removal)
Polarization	Full	Calibration, foreground removal
Integration time	> 1000 hours	H I brightness temperature
A_{eff}/T_{sys}	> 2000 m^2 K^{-1}	H I brightness temperature

2.4.1. Frequency Range

SCI-T-REQ-0010: The SKA Phase 1 shall provide frequency coverage of at least 70 to 200 MHz, with a goal of covering 50 to 200 MHz.

This requirement follows directly from the redshift coverage requirement. The rest frequency of the H I line is 1.4 GHz. The lower frequency end is determined by the requirement to reach a specified redshift [i.e., 1.4 GHz/(1 + z)]. A redshift of 30 corresponds to a lower frequency of 50 MHz.

2.4.2. Frequency Resolution

SCI-T-REQ-0020: The SKA Phase 1 shall provide a frequency resolution of at least as fine as 100 kHz.

This requirement follows directly from the radial resolution science requirement. For reference, assuming the concordance cosmology, at these redshifts, the co-moving length is given by ≈ 1.7 Mpc(Δν/100 kHz). Therefore, to match the angular resolution a frequency resolution of about 100 kHz is required. For high redshifts (z > 9), simulations have shown little difference in the sky brightness temperature difference for 0.1 and 1 MHz resolutions (Ciardi & Madau 2003). A frequency resolution of 1 MHz will probably be used in the early stages to increase the sensitivity of the observations (§2.4.4).

2.4.3. Maximum Baseline

SCI-T-REQ-0030: The SKA Phase 1 shall provide a maximum baseline of at least 5 km, and potentially as large as 50 km (TBC).

Imaging Tomography:

The nominal angular resolution requirement would imply a maximum baseline of 5 km. However, observations of the high redshift 21-cm signal are expected to be challenging because of foreground contamination. Because of their smooth and broadband signature, the foreground signal from the galaxy can be filtered out. Nevertheless, sidelobes from point sources out-of-beam will confuse the in-beam images unless these sources are removed. Accurate identification and removal of such out-of-beam sources requires higher angular resolution (~ 10"). These outer baseline stations are also required to reduce ionospheric effects for a large field of view on scales below the FWHM resolution of the core. For a 5° field of view, the requirement is nominally 50 km maximum baselines (Koopmans 2010), which is equivalent to the largest physical electron-density waves in the ionosphere at 300 km height that fits inside the field of view of the antennas. We note that ~180 km baselines are already foreseen in the SKA Phase 1 configuration (Memo 125).

Power Spectrum Analysis:

Statistical detection of the EoR does not require as great an angular resolution as imaging. For example, the decrease of angular resolution from 2' to 7' may decrease the differential sky brightness by a factor of about 5 (Ciardi et al. 2003; Furlanetto et al. 2006), but the l_{min}/l increase in sensitivity of power spectrum

analysis over imaging makes the signal still potentially detectable. Baselines of about 1 km (i.e., the power spectrum on scales of about 10') will be sufficient for power spectrum analysis, given the imaging tomography $A_{\rm eff}/T_{\rm sys}$ in §2.4.4.

2.4.4. Polarization

SCI-T-REQ-0040: The SKA Phase 1 shall provide full polarization capabilities.

The (redshifted) 21-cm signal is not expected to be polarized, but both discrete and diffuse foregrounds exhibit polarization patterns. Thus, full polarization is required for calibration and foreground removal purposes.

2.4.5. Sensitivity and Integration Time

SCI-T-REQ-0050: TBD

Imaging Tomography:

The sensitivity requirement follows directly from the brightness temperature sensitivity requirement and the angular resolution desired. Assuming a 1000 hr integration time, the $A_{\rm eff}/T_{\rm sys}$ required to obtain the sky brightness temperature noise level of 1 mK (0.09 μJy beam^{-1}) is 10400 m^2 K^{-1} for the maximum resolution of 4.2', 3.0', 2.1', 1.4', 1.1' at 50, 70, 100, 150, 200 MHz, respectively. This $A_{\rm eff}/T_{\rm sys}$ is not likely to be achieved until SKA Phase 2, so smoothing on arcminute scales (effectively a low pass filter in the *u–v* plane) will increase the sensitivity of the imaging. Table 2.3 and Figure 2.3 show the $A_{\rm eff}/T_{\rm sys}$ required to obtain a brightness temperature noise level of 1 mK rms for various smoothing scales. Sensitivities $A_{\rm eff}/T_{\rm sys}$ of 200 to 10000 m^2 K^{-1} are required across the frequency range to image the EoR at scales < 10' (Figure 2.3).

The system temperature at 50 to 240 MHz is dominated by Galactic radiation with a strong wavelength dependence: $Tsys = T_0 \lambda^{2.55}$ and $T_0 = 60 \pm 20$ K. The effective collecting area required to reach the needed $A_{\rm eff}/T_{\rm sys} > 2000$ m^2 K^{-1} may therefore be prohibitive at the lowest frequencies. For 50 to 70 MHz, direct imaging is not likely to be possible in Phase 1, but a signal should be possible from power spectrum analysis.

Power Spectrum Analysis:

Power spectrum analysis has an increase in sensitivity over imaging which is proportional to l_{min}/l, where the angular scale of the fluctuations and l_{min} *is* the angular scale of the field of view. Thus, the signal to noise ratio increases by about 5 for a power spectrum analysis of 2' scales with a 1° field of view. Figure 2.3 shows signal to noise ratios of order 10 can be achieved over a wide range of scales for a typical FoV.

The results of various pathfinder telescopes (LOFAR, MWA, and PAPER) will influence this requirement.

2.4.6. Imaging Fidelity

SCI-T-REQ-0060: The SKA Phase 1 shall be designed so that any spatial structure within the sky area of interest that results from an instrumental contribution is much less than 1 mK on arcminute scales.

In order to detect, either via a power spectrum analysis or imaging, the hydrogen signal from the EoR, a sky area sufficiently large to mitigate cosmic variance must be observed (Section 2.3.5). If there is an instrumental contribution from the SKA within this sky area that is in excess of the brightness temperature level expected, it may be difficult or impossible to recognize the astronomical signal. It is acceptable if this requirement is met after calibration.

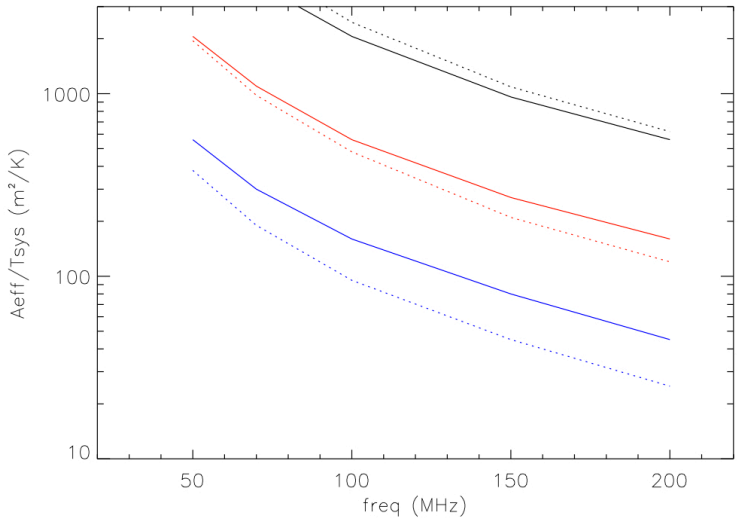

Figure 2.3. A_{eff}/T_{sys} required to reach 1 mK rms, assuming an integration time of 1000 hours and a bandwidth of 1 MHz (solid lines). The smoothing scale is 5, 10 and 20 arcmin for the black, red and blue lines, respectively. The dotted lines are for bandwidths matched to the smoothing scale.

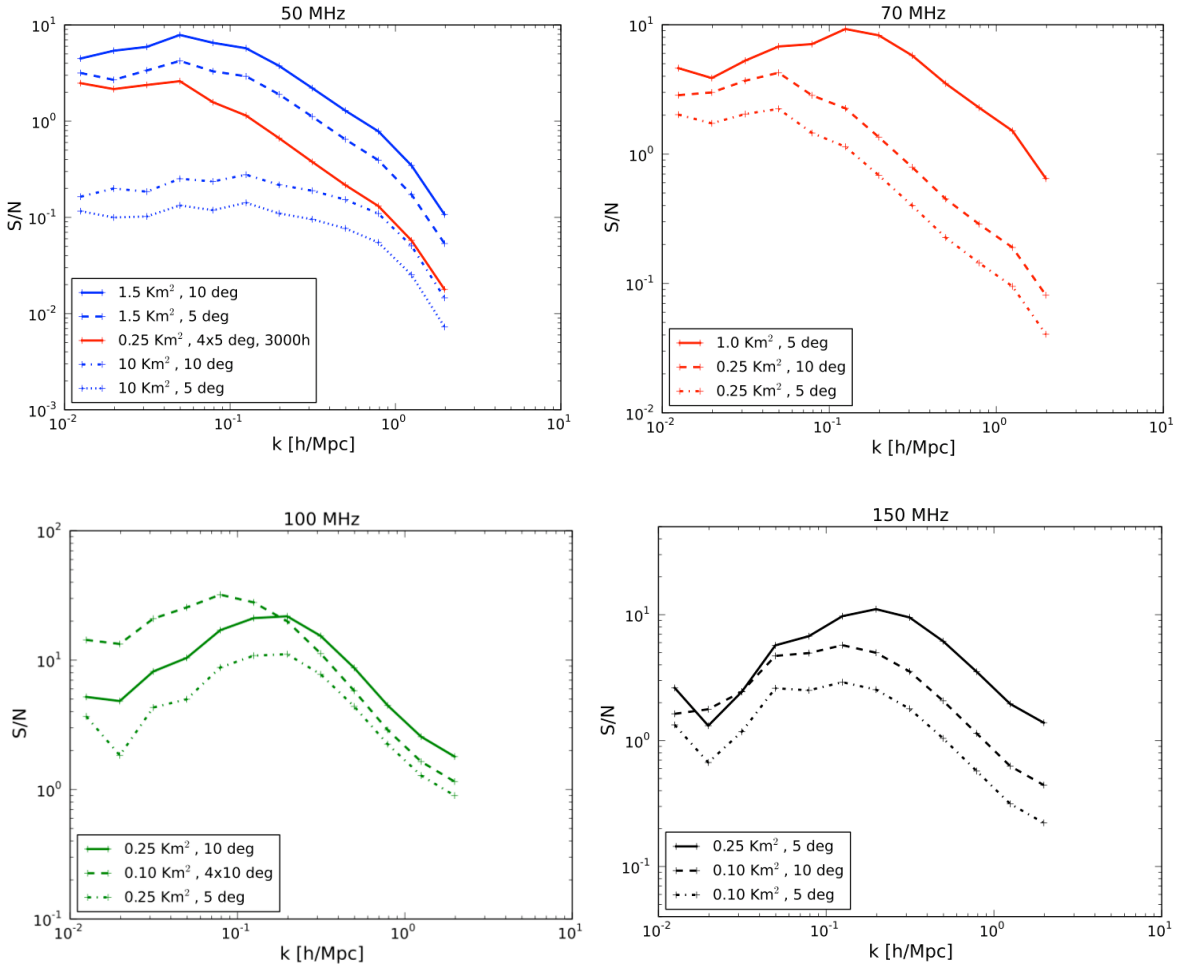

Figure 2.4. Signal to noise of power spectrum determinations, for core areas and fields of view as shown. Three top lines in 50 MHz plot show an early star formation model, which can be distinguished from later reionization models with the 50 to 70 MHz frequency coverage.

Table 2.3. Sensitivity requirements for various smoothing scales, assuming 1000 hours of integration time and bandwidths as shown, to reach sky brightness noise levels of 1 mK. It is assumed that the visibility density decreases as $1/(u^2 + v^2)$ in the *u-v* plane.

	ν = 50 MHz	ν = 70 MHz	**ν = 100 MHz**	ν = 150 MHz	ν = 200 MHz
	z = 27.4	z = 19.3	**z = 13.2**	z = 8.5	z = 6.1
Beam FWHM	4.2'	3.0'	**2.1'**	1.4'	1.1'
Bandwidth	0.47 MHz	0.38 MHz	**0.30 MHz**	0.22 MHz	0.18 MHz
equivalent Bandwidth	1.0 MHz	1.0 MHz	**1.0 MHz**	1.0 MHz	1.0 MHz
A_{eff}/T_{sys} for FWHM	10400 m^2 K^{-1}	10400 m^2 K^{-1}	**10400 m^2 K^{-1}**	10400 m^2 K^{-1}	10400 m^2 K^{-1}
A_{eff}/T_{sys} for 5' smoothing	7600 m^2 K^{-1}	4030 m^2 K^{-1}	**2060 m^2 K^{-1}**	960 m^2 K^{-1}	560 m^2 K^{-1}
A_{eff}/T_{sys} for 10' smoothing	2060 m^2 K^{-1}	1100 m^2 K^{-1}	**560 m^2 K^{-1}**	270 m^2 K^{-1}	160 m^2 K^{-1}

A_{eff}/T_{sys} for 20' smoothing	560 m^2 K^{-1}	300 m^2 K^{-1}	**160 m^2 K^{-1}**	80 m^2 K^{-1}	45 m^2 K^{-1}
Bandwidth	Matched to smoothing scale	Matched to smoothing scale	Matched to smoothing scale	Matched to smoothing scale	Matched to smoothing scale
A_{eff}/T_{sys} for 5' smoothing	10200 m^2 K^{-1}	5090 m^2 K^{-1}	**2460 m^2 K^{-1}**	1090 m^2 K^{-1}	620 m^2 K^{-1}
A_{eff}/T_{sys} for 10' smoothing	1950 m^2 K^{-1}	980 m^2 K^{-1}	**480 m^2 K^{-1}**	210 m^2 K^{-1}	120 m^2 K^{-1}
A_{eff}/T_{sys} for 20' smoothing	380 m^2 K^{-1}	190 m^2 K^{-1}	**95 m^2 K^{-1}**	45 m^2 K^{-1}	25 m^2 K^{-1}

2.5. Data Products

Visibility data cubes of full polarization (Stokes I, Q, U, and V) covering the frequency range 70–200 MHz (goal: 50–200 MHz) at 100 kHz spectral resolution and a temporal resolution sufficient to track ionospheric fluctuations above the site for baselines equivalent to 2' angular resolution.

Bibliography

Becker R. H., et al. 2001, "Evidence for Reionization at z~6: Detection of a Gunn-Peterson Trough in a z = 6.28 Quasar," AJ, 122, 2850

Bernardi, G., et al., 2009, "Foregrounds for observations of the cosmological 21 cm line. I. First Westerbork measurements of Galactic emission at 150 MHz in a low latitude field," A&A 500, 965

Bernardi, G., et al., 2010, "Foregrounds for observations of the cosmological 21 cm line. II. Westerbork observations of the fields around 3C 196 and the North Celestial Pole," A&A 522, 67

Carilli, C. L., Furlanetto, S., Briggs, F., Jarvis, M., Rawlings, S., & Falcke, H. 2004, "Probing the Dark Ages with the Square Kilometer Array," in Science with the Square Kilometre Array, eds.C. L. Carilli & S. Rawlings (Elsevier: Amsterdam) p. 1029

Carilli, C. L., & Rawlings, S. 2004, *Science with the Square Kilometer Array*, New Astron. Rev. (Elsevier: Amsterdam)

Ciardi B., & Madau P., 2003, "Probing beyond the Epoch of Hydrogen Reionization with 21 Centimeter Radiation," ApJ, 596, 1

Ciardi B., Stoehr F., & White S. D. M. 2003, "Simulating Intergalactic Medium Reionization," MNRAS, 343, 1101

Djorgovski S. G., Castro S., Stern D., & Mahabal A. A. 2001, "On the Threshold of the Reionization Epoch," ApJ, 560, L5

Fan, X., Strauss, M. A., Becker, R. H., et al., 2006, "Constraining the Evolution of the Ionizing Background and the Epoch of Reionization with z ~ 6 Quasars. II. A Sample of 19 Quasars," AJ, 132, 117

Furlanetto S. R., Sokasian A., & Hernquist L. 2004, "Observing the Reionization Epoch Through 21-centimetre Radiation," MNRAS, 347, 187

Furlanetto, S.R., Oh, S.P, Briggs, F.H, 2006, "Cosmology at low frequencies: The 21 cm transition and the high-redshift Universe," PhR 433, 181

Haslam, C. G. T., Salter, C. J., Stoffel, H., & Wilson, W. E. "A 408 MHz All-sky Continuum Survey. II - The Atlas of Contour Maps," 1982, A&AS, 47, 1

Hinshaw, G., et al. 2008, astro-ph/0803.0732

Komatsu, E., Dunkley, J., Nolta, et al. 2008, "Five-Year Wilkinson Microwave Anisotropy Probe (WMAP) Observations: Cosmological Interpretation," arXiv: 0803.0547

Koopmans, L.V.E., 2010, "Ionospheric Power-spectrum Tomography in Radio Interferometry," ApJ 718, 963

Loeb, A., Barkana, R., 2001, "The Reionization of the Universe by the First Stars and Quasars," ARA&A 39, 19

Morales, M., & Wyithe, J.S.B. 2010, "Reionization and Cosmology with 21-cm Fluctuations," ARA&A 48, 127

Pritchard, J. and Loeb, A. 2010, Physics Review D, 82, 023006

Spergel D. N., et al. 2007, ApJS, 170, 377

Wythe J. S. B., Loeb A., & Barnes D. G. 2005, ApJ, 634, 715

3. Tracking Galaxy Evolution over Cosmic Time via H I Absorption

Principal Authors: N. Kanekar, F. Briggs, C. Carilli, J. Chengalur, J. Darling, W. Lane Peters, R. Morganti, E. Sadler

This Design Reference Mission component is motivated primarily by the Key Science Project "Galaxy Evolution, Cosmology, and Dark Energy" (Rawlings et al., 2004) and has the specific goal of conducting a blind survey for H I absorption in order to track galaxy evolution over cosmic time.

This chapter is part of the Design Reference Mission because it provides requirements on the frequency range, spectral resolution, and survey speed.

3.1. Motivation

Our understanding of "normal" galaxy evolution is mainly based on samples of damped Lyman-α systems (DLAs). Current DLA samples contain two important biases: (1) Large DLA surveys have been conducted primarily with ground-based facilities and the Lyman-α line is only observable from the ground at $z > 1.7$; more than 95% of the known DLAs are hence at $z > 2$. (2) DLA samples are almost entirely drawn from optically selected surveys, which are biased against dusty absorbers (which would obscure the background QSO). Neither issue affects H I absorption studies, and it should thus be possible to assemble unbiased samples of "normal" galaxies through a *blind* H I absorption survey, in which the background sources are selected without regard to whether they are known to have absorption in their (optical) spectra or even if their redshift is known.

Further, H I absorption is directly sensitive to the physical conditions in the neutral gas in a galaxy. In comparison, optical absorption line studies can only infer the conditions in the neutral gas from low-ionization metal lines. For example, high spectral resolution H I absorption studies can measure or constrain the gas kinetic temperature in high-z galaxies. This is not possible in the optical, as the Lyman-series lines are saturated in DLAs, while low-ionization metal lines have very narrow thermal line widths (not resolvable even with 30-m class optical telescopes). H I absorption studies also provide estimates of the spin temperature (when combined with the H I column density measured from the Lyman-α line), which, for multi-phase absorbers, gives the distribution of H I between cold and warm phases, allowing a probe of the redshift evolution of the temperature distribution of the ISM.

In addition to the neutral gas throughout the galaxy, H I absorption "associated" with AGN allows detailed studies of the kinematics and distribution of gas close to the AGN, which is important for understanding the physics of AGN activity, especially as this activity may be triggered and fuelled by the neutral gas. H I observations also provide direct tests of the unification scheme for radio galaxies and quasars. For example, associated H I absorption should be systematically more common in narrow-line radio galaxies, where the line of sight is predicted to lie close to the plane of the torus, than in broad-line radio galaxies, where the line of sight is expected to lie normal to the plane of the torus.

Finally, the H I line frequency has a different dependence on the fine structure constant α, the proton-electron mass ratio $\mu \equiv m_e/m_p$, and the proton gyromagnetic ratio g_p from optical resonance and molecular rotational (or Lambda-doubled) transitions. A comparison between the redshifts of H I absorption and optical/molecular absorption is hence sensitive to changes in these constants, which are expected in modern extensions of the standard model of particle physics. Such studies of fundamental constant evolution require large samples, to average out "local" velocity offsets (arising, e.g., from intra-cloud motions) between the different lines.

3.2. Observational Summary

The notional survey is a blind survey of H I absorption over a substantial fraction of the sky. The exact survey strategy will depend, in part, upon the actual instrumental characteristics. As an illustration, however, one might envision nighttime observations with the fields observed while they are near meridian

(e.g., an hour angle of 1–2 hr). The motivation for observing only near transit is to minimize the ionospheric "air mass" for the line of sight and to minimize the extent to which any RFI emanating from emitters near the horizon would enter the receptors' near sidelobes. Depending upon the size of the field of view (FoV) and the choice of integration time per field, more than one declination strip might be acquired per night.

3.3. Scientific Requirements

Table 3-1 summarizes the scientific requirements. Motivation for and discussion of each scientific requirement follows.

Table 3-1. H I Absorption Survey Scientific Requirements

Parameter	Value
Redshift	0-6
Optical depth	0.01 toward a 50 mJy flux density background at 1400 MHz
Sky coverage	> 10000 deg^2
Velocity resolution	8 km s^{-1}

3.3.1. Redshift

SCI-S-REQ-0110: The SKA Phase 1 shall be able to access the H I line over at least the redshift range of 0 to 6.

The redshift range accessible determines the cosmic epoch over which galaxy assembly and evolution can be probed. The upper limit of 6 encompasses the range of redshifts over which galaxies have been detected. Higher redshift observations would be valuable for probing into the Epoch of Reionization and detecting the "21-cm forest" from the neutral intergalactic medium during this era; these are the subject of Chapter 4.

3.3.2. Optical Depth

SCI-S-REQ-0120: The SKA Phase 1 shall be able to detect H I absorption at optical depths of 0.01. Obtaining lower optical depths would be desirable.

The optical depth of the H I line depends upon both the column density and the spin (excitation) temperature of the gas. Current observations of H I observations tend to focus on damped Ly-α systems, both because these are easily detected in optical spectra of quasars and because they are thought to be the precursors of massive spirals seen in the local Universe (e.g., Kanekar, 2008). These systems tend to have column densities in excess of 2×10^{20} cm^{-2}, but there are also indications that the spin temperature depends upon metallicity, which likely evolves with redshift (Kanekar et al. 2009). Further, there is some expectation that at column densities below about 10^{20} cm^{-2}, the gas would no longer be able to self-shield itself from the ambient ionizing field, the efficiency of which may depend upon metallicity, density, or other parameters, all of which may evolve with redshift. The specified optical depth is characteristic of what has been detected to date and allows for a range of column densities and temperatures to be probed.

3.3.3. Sky Coverage

SCI-S-REQ-0130: The SKA Phase 1 shall be able to survey a significant fraction of the sky, at least 10000 deg^2.

Both the density of background sources and intervening absorbers, and their uncertainties, drive this requirement. At moderate redshifts ($z \sim 3$), the density of background radio sources is well known, but

the statistics of absorbers is currently quite poor. Consequently, this requirement follows from two separate approaches. Kanekar & Briggs (2004) show that, in order to exceed current surveys at moderate redshifts by an order of magnitude, of order 1000 objects must be detected, which will require covering a hemisphere. Similar estimates are obtained from the SKADS simulations.

3.3.4. Velocity Resolution

SCI-S-REQ-0140: The SKA Phase 1 shall be able to provide a velocity resolution of 8 km s^{-1} or better.

H I absorption observations favor relatively cool gas. The specified requirement is based on existing experience for H I absorption.

3.4. Technical Requirements

Table 3-2 summarizes the technical requirements derived from the scientific requirements. Discussion of each technical requirement follows.

Table 3-2. H I Absorption Survey Technical Requirements

Parameter	Value	Requirement
Frequency range	0.2–1.4 GHz	Redshift coverage
Frequency resolution	5 kHz	Velocity resolution at 200 MHz, commensurate with velocity resolution at other frequencies
Survey Speed	$> 10^6\,\mathrm{m}^4\,\mathrm{K}^{-2}\,\mathrm{deg}^2$	Optical depth, sky coverage, assumed survey time; assumed background source flux density

3.4.1. Frequency range

SCI-T-REQ-0110: The SKA Phase 1 shall provide frequency coverage of at least 0.2 GHz to 1.4 GHz.

This requirement follows directly from the redshift coverage requirement. The rest frequency of the H I line is 1.4 GHz. The lower frequency end is determined by the requirement to reach a specified redshift [i.e., 1.4 GHz/(1 + z)]. A redshift of 6 corresponds to a lower frequency of 0.2 GHz.

3.4.2. Frequency Resolution

SCI-T-REQ-0120: The SKA Phase 1 shall provide a frequency resolution commensurate with the velocity resolution, with a fiducial value of 5 kHz at 200 MHz.

The frequency resolution requirement follows directly from the velocity resolution requirement. The frequency resolution, at a frequency n, corresponding to a velocity resolution Δv is given by $\Delta\nu = \nu(\Delta v/c)$, where c is the speed of light. At a nominal frequency of 200 MHz, the required frequency resolution is 5 kHz; at higher frequencies, the required frequency resolution is less.

3.4.3. Survey Speed

SCI-T-REQ-0130: The SKA Phase 1 shall provide a survey speed of at least 10^6 m^4 K^{-2} deg^2 at a frequency of 1.4 GHz.

A specified sky coverage surveyed to a certain flux density limit (as determined from the background source strengths and H I optical depths) leads to a survey speed requirement. We adopt a survey speed figure of merit appropriate for "steady sources" (Cordes 2007),

$$\mathrm{SSFoM} = (A_{\mathrm{eff}}/T_{\mathrm{sys}})^2 \Delta\Omega \propto (\Omega/T)\ (m/\tau S)^2$$

Here m is the signal-to-noise threshold with which an absorption profile must be detected, Ω is the sky coverage, T is the allotted survey or on-sky integration time (§1.4.1), and S is the (minimum) flux density of the background sources observed.

In general, this expression should also contain a factor for the bandpass. If the processed bandpass is too small, the sky would have to be surveyed multiple times. In practice, the bandpass factor has been suppressed in typical statements of the survey speed figure of merit, and a value is quoted that is consistent with that practice.

Figure 3-1 shows the survey speed figure of merit for a range of optical depths as a function of background source strengths at fiducial redshifts, assuming a survey covering 10 000 deg^2 and an on-sky duration of 2 yr (§1.4.1). As a nominal survey, all sources stronger than 50 mJy would be searched for H I absorption in their spectra, with the specified optical depth being able to be detected with a signal-to-noise ratio of at least 7; an actual survey could target stronger sources in order to probe to lower optical depths. For this nominal survey, a survey speed of order $10^6\ \mathrm{m}^4\ \mathrm{K}^{-2}\ \mathrm{deg}^2$ at 1400 MHz is sufficient; for survey conducted with a parabolic dishes and single pixel feeds, the SSFoM naturally increases to lower frequencies. Larger survey speeds would also be valuable to probe to lower optical depths, fainter sources, or both.

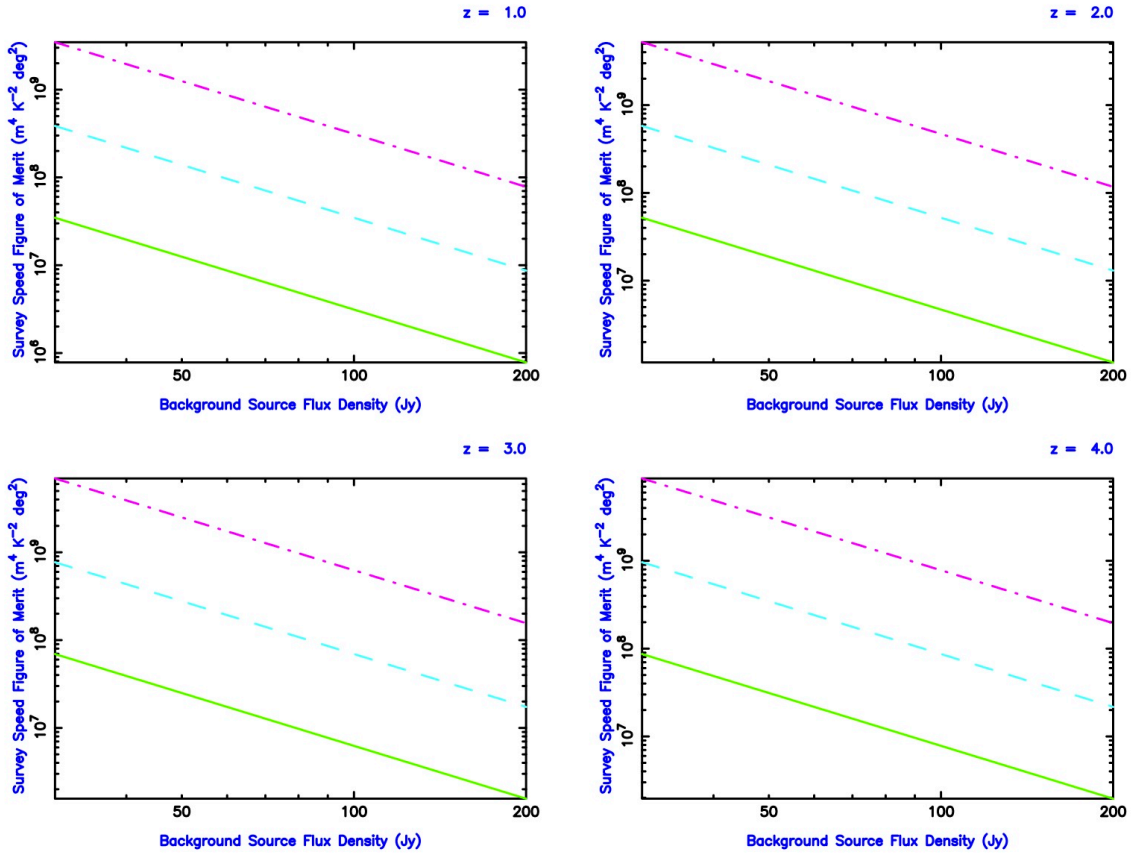

Figure 3-1. Survey speed figures of merit for a blind H I absorption survey as a function of background source strength for a variety of optical depths. The different panels show the survey speed figures of merit at fiducial redshifts. The solid (green) curves show the survey speed figure of merit for an optical depth of 10^{-2}, the dotted (cyan) curves show the figure of merit for an optical depth of 3×10^{-3}, and the purple (dot-dash) curves show the figure of merit for an optical depth of 10^{-3}. All panels assume that the survey covers 10 000 deg^2 and has an on-sky duration of 2 yr (§1.4.1).

3.5. Data Products

For all sources stronger than a specified flux density, nominally 50 mJy at 1400 MHz, a postage stamp total intensity image cube, within the frequency range 200–1500 MHz, of nominal dimensions 15" × 15", with a spectral resolution of 1 km s^{-1} and an angular resolution of 3".

Bibliography

Cordes, J. M. 2007, "The SKA as a Radio Synoptic Survey Telescope: Widefield Surveys for Transients, Pulsars and ETI," SKA Memorandum #97; http://www.skatelescope.org/PDF/memos/97_Memo_Cordes_REVISED.pdf

Kanekar, N., Smette, A., Briggs, F. H., & Chengalur, J. N. 2009, "A Metallicity-Spin Temperature Relation in Damped Lyα Systems," Astrophys. J., 705, L40

Kanekar, N. 2008, "H I 21 cm Absorption Studies: Prospects," in *The Evolution of Galaxies through the Neutral Hydrogen Window,* eds. R. Minchin & E. Momjian (AIP: Melville, NY) p. 57

Kanekar, N., & Briggs, F. H. 2004, "21-cm Absorption Studies with the Square Kilometer Array," New Astron. Rev., 48, 1259

Perley, R. A. 1989, in *Synthesis Imaging in Radio Astronomy*, eds. R. A. Perley, F. R. Schwab, & A. H. Bridle (ASP: San Francisco) p. 287

Rawlings, S., Abdalla, F. B., Bridle, S. L., Blake, C. A., Baugh, C. M., Greenhill, L. J., & van der Hulst, J. M. 2004, "Galaxy Evolution, Cosmology and Dark Energy with the Square Kilometre Array," in Science with the Square Kilometre Array, eds. C. Carilli & S. Rawlings, New Astronomy Reviews, Vol. 48, (Elsevier: Amsterdam) p. 1013

Rengelink, R. B., Tang, Y., de Bruyn, A. G., et al. 1997, "The Westerbork Northern Sky Survey (WENSS), I. A 570 square degree Mini-Survey around the North Ecliptic Pole," Astron. & Astrophys. Suppl., 124, 259

4. Probing the Epoch of Reionization Using the 21-cm Forest

Principal Authors: C. Carilli, B. Ciardi, S. Furlanetto

This Design Reference Mission component is motivated primarily by the Key Science Project "Probing the Dark Ages" (Carilli et al., 2004) and has the specific goal of probing the neutral intergalactic medium (IGM) during the Epoch of Reionization (EoR) via absorption of the (redshifted) 21-cm line.

This chapter is part of the Design Reference Mission because it provides requirements on the frequency range, spectral resolution, sky coverage, and sensitivity.

4.1. Motivation

The EoR sets a fundamental benchmark in cosmic structure formation, corresponding to the formation of the first luminous objects that act to ionize the neutral IGM. Observations at near-IR wavelengths of absorption by the IGM in the spectra of the highest redshift quasars (Becker et al., 2001; Djorgovski et al., 2001; Fan et al., 2006) and at radio wavelengths of the electron scattering optical depth for the cosmic microwave background (CMB, Spergel et al. 2007; Hinshaw et al., 2009; Komatsu et al. 2009) imply that we are finally probing into this key epoch of galaxy formation at $z > 6$. The application of radio technologies to probing the EoR forms the basis for several chapters in the SKA Science Case (Carilli & Rawlings, 2004).

Theoretical modeling based on the above existing observational constraints, gives the impression conveyed in Figure 2-1 of an IGM that becomes filled with growing ionized bubbles on a range of size scales. With the passage of time, the bubbles finally punch through the walls separating each other, to leave behind a fully ionized IGM, which remains ionized to the present. The SKA, and its pathfinder telescopes, will provide critical insight into the EoR in a number of ways. One of those methods is via the "21-cm forest": Analogous to the Lyman-α forest, radio sources that form prior to the full reionization of the Universe should show absorption features in their spectrum due to the hyperfine transition (21-cm) of hydrogen (Carilli et al. 2002; Furlanetto & Loeb 2002; Inoue et al. 2007; Xu et al. 2009; Toma et al. 2010). Although this method depends upon the presence of such background sources, as the Lyman-α forest observations have shown, considerable information can be extracted from such absorption spectra.

4.2. Observational Summary

The exact observational strategy will depend, in part, upon what is known about the radio luminosity function of sources at times prior to reionization. Here it assumed that targeted observations of sources known to be a high redshift will be performed. A blind survey would have similar requirements, but would probably require a higher survey speed than specified in §3.4.3 in order to be profitable.

4.3. Scientific Requirements

Table 4-1 summarizes the scientific requirements. Motivation for and discussion of each scientific requirement follows.

Table 4-1. 21-cm Forest Observation Scientific Requirements

Parameter	Value
Redshift	6-20
Optical depth	0.001
Velocity resolution	0.2 km s^{-1}
Sky coverage	> 2π sr

4.3.1. Redshift

SCI-S-REQ-0210: The SKA Phase 1 shall be able to access the H I line over at least the redshift range of 6 to 20.

The redshift range accessible determines the cosmic epoch over which the Epoch of Reionization can be probed. The lower limit of 6 is set by the existing observations of QSOs while the upper limit of 20 is set by the objective of probing deeply into the Epoch of Reionization (Carilli et al., 2002). H I absorption observations at lower redshifts would also be useful; these are discussed in Chapter 3. The upper redshift limit is highly uncertain, because the radio luminosity function of high redshift objects is poorly determined, but radio-loud objects at redshifts of 30 have been discussed in the literature (Inoue et al. 2007). To date, objects with redshifts $z \approx 6.5$ have been detected at SKA frequencies.

4.3.2. Optical Depth

SCI-S-REQ-0220: The SKA Phase 1 shall be able to detect H I absorption at optical depths of 0.001 or lower.

Estimates in the literature of the optical depth in the 21-cm forest vary, depending upon what is assumed about the state of the gas, the overdensity responsible for the absorption, and the redshift (Carilli et al. 2002; Furlanetto & Loeb 2002; Inoue et al. 2007; Xu et al. 2009). The specified optical depth is at or near the lower limit predicted by various authors and should allow a range of conditions to be probed.

4.3.3. Velocity Resolution

SCI-S-REQ-0230: The SKA Phase 1 shall be able to provide a velocity resolution of 0.2 km s^{-1} or better.

H I absorption observations favor cool gas. The deepest absorption features could potentially result from gas having a velocity width of less than a few kilometers per second (Furlanetto & Loeb 2002).

4.3.4. Sky Coverage

SCI-S-REQ-0235: The SKA Phase 1 shall be able to provide access as large a fraction of the sky as feasible, notionally at least 2π steradians.

To date, no radio-loud objects are known within the redshift range over which 21 cm absorption experiments would be relevant. However, these are likely to be rare objects, implying that a large fraction of the sky must be accessible in order to have a reasonable likelihood of being able to observe one. Further, one possible source for such conducting such measurements is the radio afterglow from a gamma-ray burst (GRB). Should such a GRB radio afterglow be detected, it could be at essentially any location on the sky, given the essentially random sky distribution for GRBs.

4.4. Technical Requirements

Table 4-2 summarizes the technical requirements derived from the scientific requirements. Discussion of each technical requirement follows.

Table 4-2. 21-cm Forest Observation Technical Requirements

Parameter	Value	Requirement
Frequency range	70–200 MHz	Redshift coverage
Frequency resolution	0.1 kHz	Velocity resolution at 150 MHz, commensurate with velocity resolution at other frequencies
Sensitivity	1300 m^2 K^{-1}	fiducial value; H I optical depth

4.4.1. Frequency range

SCI-T-REQ-0210: The SKA Phase 1 shall provide a frequency range of at least 70 to 200 MHz.

This requirement follows directly from the redshift coverage requirement. The rest frequency of the H I line is 1.4 GHz. The lower frequency end is determined by the requirement to reach a specified redshift [i.e., 1.4 GHz/(1 + z)]. A redshift of 20 corresponds to a lower frequency of 70 MHz.

4.4.2. Frequency Resolution

SCI-T-REQ-0220: The SKA Phase 1 shall provide a frequency resolution commensurate with the velocity resolution, with a fiducial value of 0.1 kHz at an observation frequency of 150 MHz.

The frequency resolution follows directly from the stated velocity resolution requirement. The frequency resolution, at a frequency ν, corresponding to a velocity resolution Δv is given by $\Delta\nu = \nu(\Delta v/c)$, where c is the speed of light. At a nominal frequency of 150 MHz, the required frequency resolution is 0.1 kHz; a frequency of 150 MHz corresponds to a redshift 8.5.

4.4.3. Sensitivity

SCI-T-REQ-0230 The SKA Phase 1 shall have a sensitivity of at least 1300 m^2 K^{-1}.

No radio sources are known currently that are at a redshift greater than 6.5. Typical flux densities assumed in theoretical treatments are 20 mJy, based on shifting a source such as Cygnus A to these redshifts.

4.5. Data Products

For any identified radio-loud source with a redshift $z > 6$, nominally stronger than about 20 mJy at 150 MHz, a postage stamp total intensity image cube, over the frequency range 70–200 MHz (goal: 50–200 MHz), of nominal dimensions 75" × 75", with a spectral resolution of 0.2 km s^{-1} and an angular resolution of 15".

Bibliography

Becker R. H., et al., 2001, "Evidence for Reionization at z~6: Detection of a Gunn-Peterson Trough in a z = 6.28 Quasar," AJ, 122, 2850

Carilli, C. L., Furlanetto, S., Briggs, F., Jarvis, M., Rawlings, S., & Falcke, H. 2004, "Probing the Dark Ages with the Square Kilometer Array," in Science with the Square Kilometre Array, eds.C. L. Carilli & S. Rawlings (Elsevier: Amsterdam) p. 1029

Carilli, C. L., & Rawlings, S. 2004, *Science with the Square Kilometer Array*, New Astron. Rev. (Elsevier: Amsterdam)

Carilli, C., Gnedin, N., & Owen, F. 2002, "H I 21 Centimeter Absorption beyond the Epoch of Reionization," Astrophys. J., 577, 22

Djorgovski S. G., Castro S., Stern D., & Mahabal A. A. 2001, "On the Threshold of the Reionization Epoch," Astrophys. J., 560, L5

Fan, X., Strauss, M. A., Becker, R. H., et al., 2006, "Constraining the Evolution of the Ionizing Background and the Epoch of Reionization with z ~ 6 Quasars. II. A Sample of 19 Quasars," AJ, 132, 117

Furlanetto S. R., Sokasian A., & Hernquist L. 2004, "Observing the Reionization Epoch Through 21-centimetre Radiation," MNRAS, 347, 187

Furlanetto, S. R., & Loeb, A. 2002, "The 21 Centimeter Forest: Radio Absorption Spectra as Probes of Minihalos before Reionization," Astrophys. J., 579, 1

Hales, S. E. G., Riley, J. M., Waldram, E. M., Warner, P. J., & Baldwin, J. E. 2007, "A final non-redundant catalogue for the 7C 151-MHz survey," MNRAS, 382, 1639

Inoue, S., Omukai, K., & Ciardi, B. 2007, "The radio to infrared emission of very high redshift gamma-ray bursts: probing early star formation through molecular and atomic absorption lines," MNRAS, 380, 1715

Komatsu, E., Dunkley, J., Nolta, et al. 2009, "Five-Year Wilkinson Microwave Anisotropy Probe (WMAP) Observations: Cosmological Interpretation," Astrophys. J. Supp., 180, 330

Hinshaw, G., Weiland, J. L., Hill, R. S., et al. 2009, "Five-Year Wilkinson Microwave Anisotropy Probe Observations: Data Processing, Sky Maps, and Basic Results," Astrophys. J. Supp., 180, 225

Perley, R. A. 1989, in *Synthesis Imaging in Radio Astronomy*, eds. R. A. Perley, F. R. Schwab, & A. H. Bridle (ASP: San Francisco) p. 287

Spergel D. N., et al. 2007, "Three-Year Wilkinson Microwave Anisotropy Probe (WMAP) Observations: Implications for Cosmology," Astrophys. J. Supp., 170, 377

Toma, K., Sakamoto, T., & Meszaros, P. 2010, "Population III GRB Afterglows: Constraints on Stellar Masses and External Medium Densities," Astrophys. J., in press; arXiv:1008.1269

Xu, Y., Chen, X., Fan, Z., Trac, H., & Cen, R. 2009, "The 21 cm Forest as a Probe of the Reionization and The Temperature of the Intergalactic Medium," Astrophys. J., 704, 1396

5. Pulsar Surveys with Phase 1 of the SKA

Principal Authors: R. Smits, B. Stappers, J. Cordes, M. Kramer, S. Ransom, I. Stairs

This Design Reference Mission component is motivated by the Key Science Project "Strong-field Tests of Gravity Using Pulsars and Black Holes," (Cordes et al. 2004; Kramer et al. 2004) to probe fundamental physics including tests of theories of gravity using ultra-relativistic binaries and studying gravitational waves with a pulsar timing array (PTA). Secondary motivations include using pulsars to constrain fundamental nuclear physics. This Key Science Project has two goals: (1) Increase by an order of magnitude the number of known radio pulsars, with the goal of detecting every radio pulsar in the Galaxy that is beamed toward us; and (2) Conduct precision timing observations of a subset of these in order to extract constraints on fundamental physical theories. The SKA Phase 1 will not have the sensitivity to detect every pulsar in the Galaxy that is beamed toward us, but it will be able to make a substantial contribution to the Galactic pulsar census. In contrast to other components of the Design Reference Mission that focus on a specific scientific issue, this chapter will focus on the first goal, that of improving the Galactic pulsar census. A companion chapter (Chapter 6) focuses on the timing goal. The motivation for this slightly different approach is that, while there are different scientific motivations for conducting timing programs, they often result in similar technical requirements, and the surveys required to find the pulsars of interest also have similar technical requirements. Cordes (2007) and Smits et al. (2009) also have addressed much of this material.

This chapter is part of the Design Reference Mission because it provides requirements on the array configuration, frequency range, sensitivity, sky coverage, and non-imaging processing.

5.1. Motivation

Neutron stars have magnetic field strengths exceeding 10^{14} G, rotation rates approaching 1000 Hz, central densities exceeding 10^{14} g cm^{-3}, and normalized gravitational strengths of order 0.4. With their large moments of inertia, when detected as radio pulsars, their pulses provide a highly regular clock. Long-term, high-precision timing programs, in which the arrival times of pulses are monitored, can produce constraints on theories of gravity, the existence of gravitational waves, and fundamental nuclear physics.

As examples of the constraints that can be provided, one member of a double neutron star system is detected as PSR B1913+16. Precise measurements of its pulse arrival times over an interval of decades revealed that this system is losing energy at a rate that is consistent with the emission of quadrupolar gravitational waves as predicted by General Relativity (GR, Taylor & Weisberg 1989). The discovery and subsequent timing of this pulsar resulted in the 1993 Nobel Prize in Physics. More recently, the double pulsar PSR J0737−3039A/B was discovered in an extension of a large Galactic plane survey and is proving to be a spectacular gravitational and plasma physics laboratory (Kramer et al. 2006; Kramer & Stairs 2008). Another exotic pulsar system that demonstrates the potential of pulsars for testing fundamental physics is the pulsar J1744−2446ad, in the globular cluster Terzan 5, which has a pulse period of 1.4 ms (implied rotation rate of 716 Hz, Hessels et al. 2006). In order for it to maintain its structural integrity, the nuclear equation of state must be such that it can withstand the centrifugal force on its equator.

Finally, while compelling and consistent with GR, the behavior of PSR B1913+16 is only an indirect detection of gravitational waves. A laboratory demonstration of gravitational waves, akin to Hertz's demonstration of electromagnetic waves, is not possible due to the large masses and high velocities required. Rather, gravitational waves will be found in an astronomical context, such as the change in the time of periastron of PSR B1913+16. The SKA objective is the *direct* detection and exploitation of gravitational waves for a non-photonic probe of the Universe. The SKA will construct a *Pulsar Timing Array* (PTA) gravitational wave observatory in which each "arm" is the path to a millisecond pulsar (MSP). Changes in the spacetime metric between an MSP and the Earth are reflected as changes in the time of arrival for that pulsar. The SKA PTA will be sensitive to gravitational waves with frequencies $f \sim$

10 nHz. Thus, the SKA PTA will complement both terrestrial and space-borne observatories: the Laser Interferometer Gravitational wave Observatory (LIGO) is most sensitive to gravitational waves of frequencies $f \sim 100$ Hz and the Laser Interferometer Space Array (LISA) is most sensitive to $f \sim 1$ mHz.

A significant constraint on the utility of radio pulsars is the scarcity of "useful" pulsars. Until recently, the most significant constraints on the nuclear equation of state derived from radio pulsars resulted from the first millisecond pulsar, PSR B1937+21, discovered in the *early 1980s*. Similarly, many of the tests of theories of gravity and for gravitational wave emission rely on one or a few objects, but detection of gravitational waves may require as many as several tens of millisecond pulsars (Shannon & Cordes 2010). Recent surveys have begun to demonstrate the potential for vastly increasing the number of radio pulsars and thereby increasing the number of "significant" systems. Finally, even if no pulsars are found to provide higher individual timing precision, the overall sensitivity of the PTA does depend upon the number of pulsars in the "array."

The wide range of physical theories and models that can be tested with neutron stars, and particularly radio pulsars, motivate pulsar searches and timing as a key science driver. Significant selection effects have been present in previous pulsar programs, selection effects that an increase in sensitivity will mitigate. With the SKA Phase 1, shorter integration times will likely be possible, which will reduce the effects of orbital modulations of pulsars in tight binaries and potentially the interstellar propagation effects for all pulsars. Continuing improvements in computational power have begun to mitigate orbital effects, but full acceleration searches remain computationally daunting.

5.2. Survey Summary

In general, pulsars become brighter towards lower frequencies. However, scattering due to the interstellar medium and the increase of the sky temperature towards lower frequencies lead to an optimal survey frequency that is dependent on the location on the sky. In the Galactic plane, where scattering is severe, the optimal survey frequency is between 1 and 3 GHz (Smits et al. 2009), whereas at higher Galactic latitudes, lower survey frequencies are acceptable.

The SKA Phase 1 pulsar survey will cover the entire sky, as pulsars useful for different science programs tend to be found in different portions of the sky. However, the essential observation remains the same regardless of the pointing direction. Within the field of view (FoV), the data are acquired with both high frequency and time resolution, compensation is made for various propagation and orbital effects that have the effect of smearing the pulsar signal, and a periodic signal is sought by summing one or more harmonically related powers from a power spectrum. The high time and frequency resolution is required both because of the duration of the typical pulsar signal as well as by the fact that pulsar signals are dispersed by their passage through the Galactic interstellar medium, and the high frequency and time resolution allows for "de-dispersion" before searching for a periodic signal, which is essential to detect fast rotating pulsars that are otherwise completely smeared out. Finally, there are strong motivations for the survey program to cover the same region of the sky multiple times. These include mitigation of scintillation (from the standpoint of finding and timing pulsars) and the detection of radio transients.

Conceptually, the survey and timing aspects of this Key Science Project are distinct, although depending upon the FoV and the pointing direction, it may be possible to conduct some timing and search observations simultaneously. A notional survey strategy could involve a rank-ordered list of pulsars to be timed combined with a search. The rank ordering will depend upon parameters such as the sensitivity required for each pulsar and the cadence. As pulsars to be timed approach transit, the array would slew to time them, then return to the search. Moreover, the balance between search and timing observations may evolve during the course of the SKA's lifetime, with an initial emphasis on finding new pulsars gradually being replaced by timing observations as essentially the entire Galactic pulsar population is discovered.

5.3. Scientific Requirements

Table 5-1 summarizes the scientific requirements. Motivation for and discussion of each scientific requirement follows.

Table 5-1. Pulsar Survey Scientific Requirements

Parameter	Value
Pulsar luminosity	0.1 mJy kpc^2 at 1400 MHz
Pulsar period	0.5 ms–10 s
Dispersion measure	At least 1000 pc cm^{-3}
Sky coverage	Entire sky visible from its latitude on Earth, above notional elevation limit of 10 deg (TBC)
Pulsar orbits	Orbital periods at least as short as 30 minutes

5.3.1. Pulsar Luminosity

SCI-S-REQ-0310: The SKA Phase 1 shall be capable of detecting pulsars beamed in the direction of Earth with (pseudo)-luminosities as low as 0.1 mJy kpc^2 at 1400 MHz within 10 kpc.

A pulsar's (pseudo-)luminosity is given by SD^2, for a pulse-averaged flux density S and distance D, with units of mJy kpc^2 (equivalent to W Hz^{-1}). The details of a particular pulsar's luminosity and whether it can be detected may depend upon factors such as its pulse profile, period, duty cycle, age, orientation with respect to the Earth, position in the Galaxy (vis-a-vis the strength of interstellar scattering), and the presence of a companion(s). However, the quantity SD^2 provides a useful measure by which to compare pulsars at different distances and flux densities.

The stated requirement (0.1 mJy kpc^2) is sufficient to detect more than 99.9% of the currently known pulsar population, including objects such as the double pulsar J0737−3039A/B ($SD^2 \approx 0.18$ mJy kpc^2), and the simulations by Smits et al. (2009) suggest that approximately 50% of the Galactic pulsar population could be recovered.

5.3.2. Pulsar Period

SCI-S-REQ-0320: The SKA Phase 1 shall be capable of detecting pulsars with periods at least in the range 0.5 ms to 10 s, for a nominal duty cycle of 5%, for at least a subset of the specified range in dispersion measure (DM).

The range of periods in the known pulsar population ranges from as short as 1.4 ms to almost 10 s. Short-period pulsars are useful for testing equations of state of nuclear matter (§5.1) while it is possible that a pulsar-black hole binary will involve a relatively slow-period pulsar (of order 1 s or longer). A number of authors have summarized the details involved in finding short-period pulsars (e.g., Keith et al. 2010). Briefly, as the DM of a short-period pulsar increases, it must have a larger flux density to be detected, due primarily to dispersion smearing.

5.3.3. Dispersion Measure

SCI-S-REQ-0330: The SKA Phase 1 shall be capable of detecting pulsars with dispersion measures (DM) of at least 1500 pc cm^{-3}, for at least a fraction of the pulsars in the specified range in pulse period.

The range of DMs in the known pulsar population ranges from only a few to nearly 1500 pc cm^{-3}. Pulsars with large DM values will likely be those at large distances in the Galactic plane, such as additional ultra-relativistic binaries, though pulsars behind nearby H II regions may also have large values of DM. Various authors have summarized the details involved in finding high-DM pulsars (e.g., Keith et al.

2010). Briefly, pulsars with larger values of DM require higher effective frequency resolution to mitigate dispersion smearing, and it is likely that only the most luminous pulsars will be detected at high DM.

5.3.4. Sky Coverage

SCI-S-REQ-0340: The SKA Phase 1 shall provide access to the entire sky visible from its latitude on the Earth, above a notional elevation limit of 10 deg (TBC).

There are multiple radio pulsar populations, including a young population with a strong concentration toward the Galactic plane and an older population that has had time to thermalize in the Galactic disk and migrate to large distances above the Galactic plane, implying high Galactic latitudes. Coverage of the entire sky accessible to the SKA Phase 1 is required, in order to survey these populations, including the maximal Galactic longitude coverage, though, this will be dictated largely by the choice of site, and both candidate sites are comparable.

A nominal Galactic plane survey, most likely to find pulsars in ultra-relativistic binaries such as PSR J0737−3039A/B, consists of the Galactic plane itself (e.g., $|b| < 3°$) and likely a flanking mid-latitude survey. Initially, the Galactic plane survey will take place at a frequency near 1.4 GHz. A possible follow-up survey could be performed at a higher frequency of about 2 GHz, depending on the outcome of the first survey.

From the perspective of the PTA, having MSPs distributed over a substantial fraction of the sky improves the ability to detect and study gravitational waves (Jenet et al. 2005), and work is in progress to quantify this further. Further, a number of the pulsars already being timed at existing facilities have Galactic latitudes above the nominal Galactic latitude value for an optimal search. Cordes & Chernoff (1997) discuss optimal search strategies, emphasizing the distinction between *search volume* and *detection volume*. At high Galactic latitudes, large search volumes can be obtained because scattering effects are generally small and the system sensitivity is less affected by the Galactic nonthermal emission. However, the detection volume is maximized at intermediate Galactic latitudes ($|b| \approx 20°$) because of the (assumed) MSP population distribution.

The elevation limit is specified as being consistent with current practice from existing instruments.

5.3.5. Pulsar Orbits

SCI-S-REQ-0350: The SKA Phase 1 shall provide the capability to search for pulsars in binary systems with orbital periods as short as 30 minutes.

The formation of millisecond pulsars is widely agreed to proceed through a process of mass transfer in a binary system, and many "recycled" and millisecond pulsars are known to have companions. Notably these systems include PSR B1913+16, PSR J0737−3039A/B, and PSR J1719−1438.

5.4. Technical Requirements

Table 5-2 summarizes the technical requirements. Discussion of each requirement follows.

Table 5-2 Pulsar Survey Technical Requirements

Parameter	Requirement	Comment
$A_{\rm eff}/T_{\rm sys}$	500 m^2 K^{-1}	Pulsar luminosity, period, DM
Frequency range	0.3–3 GHz	Pulsar spectra, period, DM
Frequency resolution	< 10 kHz	DM
Temporal resolution	50 μs	Pulsar duty cycle, period, DM
Array filling factor	"high"	Pulsar luminosity, processing; see text
Array data product	voltage time series over entire FoV	Processing, pulsar period, DM

5.4.1. A_{eff}/T_{sys}

SCI-T-REQ-0310: The SKA Phase 1 shall provide an instantaneous sensitivity of at least 500 m^2 K^{-1}.

Cordes et al. (2004) illustrate the performance of the SKA (and implicitly the SKA Phase 1) relative to existing facilities (Arecibo, the GBT, and Parkes). The A_{eff}/T_{sys} of the array defines an effective distance to which a pulsar of a given pseudo-luminosity and period can be detected. The specified requirement allows one to probe approximately a factor of 1.5, and 3 times farther into the Galaxy than the GBT or Parkes, respectively, for MSPs at the low-end of the pulsar luminosity function. The actual number of MSPs to be detected will depend, in part, upon the distribution of MSPs within the Galaxy. Figure 5-1 illustrates the likely performance of the SKA Phase 1 with respect to pulsar searching, and specifically for finding *ultra-relativistic binaries*, assuming that the fraction of such objects in the Galaxy is 5×10^{-4} (= 1/2000, which is the approximate fraction of currently known ultra-relativistic binaries).

Particularly for ultra-relativistic binaries whose orbital periods may be of the order of 1 hr or shorter, it is required that the integration time for the survey observations be only a fraction of the binary period. As the integration time approaches or exceeds the binary period, orbital terms have to be included in the searching, which makes the searching parameter space both of much higher dimensionality and much more computationally expensive. Consequently, pulsar searching represents a scientific program for which it is *not* possible to reduce A_{eff}/T_{sys} and compensate with longer integration times.

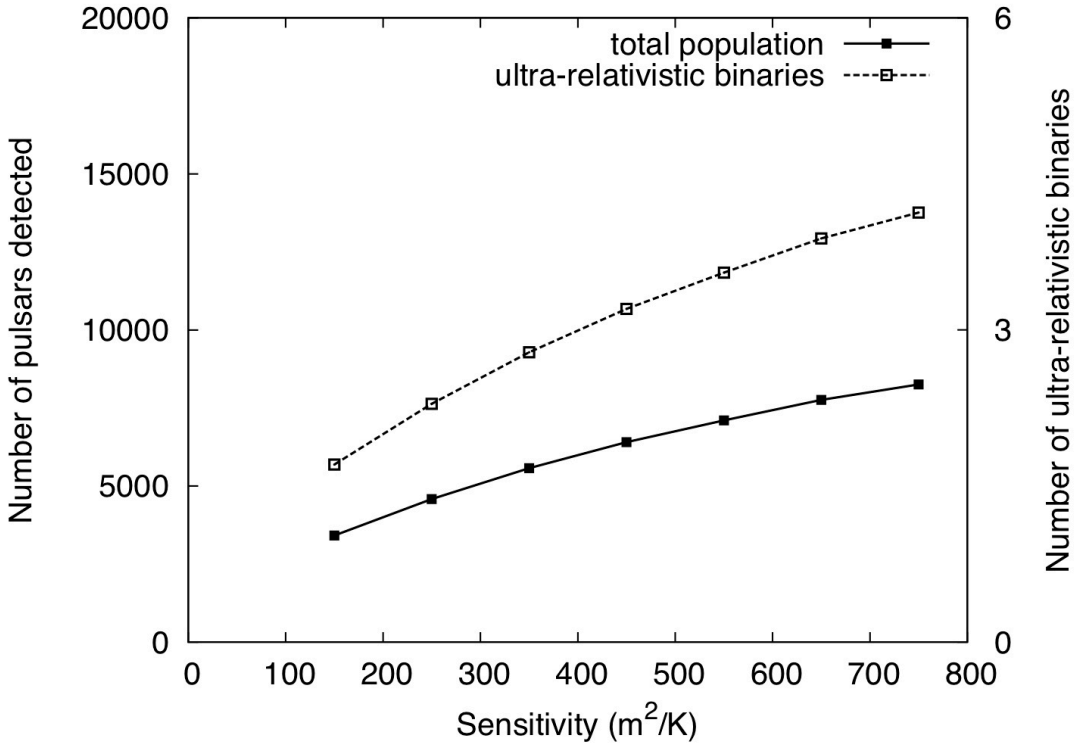

Figure 5-1. Estimated number of pulsars detected as a function of available sensitivity. *Left* axis shows the total number of Galactic pulsars (solid red curve). *Right* axis shows the number of *ultra-relativistic binaries* assuming that the fraction of such systems is 5×10^{-4} (1/2000) of the total population (dotted green curve). Adapted from Smits et al. (2009).

5.4.2. Frequency Range

SCI-T-REQ-0320: The SKA Phase 1 shall have a frequency range of at least 0.3–3 GHz.

The specified frequency range reflects a balance between pulsar spectra and the effects of interstellar propagation. Pulsars tend to have steep spectra with a characteristic frequency dependence $\nu^{-1.6}$, though often with a low frequency turnover occurring at a few hundred MHz (e.g., Malofeev et al. 1994; Lorimer et al. 1995; Maron et al. 2000).

However, interstellar propagation effects have strong frequency dependences, becoming stronger at lower frequencies; dispersion smearing scales as ν^{-2} while scattering effects tend to scale as ν^{x}, with $x \approx -4$. The range of frequencies specified is in accord with traditional pulsar searches (e.g., Hulse & Taylor 1974; Manchester et al. 1978; Manchester, D'Amico, & Tuohy 1985; Dewey et al. 1985; Stokes et al. 1986; D'Amico et al. 1988; Biggs & Lyne 1992; Johnston et al. 1992; Thorsett et al. 1993; Foster et al. 1995; Manchester et al. 1996; Manchester et al. 2001). The higher end of the range is likely to be needed for searches closer to the Galactic plane while the lower end of the range will suffice for the highest Galactic latitudes (Cordes & Chernoff 1997).

5.4.3. Frequency Resolution

SCI-T-REQ-0330: The SKA Phase 1 shall have an attainable frequency resolution of at least as narrow as 10 kHz.

Pulsar signals undergo frequency-dependent dispersion by the interstellar medium. This causes the pulsar intensity profiles to be broadened significantly, making them harder to detect. Given the value for the dispersion measure (DM), the observed signal can be de-dispersed. In a survey, the original observed signal needs to be de-dispersed many times, each with a different trial DM value. This process requires the data to be split up in frequency channels with a width of no more than 10 kHz.

5.4.4. Time Resolution

SCI-T-REQ-0340: The SKA Phase 1 shall have an attainable time resolution of at least as short as 50 μs.

Finding short-period pulsars is desired because these pulsars often provide the highest timing precision and the most stringent constraints on the nuclear equation of state. If the survey is to be sensitive to pulsars with spin periods as short as 1 ms, and assuming a typical pulse width of 10% of the period, the required time resolution is 50 μs.

5.4.5. Array Filling Factor

SCI-T-REQ-0350: The SKA Phase 1 shall have as compact an array configuration as possible.

There is no specific scientific requirement that drives a requirement on the array configuration. However, the processing requirements for pulsar searching depend upon the filling factor f of the portion of the array used for pulsar searching. The filling factor is typically defined as A/b^2, for an array composed of receptors in which the collecting area of an individual receptor is A and the maximum baseline in the array, or the portion of the array being processed, is b. Lower values of f increase the processing cost, and sufficiently low values of f easily could produce an array for which pulsar searching at an acceptable sensitivity (SYS-T-REQ-0310, §5.4.1) could not be done for an affordable cost. Cordes (2007) provides an illustration in which $f \sim 0.5$ implies a computational processing budget of order 10^{16} operations per second for the SKA2; see also Smits et al. (2009). While the specific computational cost will depend upon the details of the configuration, we take $f \approx 0.3$ as a fiducial benchmark.

5.4.6. Array Data Product

SCI-T-REQ-0360: The SKA Phase 1 shall be capable of searching across the entire field of view of the telescope.

Pulsar searching and timing is an example of a *non-imaging* use of the telescope. As such, the traditional data product of a set of interferometric visibilities may not be sufficient, unless produced at a significantly faster rate than has traditionally been the case. An alternate approach is to form a time series of the electric field as measured at the apertures or receptors. Cordes (2007) provides additional discussion of the kinds of processing to be done, but a summary is that a minimal need is to pixellate the entire field of view to produce a time series for each pixel within the field of view, and then de-disperse each time series. To detect certain classes of pulsars, e.g., those in ultra-relativisitic binaries, additional (more computational demanding) processing such as orbital searches will also be necessary.

5.4.7. Single Pulse Searches

SCI-T-REQ-0370: The SKA Phase 1 shall be capable of searching for both periodic and single dispersed pulses.

The canonical "strong magnetic field" pulsar, with a pulse period of order 1 s, has traditionally been considered to be intrinsically stable emitter with a constant luminosity, an assumption that has been verified in some limited observational cases (e.g., Stinebring & Condon 1990). Although interstellar propagation effects have long been recognized to affect observed pulsar flux densities, as the census of radio-emitting neutron stars has grown, it has become clear that there are potentially valuable objects that do not have constant luminosities (e.g., XTE J1810−197, Camilo et al. 2006; PSR B1931+24, Rea et al. 2008). Consequently, it is increasingly *de rigueur* for pulsar searches to incorporate into their pipelines procedures for searching for both periodic and single dispersed pulses. In particular, once de-dispersed time series have been produced, searching for single pulses is computationally less demanding than searching for a periodic pulse train.

5.5. Data Products

For a candidate periodic dispersed signal, the data products are sky position, pulse-average total intensity flux density, period, DM, and, if a binary orbit is found, a preliminary indication of the orbital parameters, as well as with the de-dispersed time series for each candidate.

For a candidate non-periodic dispersed signal, the data products are sky position and DM.

Bibliography

Biggs, J. D., & Lyne, A. G. 1992, "The Jodrell bank 'C' pulsar survey - A survey of the northern Galactic plane for rapidly rotating pulsars," Mon. Not. R. Astron. Soc., 254, 257

Camilo, F., Ransom, S. M., Halpern, J. P., Reynolds, J. Helfand, D. J., Zimmerman, N., & Sarkissian, J. 2006, "Transient pulsed radio emission from a magnetar," Nature, 442, 892

Cordes, J. M. 2007, SKA Memorandum #97

Cordes, J. M., Kramer, M., Lazio, T. J. W., Stappers, B. W., Backer, D. C., & Johnston, S. 2004, "Pulsars as Tools for Fundamental Physics & Astrophysics," New Astron. Rev., 48, 1413

Cordes, J. M., & Chernoff, D. F. 1997, "Neutron Star Population Dynamics. I. Millisecond Pulsars," Astrophys. J., 482, 971

D'Amico, N., Manchester, R. N., Durdin, J. M., Stokes, G. H., Stinebring, D. R., Taylor, J. H., & Brissenden, R. J. V. 1988, "A survey for millisecond pulsars at Molonglo," Mon. Not. R. Astron. Soc., 234, 437

Dewey, R. J., Taylor, J. H., Weisberg, J. M., & Stokes, G. H. 1985, "A search for low-luminosity pulsars," Astrophys. J., 294, L25

Foster, R. S., Cadwell, B. J., Wolszczan, A., & Anderson, S. B. 1995, "A High Galactic Latitude Pulsar Survey of the Arecibo Sky," Astrophys. J., 454, 826

Hessels, J. W. T., Ransom, S. M., Stairs, I. H., Freire, P. C. C., Kaspi, V. M., & Camilo, F. 2006, "A Radio Pulsar Spinning at 716 Hz," Science, 311, 1901

Hulse, R. A., & Taylor, J. H. 1974, "A High-Sensitivity Pulsar Survey," Astrophys. J., 191, L59

Jenet, F. A., Hobbs, G. B., Lee, K. J., & Manchester, R. N. 2005, "Detecting the Stochastic Gravitational Wave Background Using Pulsar Timing," Astrophys. J., 625, L123

Johnston, S., Lyne, A. G., Manchester, R. N., Kniffen, D. A., D'Amico, N., Lim, J., & Ashworth, M. 1992, "A high-frequency survey of the southern Galactic plane for pulsars," Mon. Not. R. Astron. Soc., 255, 401

Keith, M. J., Jameson, A., van Straten, W., et al. 2010, "The High Time Resolution Universe Pulsar Survey - I. System configuration and initial discoveries," Mon. Not. R. Astron. Soc., 409, 619

Kramer, M., & Stairs, I. H. 2008, "The Double Pulsar," Ann. Rev. Astron. Astrophys., 46, 541

Kramer, M., Stairs, I. H., Manchester, R. N., et al. 2006, "Tests of General Relativity from Timing the Double Pulsar," Science, 314, 97

Kramer, M., Backer, D. C., Cordes, J. M., Lazio, T. J. W., Stappers, B. W., & Johnston, S. 2004, "Strong-field Tests of Gravity Using Pulsars and Black Holes," New Astron. Rev., 48, 993

Lorimer, D. R., Yates, J. A., Lyne, A. G., & Gould, D. M. 1995, "Multifrequency flux density measurements of 280 pulsars," Mon. Not. R. Astron. Soc., 273, 411

Malofeev, V. M., Gil, J. A., Jessner, A., Malov, I. F., Seiradakis, J. H., Sieber, W., & Wielebinski, R. 1994, "Spectra of 45 pulsars," Astron. & Astrophys. 285, 201

Manchester, R. N., Lyne, A. G., Camilo, F., et al. 2001, "The Parkes multi-beam pulsar survey - I. Observing and data analysis systems, discovery and timing of 100 pulsars," Mon. Not. R. Astron. Soc., 328, 17

Manchester, R. N., Lyne, A. G., D'Amico, N., Bailes, M., Johnston, S., Lorimer, D. R., Harrison, P. A., Nicastro, L., & Bell, J. F. 1996, "The Parkes Southern Pulsar Survey. I. Observing and data analysis systems and initial results," Mon. Not. R. Astron. Soc., 279, 1235

Manchester, R. N., Damico, N., & Tuohy, I. R. 1985, "A search for short-period pulsars," Mon. Not. R. Astron. Soc., 212, 975

Manchester, R. N., Lyne, A. G., Taylor, J. H., Durdin, J. M., Large, M. I., & Little, A. G. 1978, "The second Molonglo pulsar survey - discovery of 155 pulsars," Mon. Not. R. Astron. Soc., 185, 409

Maron, O., Kijak, J., Kramer, M., & Wielebinski, R. 2000, "Pulsar spectra of radio emission," Astron. & Astrophys. Suppl., 147, 195

Rea, N., Kramer, M., Stella, L., Jonker, P. G., Bassa, C. G., Groot, P. J., Israel, G. L., Méndez, M., Possenti, A., & Lyne, A. 2008, "On the nature of the intermittent pulsar PSR B1931+24," Mon. Not. R. Astron. Soc., 391, 663

Shannon, R. M., & Cordes, J. M. 2010, "Assessing the Role of Spin Noise in the Precision Timing of Millisecond Pulsars," Astrophys. J., in press; arXiv1010.4794

Smits, R., Kramer, M., Stappers, B., Lorimer, D. R., Cordes, J., & Faulkner, A. 2009, "Pulsar Searches and Timing with the Square Kilometre Array," Astron. & Astrophys., 493, 1161

Stinebring, D. R., & Condon, J. J. 1990, "Pulsar flux stability and refractive interstellar scintillation," Astrophys. J., 352, 207

Stokes, G. H., Segelstein, D. J., Taylor, J. H., & Dewey, R. J. 1986, "Results of two surveys for fast pulsars," Astrophys. J., 311, 694

Taylor, J. H., & Weisberg, J. M. 1989, "Further Experimental Tests of Relativistic Gravity using the Binary Pulsar PSR 1913+16," Astrophys. J., 345, 434

Thorsett, S. E., Deich, W. T. S., Kulkarni, S. R., Navarro, J., & Vasisht, G. 1993, "A Search for Pulsars at High Galactic Latitudes," Astrophys. J., 416, 182

6. Pulsar Timing with Phase 1 of the SKA

Principal Authors: R. Smits, J. Cordes, M. Kramer, A. Lommen, S. Ransom, I. Stairs, B. Stappers

This Design Reference Mission component is motivated by the Key Science Project "Strong-field Tests of Gravity Using Pulsars and Black Holes,"(Cordes et al. 2004; Kramer et al. 2004) to probe fundamental physics including tests of theories of gravity using ultra-relativistic binaries and studying gravitational waves with a pulsar timing array (PTA). Secondary motivations include using pulsars to constrain fundamental nuclear physics. This Key Science Project has two goals: (1) Increase by an order of magnitude the number of known radio pulsars, with the goal of detecting every radio pulsar in the Galaxy that is beamed toward us; and (2) Conduct precision timing observations of a subset of these in order to extract constraints on fundamental physical theories. In contrast to other components of the Design Reference Mission that focus on a specific scientific issue, this chapter will focus on the second goal, that of precision timing. Chapter 5 focuses on the survey goal. The motivation for this slightly different approach is that, while there are different scientific motivations for conducting timing programs, they often result in similar technical requirements, and the surveys required to find the pulsars of interest also have similar technical requirements.

This chapter is part of the Design Reference Mission because it provides requirements on the sensitivity and polarization properties.

6.1. Motivation

Neutron stars have magnetic field strengths exceeding 10^{14} G, rotation rates approaching 1000 Hz, central densities exceeding 10^{14} g cm^{-3}, and normalized gravitational strengths of order 0.4. With their large moments of inertia, when detected as radio pulsars, their pulses provide a highly regular clock that can be used to probe their spacetime environment or to constrain the properties of the star itself.

Specific examples of constraints on fundamental physical theories that have already been provided by pulsar timing include

- One member of a double neutron star system is detected as PSR B1913+16. Precise measurements of its pulse arrival times over an interval of decades revealed that this system is losing energy at a rate that is consistent with the emission of quadrupolar gravitational waves as predicted by General Relativity (GR, Taylor & Weisberg 1989). The discovery and subsequent timing of this pulsar resulted in the 1993 Nobel Prize in Physics.
- Both members of the double neutron star system are detected in the double pulsar PSR J0737−3039A/B, and the system is proving to be a spectacular gravitational and plasma physics laboratory (Kramer et al. 2006; Kramer & Stairs 2008).
- The pulsar PSR J1744−2446ad, in the globular cluster Terzan 5, which has a pulse period of 1.4 ms (implied rotation rate of 716 Hz, Hessels et al. 2006). In order for it to maintain its structural integrity, the nuclear equation of state must be such that it can withstand the centrifugal force on its equator.

In addition to improved timing, either of existing systems or of new ultra-relativistic binaries to be found by SKA pulsar surveys (Chapter 5), pulsar timing with the SKA has the opportunity for the direct detection of gravitational waves. A laboratory demonstration of gravitational waves, akin to Hertz's demonstration of electromagnetic waves, is not possible due to the large masses and high velocities required. Rather, gravitational waves will be found in an astronomical context, such as the change in the time of periastron of PSR B1913+16. While compelling and consistent with GR, the behavior of PSR B1913+16 is only an indirect detection of gravitational waves—the SKA objective is the *direct* detection and exploitation of gravitational waves for a non-photonic probe of the Universe.

The SKA *Pulsar Timing Array* (PTA) will construct a gravitational wave observatory in which each "arm" is the path to a millisecond pulsar (MSP). Changes in the spacetime metric between an MSP and the Earth are reflected as changes in the time of arrival for that pulsar. The SKA PTA will be sensitive to gravitational waves with frequencies $f \sim 10$ nHz. Thus, the SKA PTA will complement both terrestrial and space-borne observatories: LIGO's sensitivity is for $f \sim 100$ Hz and LISA's sensitivity is for $f \sim 1$ mHz. In principle, timing observations of a single pulsar could detect gravitational waves. In practice, no pulsar has yet been timed with sufficient accuracy that would enable detection of gravitational waves, hence the "array" nature of the PTA.

The SKA PTA will probe two classes of sources. The first is supermassive black hole binaries, particularly those in the last few years before in-spiral. Mergers are recognized to be an important part of galaxy and cluster growth, leading to the expectation that there should be a large number of supermassive black hole binaries in the observable Universe. The aim of the SKA PTA is detecting the combination of the gravitational wave emission from all of the systems. In addition to complementary frequency ranges, the SKA PTA and LISA also probe complementary redshift ranges. The LISA redshift range is $z > 7$ while the SKA PTA range is $z < 2$. Taken together, LISA and the SKA PTA will probe the evolution of merging activity.

The second SKA PTA source is cosmological, related to strings, topological defects, or similar effects. The current limit arises from a single pulsar, PSR B1855+09, for which $\Omega_{str}h^2 < 4 \times 10^{-9}$ (Lommen & Backer 2001), where Ω_{str} is the energy density of gravitational waves due to cosmic strings in units of the critical density and h is the normalized Hubble constant, $H_0 = 100h$ kms^{-1}Mpc^{-1}. (See also Jenet et al. 2006.) Increasing the number of MSPs timed, and the precision at which they are timed, can improve upon this limit by as much as three orders of magnitude. Further, this probe of the gravitational wave background will complement CMB experiments, which constrain (or will detect) the amplitude of any inflationary signal, $\Omega_{inflat}h^2$.

6.2. Observational Summary

Timing pulsars involves re-observing them on a regular basis to obtain accurate values for the arrival time of their radio pulse. Initially, this can be used to obtain the pulsar period and the rate at which the pulsar spins down. It is therefore required that all pulsars detected in the survey are re-observed, perhaps about once every two weeks for a period of at least 1year. Doing so will "weed out" the less interesting pulsars.

Once timing solutions are obtained, further timing is required to extract gravitational or nuclear physics information from the most "interesting" objects. This involves obtaining arrival times from pulsars in compact binaries and a selection of millisecond pulsars to a high accuracy. This high-precision timing needs to be performed on a regular basis. As a nominal value, timing measurements on a 2-week cadence might be necessary, though the actual value will likely vary depending upon the pulsar.

For the specific case of the PTA, the gravitational wave signal is extracted from the time series of pulse time of arrivals (TOAs) from an ensemble of pulsars. The precision with which the TOAs can be measured, in an rms sense, determines the strength of the gravitational wave signal that can be detected. Estimates of the number of pulsars and the precision to which they must be timed vary, but could be as high as several tends of millisecond pulsars to better than 100 ns timing precision on 40 pulsars (Jenet et al. 2005; Shannon & Cordes 2010; Zarb Admai et al. 2010). Not all pulsars can be timed to the same precision, some pulsars display "timing noise," a spectrally "red" component to the TOA residual time series that may reflect internal structure of the neutron star. Further, interstellar and interplanetary propagation effects can contribute to the rms TOA level (Cordes et al. 2004). As Jenet et al. (2005) discuss in more detail, generally a larger number of pulsars at comparable timing precision improves the significance of the detection while a lower timing precision decreases the effective strain rate amplitude that can be detected. Many of the technical requirements described in the remainder of this section relate to obtaining a timing precision of 100 ns or better.

An important distinction between the timing and survey observations is that the dimensionality of the timing observations is much smaller than that of the survey observations. Consequently, the computational expense is much reduced, and a much larger fraction (potentially as much as 100%) of the array can be used for timing observations.

Conceptually, timing and searching are distinct, although depending upon the field of view of the instrument, it may be possible to conduct some timing and search observations simultaneously. Moreover, the balance between search and timing observations may evolve during the course of the SKA's lifetime, with an initial emphasis on finding new MSPs gradually being replaced by timing observations as essentially the entire Galactic MSP population is discovered.

6.3. Scientific Requirements

Table 6-1 summarizes the scientific requirements. Motivation for and discussion of each scientific requirement follows.

Table 6-1. Pulsar Timing Scientific Requirements

Parameter	Value
Pulsar luminosity	0.1 mJy kpc^2 at 1400 MHz
Sky coverage	$> 2\pi$ sr
Gravitational wave strain	10^{-16}
Time resolution capability	100 ns

6.3.1. Pulsar Luminosity

SCI-S-REQ-0410: The SKA Phase 1 shall be capable of timing pulsars with (pseudo)-luminosities as low as 0.1 mJy kpc^2 at 1400 MHz.

A pulsar's (pseudo-)luminosity is given by SD^2, for a pulse-averaged flux density S and distance D, with units of mJy kpc^2 (equivalent to W Hz^{-1}). The details of a particular pulsar's luminosity and its suitability for timing may depend upon factors such as its pulse profile, period, duty cycle, age, orientation with respect to the Earth, position in the Galaxy (vis-a-vis the strength of interstellar scattering), and the presence of a companion(s). However, the quantity SD^2 provides a useful measure by which to compare pulsars at different distances and flux densities.

The stated requirement (0.1 mJy kpc^2) is sufficient to detect more than 99.9% of the currently known pulsar population, including objects such as the double pulsar J0737−3039A/B ($SD^2 \approx 0.18$ mJy kpc^2).

6.3.2. Sky coverage

SCI-S-REQ-0420: The SKA Phase 1 shall provide access to the entire sky visible from the site with no more than a 10% (TBC) loss in sensitivity in any direction.

From the timing and gravitational wave study perspective, the motivation for a large sky coverage is that having MSPs distributed over a substantial fraction of the sky improves the ability to detect and study gravitational waves (Jenet et al. 2005), and work is in progress to quantify this improvement in gravitational wave detection as a function of sky coverage (e.g., Burt et al. 2011). Further, a number of the pulsars already being timed at existing facilities cover a significant fraction of the sky. The specified requirement is comparable to the extent of current sky coverage of timing programs.

6.3.3. Gravitational Wave Strain

SCI-S-REQ-0430: The SKA Phase 1 shall be able to provide measurements that will enable the detection of gravitational waves with strain amplitudes of 10^{-16}.

The amplitude of a gravitational wave signal commonly is parameterized in terms of an amplitude spectrum, $h_c(f) = Af^{\alpha}$, for a gravitational wave frequency f (Jenet et al. 2006). In turn, for many classes of sources, this spectrum can be related to the cosmological density in gravitational waves. The current focus for pulsar timing experiments is on the *detection* of gravitational waves (Hobbs 2005; Jenet et al. 2005). Limits on a gravitational wave background are $A < 7 \times 10^{-15}$, depending somewhat on the value of α, implying a gravitational wave density $\Omega_{gw}h^2 < 2 \times 10^{-8}$, for $f = 1$ yr^{-1} and a normalized Hubble constant, $H_0 = 100h$ kms^{-1} Mpc^{-1}. Expectations are that, with ongoing efforts (the Parkes Pulsar Timing Array, the European Pulsar Timing Array, the North American Nanohertz Observatory for Gravitational waves, the International Pulsar Timing Array, Hobbs et al. 2010), either a detection will be made or these limits can be improved upon by approximately an order of magnitude. If no detection is obtained, the resulting limits will be approximately one order of magnitude better for A (and two orders of magnitude for $\Omega_{gw}h^2$). The stated requirement is a factor of several better than is expected from current systems. The justification for such an improvement is that, if a detection is made, attention will turn to understanding the physics or astrophysics of the source(s). Doing so will require a higher signal-to-noise ratio than simply a detection. Alternately, if no detection is made, fundamental aspects of our understanding of the generation of gravitational waves from many classes of sources is incorrect. New models will have to be developed, and testing those will require an attendant improvement in signal-to-noise ratio.

6.3.4. Time Sampling Capability

SCI-S-REQ-0440: The SKA Phase 1 shall provide data that enable the measurements of average pulse profiles to a precision of at least 100 ns.

Precision timing requires that the pulse profile be well resolved. Taking a 1 ms pulse period and a 5% duty cycle as nominal values, the typical millisecond pulsar pulse profile has a width of order 50 μs. Current experience is that the required time resolution required is approximately 500 to 1000 ns. This time resolution is achieved currently by processing large fractional bandwidths at baseband. We specify a requirement that the SKA Phase 1 be able to achieve a resolution of 100 ns in order to allow for the possibility that future pulsar discoveries may include shorter period pulsars, smaller duty cycle pulsars, or both.

This time resolution is a *post-calibration* requirement, and there is *not* a simple relation between this requirement and the instantaneous bandwidth.

6.4. Technical Requirements

Table 6-2 summarizes the technical requirements.

Table 6-2. Pulsar Timing Technical Requirements

Parameter	Requirement	Comment
A_{eff}/T_{sys}	> 1000 m^2 K^{-1}	Pulsar luminosity
Array data product	multiple independent voltage time series, notionally at least 20 such data streams	Processing
Frequency range	0.8–3 GHz	Pulsar spectra, timing precision
Frequency agility	switch between observing frequencies within 10 minutes or less	Timing precision
Polarization purity	40 dB	Timing precision, coupled to Array Data Product requirement; see text
Timing stability	connect pulse time of arrivals over at least 10 yr	Longer programs lead to ever higher precision tests; see text

6.4.1. A_{eff}/T_{sys}

SCI-T-REQ-0410: The SKA Phase 1 shall provide an instantaneous sensitivity of at least 1000 m^2 K^{-1}.

The sensitivity of the telescope affects the timing precision attainable, via simple radiometer noise (Cordes et al. 2004). Figure 6-1 illustrates the sensitivity required to obtain a range of timing precisions (σ_{TOA}) as a function of pulsar period and flux density. While the values shown are for typical pulsar values, they may not describe any actual pulsar in the SKA PTA. Nonetheless, for the radiometer noise contribution to the TOA error budget not to exceed 100 ns requires A_{eff}/T_{sys} > 1000 m^2 K^{-1} for all but the strongest and shortest period MSPs.

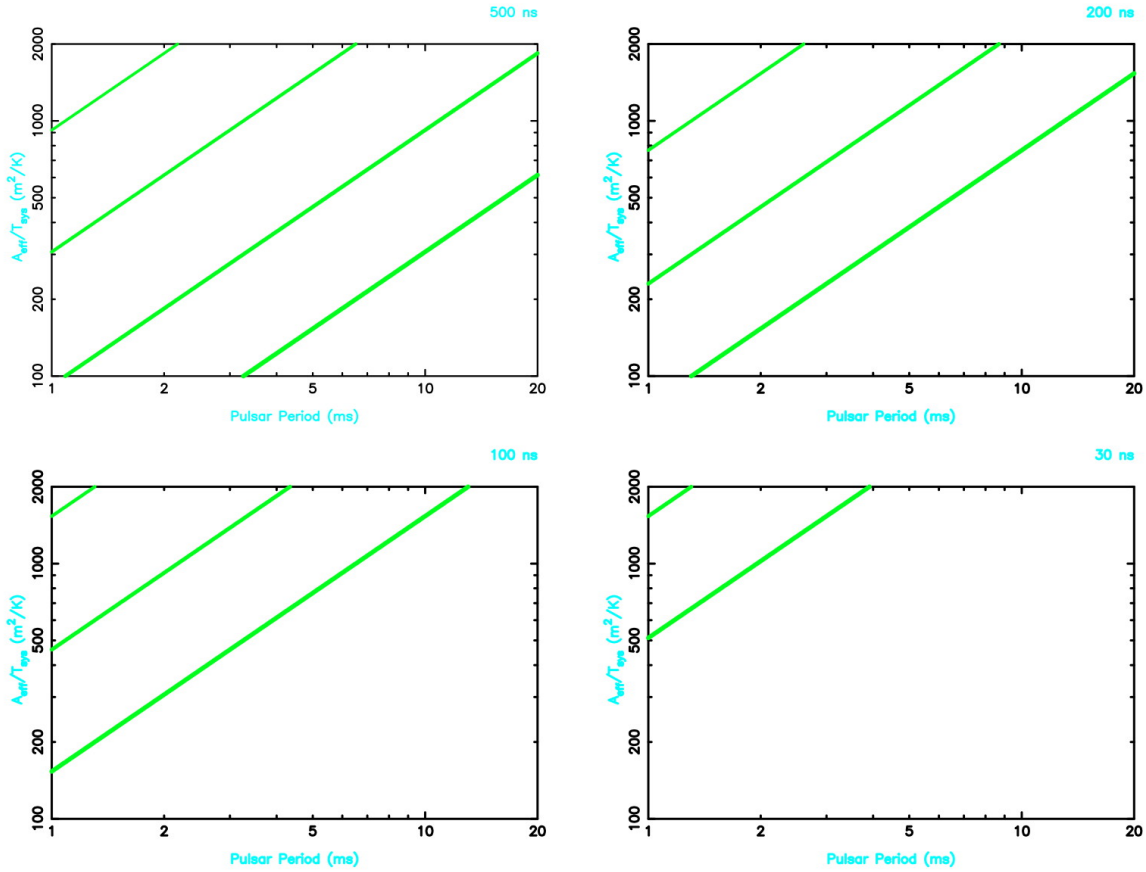

Figure 6-1. Each panel shows the sensitivity required, as a function of pulsar period, to obtain the required rms TOA level (500, 200, 100, and 30 ns). The curves are for flux densities of 30, 10, 3, and 1 mJy (in thickness, from stronger to weaker, or lower right to upper left). The curves also assume that the pulsar duty cycle is 10%, the time to acquire a pulse profile is 1 hr, and the bandwidth is 500 MHz for an observation frequency of 1400 MHz. These curves show the contribution from "white noise" or uncorrelated uncertainties; "red noise" contributions, e.g., from pulsar timing noise will lead to larger rms TOA levels.

Alternately, depending upon the sensitivity required, multiple pulsars may be able to be timed simultaneously by *sub-arraying* the SKA Phase 1, but it is likely that there will be some pulsars that will require the full sensitivity of the array for the highest precision timing.

6.4.2. Array data product

SCI-T-REQ-0420: The SKA Phase 1 shall be capable of delivering the voltage time series from multiple independent directions within the field of view of the telescope, notionally at least 20.

Pulsar timing (and searching) is an example of a *non-imaging* use of the telescope. For timing observations, in contrast to the searching requirement, phased, baseband voltage streams are required from only a relatively small number of independent pixels in the primary beam. For example, if there are 400 pulsars to be timed spread across the sky, the typical separation between pulsars would be of order 7 deg. However, the actual number of independent pixels will likely differ with direction, and, in some directions, e.g., along the Galactic plane or toward a globular cluster, a more typical number might be 10–20. This requirement will depend upon the results of pulsar search programs to be conducted by SKA Precursors and pathfinders.

6.4.3. Frequency range

SCI-T-REQ-0420: The SKA Phase 1 shall have a frequency range of at least 0.8–3 GHz.

The specified frequency range is largely driven by a need to mitigate interstellar (and to a lesser extent interplanetary) propagation effects. There are a variety of propagation effects, ranging from dispersive smearing which scales as ν^{-2} to scattering effects which tend to scale as ν^{x}, with $x \approx -4$. Further, the magnitude of propagation effects is direction dependent.

6.4.4. Frequency agility

SCI-T-REQ-0430: The SKA Phase 1 shall be capable of switching the observational frequency on a time scale of 10 minutes or faster.

Interstellar propagation effects have strong frequency dependences. As You et al. (2007) discuss, a DM variation of order 5×10^{-5} pc cm^{-3} produces a time delay of order 100 ns, comparable to the level of timing precision required. Both the solar wind and the Galactic interstellar medium can produce DM variations, in some cases over the relatively short time scales of order 30 minutes. Simultaneous, or nearly simultaneous, multi-frequency observations, in which the center frequencies of the observations differ by of order the observation frequency, can exploit the frequency dependence of the propagation effects, particularly dispersion smearing, to mitigate or remove them. The optimal set of frequencies is likely to be direction dependent, and even the number of frequencies required is a topic of active investigation. Current results suggest that 3, and perhaps 4, frequencies will be required. Observations with frequencies at 0.8, 1.4, and 3 GHz are examples of suitable observing frequencies.

6.4.5. Polarization purity

SCI-T-REQ-0440: The SKA Phase 1 shall be capable of maintaining a polarization purity between different senses of polarization that is at least 40 dB toward all directions within the field of view over which timing is being conducted.

Pulsars typically generate highly polarized emission. Cordes et al. (2004) discuss how instrumental polarization and errors in gain calibration can affect TOA precision. The polarization contribution to the TOA error budget scales as $\varepsilon\pi_V W$, for a pulse of width W, a circular polarization fraction π_V, and fractional gain calibration errors ε; a similar scaling holds for linear polarization. In order that the polarization contribution to the error budget not be more than 100 ns, for typical pulse widths, $W \sim 1$ ms, and pulsar polarizations, a polarization purity of 40 dB is required. The incorporation of full polarization information into pulsar timing models is an area of on-going work, but current indications are that significant improvements in precision are available and that the highest precisions may require full polarization information (van Straten 2006). This requirement is coupled to the Array Data Product requirement (§6.4.2), as that requirement determines the fraction of the field of view over which the polarization purity must be maintained.

This requirement is a *post-calibration* requirement, rather than a native performance requirement.

6.4.6. Timing stability

SCI-T-REQ-0450: The SKA Phase 1 shall be capable of conducting phase-coherent pulsar timing observations over durations of at least 10 years.

The observation time required per pulsar is often not long—the integration time to acquire a pulse time of arrival is determined by a combination of signal-to-noise ratio and the intrinsic pulse profile stabilization time scale, but is typically less than 1 hr. However, the acquiring a sufficient time series from which to extract signatures of gravitational waves, relativistic effects from orbits, or constraints on other fundamental physical theories typically requires sustaining a pulsar timing program for many years. Over the duration of the timing program, the system must be stable such that pulse times of arrival can be connected. We adopt a nominal duration of 10 years, as this is comparable to or longer many of the on-going pulsar timing programs on existing instruments, though some pulsars have been timed for even longer durations with existing instrumentation.

6.4.7. Cadence

SCI-T-REQ-0460: The SKA Phase 1 shall support an observing cadence of at least one time of arrival every two weeks for any given pulsar that is timed regularly. More rapid, shorter duration, cadences shall also be supported.

The observing cadence is connected directly to the highest frequency gravitational wave that can be detected, by the Nyquist theorem. Current timing programs obtain a cadence of a time of arrival from each pulsar in the timing program at least once every two weeks. Higher cadences (i.e., more frequent measurements) are desired because they both enable the detection of higher frequency gravitational waves and of "burst" sources (e.g., Finn & Lommen 2010). For some timing programs, e.g., tests of theories of gravity, higher cadences need to be supported for short durations.

6.4.8. Sub-Array Capabilities

SCI-T-REQ-470: The SKA Phase 1 shall be capable of timing multiple pulsars simultaneously, separated by distances larger than the nominal field of view, with a minimal number of pulsars being 5.

The precision to which a pulsar can be timed is dependent upon a number of factors, including its intrinsic spin properties, the magnitude of interstellar scattering along its line of sight, and the telescope sensitivity. Currently, high precision timing is being obtained with 100 m class telescopes, suggesting that there may be a subset of pulsars for which the full SKA Phase 1 sensitivity may not be needed. For the overall timing program, a significant factor may be the overall "throughput," i.e., the rate at which pulse times of arrival can be obtained. For those pulsars for which additional sensitivity would not improve the precision, it would be advantageous to acquire times of arrival from multiple pulsars simultaneously. In general, the pulsars to be timed will be widely dispersed on the sky, requiring the capability of the array to be configured in "sub-arrays," subsets of the receptors operating independently.

6.5. Data Products

Folded pulse profiles, at full polarization, and pulse times of arrival, with estimates of the uncertainties on those, in the solar system barycenter for a specified ephermeris, as derived from full polarization observations, for a specified list of timed pulsars, which specifies the cadence and integration time for each pulsar.

Bibliography

Burt, B. J., Lommen, A. N., & Finn, L. S. 2011, "Optimizing Pulsar Timing Arrays to Maximize Gravitational Wave Single Source Detection: a First Cut," Astrophys. J., in press; arXiv:1005.5163

Cordes, J. M., Kramer, M., Lazio, T. J. W., Stappers, B. W., Backer, D. C., & Johnston, S. 2004, "Pulsars as Tools for Fundamental Physics & Astrophysics," New Astron. Rev., 48, 1413

Finn, L. S., & Lommen, A. N. 2010, "Detection, Localization, and Characterization of Gravitational Wave Bursts in a Pulsar Timing Array," Astrophys. J., 718, 1400

Hessels, J. W. T., Ransom, S. M., Stairs, I. H., Freire, P. C. C., Kaspi, V. M., & Camilo, F. 2006, "A Radio Pulsar Spinning at 716 Hz," Science, 311, 1901

Hobbs, G., Archibald, A., Arzoumanian, Z., et al. 2010, "The International Pulsar Timing Array project: using pulsars as a gravitational wave detector," Class. Quant. Grav., 27h, 4013

Hobbs, G. 2005, "Pulsars and Gravitational Wave Detection," Publ. Astron. Soc. Aust., 22, 179

Jenet, F. A., Hobbs, G. B., van Straten, W., et al. 2006, "Upper Bounds on the Low-Frequency Stochastic Gravitational Wave Background from Pulsar Timing Observations: Current Limits and Future Prospects," Astrophys. J., 653, 1571

Jenet, F.A., Hobbs, G. B., Lee, K. J., & Manchester, R. N. 2005, "Detecting the Stochastic Gravitational Wave Background Using Pulsar Timing," Astrophys. J., 625, L123

Kramer, M., & Stairs, I. H. 2008, "The Double Pulsar," Ann. Rev. Astron. & Astrophys., 46, 541

Kramer, M., Stairs, I. H., Manchester, R. N., et al. 2006, "Tests of General Relativity from Timing the Double Pulsar," Science, 314, 97

Kramer, M., Backer, D. C., Cordes, J. M., Lazio, T. J. W., Stappers, B. W., & Johnston, S. 2004, "Strong-field Tests of Gravity Using Pulsars and Black Holes," New Astron. Rev., 48, 993

Lommen, A. N., & Backer, D. C. 2001, "Using Pulsars to Detect Massive Black Hole Binaries via Gravitational Radiation: Sagittarius A* and Nearby Galaxies," Astrophys. J., 562, 297

Shannon, R. M., & Cordes, J. M. 2010, "Assessing the Role of Spin Noise in the Precision Timing of Millisecond Pulsars," Astrophys. J., in press; arXiv1010.4794

Taylor, J. H., & Weisberg, J. M. 1989, "Further Experimental Tests of Relativistic Gravity using the Binary Pulsar PSR 1913+16," Astrophs. J, 345, 434

van Straten, W. 2006, "Radio Astronomical Polarimetry and High-Precision Pulsar Timing," Astrophys. J., 642, 1004

You, X. P., Hobbs, G., Coles, W. A., et al. 2007, "Dispersion Measure Variations and Their Effect on Precision Pulsar Timing," Mon. Not. R. Astron. Soc., 378, 493

Zarb Adami, K., Gauci, A., & Abela, J. 2010, "Gravitational wave detection and cosmic string detection with current radio interferometers," arXiv:1011.1018

7. Pulsar Astrometry with Phase 1 of the SKA

Principal Authors: S. Chatterjee, A. Deller, B. Stappers, M. Kramer, J. Lazio, M. Huynh, A. Lommen, R. Manchester, S. Ransom, G. Theureau

This Design Reference Mission component is motivated by the Key Science Project "Strong-field Tests of Gravity Using Pulsars and Black Holes,"(Cordes et al. 2004; Kramer et al. 2004) to probe fundamental physics including tests of theories of gravity. Other chapters of the Design Reference Mission focus on the finding (Chapter 5) and timing (Chapter 6) of pulsars. This chapter focuses on the goal of obtaining accurate astrometry of pulsars to allow more precise tests of gravity, as well as enabling other astrophysics such as stellar evolution and structure of the Milky Way.

This chapter is part of the Design Reference Mission because it provides requirements on the maximum baseline and image processing.

7.1. Motivation

Neutron stars are one of the most extreme astrophysical objects known. They are formed in a supernova explosion, which marks the end of massive star evolution, and they have mass densities greater than that of atomic nuclei as well as the strongest magnetic fields ever measured. Their violent birth often imparts a "kick" which means that neutron stars have the highest space velocities of any other class of stars. Radio pulsars are rapidly rotating neutron stars that emit beams of radio emission from the magnetic poles. The large moment of inertia of the underlying neutron star means that as these radio beams sweep across the Earth, the received pulses provide a clock-like signal that has an accuracy rivaling the best atomic clocks on Earth. This remarkable property means that pulsars in binary systems can be used to perform some of the most stringent tests of the theories of gravity. These pulses also provide a probe of the interstellar medium via the frequency dependent delay generated by the free electrons along the line of sight.

In all aspects of the astrophysics and physics that can be probed with pulsars, the highest precisions are obtained when model-independent, accurate trigonometric distances and velocities are known. The SKA is an excellent facility for increasing greatly the number of pulsars for which accurate parallaxes and the proper motion are measured.

More accurate tests of theories of gravity with neutron star binaries are possible once we know the distance to the binary pulsar. In order to compare the rate of change of orbital period ($\dot{P}_b$) due to the loss of energy from gravitational radiation with predictions from general relativity (GR), the contributing factors to $\dot{P}_b$ other than GR must be estimated and subtracted. These other factors include the acceleration at the location of the binary system, acceleration at the solar system barycentre, and the apparent acceleration due to the transverse velocity (known as the Shklovskii effect; Shklovskii 1970). For example, VLBI measurements of PSR J0737−3039A/B revised its distance to 1150 pc (Deller et al. 2009), more then twice the distance estimated using the pulsar dispersion measure and models of the ionized component of the Milky Way (Cordes & Lazio 2002). With the new distance and proper motion measure, the Galactic and kinematic contributions to the orbital period derivative, $\dot{P}_b$, were determined to four orders of magnitude below the GR contribution, allowing GR tests to be made to within 0.01% accuracy (Deller et al. 2009). Measuring $\dot{P}_b$ to this level will place constraints on alternative gravitational theories and surpass the best solar system tests (Kramer et al. 2006; Damour 2006).

Pulsar astrometry is also important for a wide variety of other astrophysics. The true space velocity of pulsars provides us with vital insight into the physics of their formation in supernovae. Knowing the distance and the velocity also allows us to determine the birth locations of young pulsars and thus potentially associate them with the supernova remnants in which they were born and again allow us to study the physics of their birth. Accurate distances combined with our knowledge of the total electron content (obtained through the delay of the pulses) along the line of sight allows a better determination of

the structure of the electron distribution in the Milky Way. This has important implications for Galaxy modelling but also for predicting distances to pulsars without measured parallaxes. Accurate distances can be also used to constrain the "size" of the neutron star photosphere, which has important implications for the neutron star equation of state.

7.2. Observational Summary

The measurement of the position of an individual object is relative in nature, and absolute positions are inferred when positions are determined relative to sources that define the International Celestial Reference Frame (ICRF, Ma et al. 1998). Over time, repeated position measurements allow a proper motion to be derived. The main consideration of such astrometric measurements is a long time baseline, limited by the stability of the reference frame and the variability of the frame-defining sources. Given enough astrometric precision, a trigonometric parallax may also be measurable. The primary consideration for parallax measurements is appropriate sampling over the Earth's orbital phase, not just a long time baseline, and precise single-epoch positions.

Neutron stars emit over a broad range of wavelengths, and astrometric observations have been conducted at wavelengths from radio to X-rays. For example, Kaplan et al. (2007) have used optical observations with the Hubble Space Telescope to measure a proper motion $\mu = 107.8 \pm 1.2$ mas yr^{-1} and a parallax $\pi = 2.8 \pm 0.9$ mas for RX J0720.4−3125. At X-ray wavelengths, the resolution that can be achieved with the current generation of telescopes is a limiting factor, but Winkler & Petre (2007) have used the Chandra X-ray Observatory to measure a proper motion of 165±25 mas yr^{-1} for the RX J0822−4300, in the center of the Puppis A supernova remnant. Radio observations have an advantage over the X-ray in that they can achieve greater resolution.

Pulse timing is routinely used to refine the positions and proper motions of pulsars. A subset of recycled ("millisecond") pulsars have rotation rates that are stable enough to permit sub-milliarcsecond astrometry based on pulse time of arrival. For example, the general relativistic Shapiro delay, proper motion and parallax for the binary pulsar J0437−4715 has been measured based on pulse timing (van Straten et al. 2001; Verbiest et al. 2008). A precise position for pulsars such as J0437−4715, whose positions can be determined from pulsar timing, allows a timing solution to be obtained more rapidly. However, most pulsars do not have such stable rotation, particularly when they are young, and Very Long Baseline Interferometry (VLBI) has usually been utilized to determine their astrometric parameters (e.g., Brisken et al. 2002; Chatterjee et al. 2004, 2009).

The initial SKA Phase 1 sample will consist of known pulsars for which no accurate parallax or proper motion measurements are available. Astrometric observations of individual pulsars would take place over a period of 1–2 years, and typically 6 epochs of observations obtained for individual pulsars over this period to obtain a good parallax and proper motion measurement (Figure 7.1).

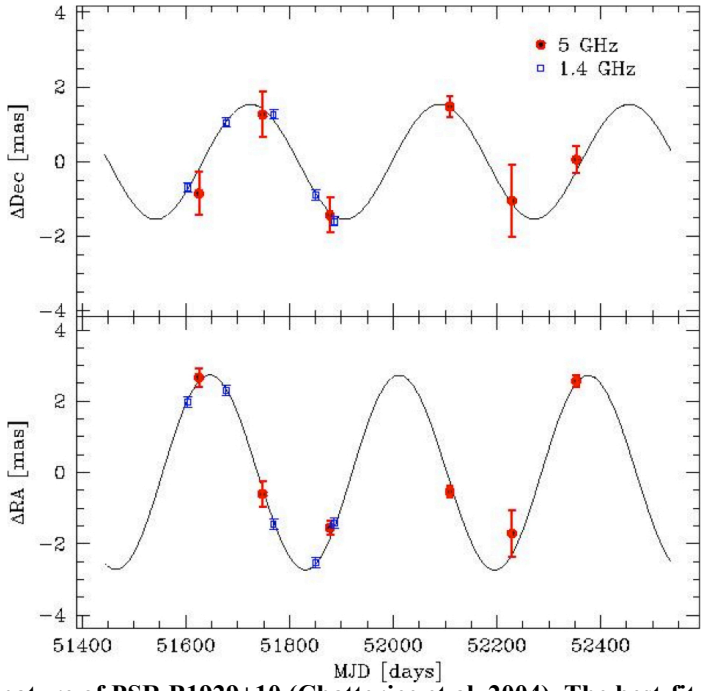

Figure 7-1. Parallax signature of PSR B1929+10 (Chatterjee et al. 2004). The best-fit proper motion from the astrometric positions has been subtracted. Sinusoids corresponding to the best-fit parallax π = 2.77 mas are superposed.

7.3. Scientific Requirements

Table 7.1 summarizes the scientific requirements. Motivation for and discussion of each scientific requirement follows.

Table 7.1. Scientific Requirements

Parameter	Value
Positional Accuracy	20 mas at low signal-to-noise ratio (5) 1 mas at high signal-to-noise-ratio (100)
Sky coverage	> 2π sr

7.3.1. Positional Accuracy

SCI-S-REQ-0500: The SKA Phase 1 shall be capable of providing positions, relative to the International Celestial Reference Frame, to at least 20 mas precision for relatively low signal-to-noise ratio observations (notionally at a signal-to-noise level of 5).

SCI-S-REQ-0505: The SKA Phase 1 shall be capable of providing positions, relative to the International Celestial Reference Frame, to at least 1 mas precision for relatively high signal-to-noise ratio observations (notionally at a signal-to-noise ratio of 100).

There are several goals of pulsar astrometry. Most importantly, a precise position can break the degeneracy between positional uncertainty and pulsar spin-down, decreasing the amount of observing time needed to obtain a coherent timing solution. Further, precise positions allow reference frame ties and improved timing solutions. Over the longer term, proper motions and parallaxes can be measured with multi-epoch observations over a longer time baseline.

This requirement follows from considering the relative magnitude of pulse phase errors related to a positional uncertainty or an uncertainty in the spin-down parameters. To be specific, we consider the

phase errors related to an uncertainty in the period determination, though the same approach follows in considering spin-down parameters (e.g., period-derivative or period-double derivative). The astrometric contribution to the pulse phase is $\nu \mathbf{r} \cdot \mathbf{n}/c$. Here, ν is the pulsar spin frequency (and *not* the observational frequency) and is related to the pulsar's period as $\nu = 1/P$, **r** is the vector between the Earth and the solar system barycenter, **n** is the unit vector in the direction of the pulsar's position, and *c* is the speed of light. In pulsar time of arrival measurements, an error in the pulsar position appears as a sinusoidal term with an amplitude of about $[(500\ \text{s})/P]\Delta\alpha$, where $\Delta\alpha$ is the positional uncertainty and the radius of the Earth's orbit has been measured in units of time (namely 500 s). Similarly, the pulse phase error due to uncertainties in the pulsar period is given by $t\Delta\nu$, where $\Delta\nu$ is the uncertainty in the pulsar spin frequency.

We require that the pulse phase error due to the position should remain below that due to uncertainties in the spin period on time scales of approximately 6 months; on longer time scales, more accurate astrometric information may be derived from a timing program, depending upon the characteristics of the pulsar. For a demanding case of a 1 ms pulsar, for the pulse phase error due to its positional uncertainty to be much less than 1, its position must be known to better than about 40 mas. To be specific, we choose 20 mas as the requirement.

7.3.1. Sky Coverage

SCI-S-REQ-0510: The SKA Phase 1 shall provide access to the entire sky visible from its latitude on the Earth, above a notional elevation limit of 10 deg (TBC).

Pulsars have and will be found all over the sky. In particular, a wide angular distribution of millisecond pulsars will allow a better constraint on gravitational waves. Astrometry thus has the same sky coverage requirement as pulsar surveys and timing (Chapters 5 and 6).

7.4. Technical Requirements

Table 7.2 summarizes the technical requirements for pulsar astrometry, which are similar to that of pulsar timing (Table 6-2).

Table 7.2. Pulsar Astrometry Technical Requirements

Parameter	Requirement	Comment
Observing Frequency	1 – 3 GHz	High signal-to-noise ratio, resolution, ionosphere calibration
Maximum baseline	100 km	positional accuracy
Instantaneous Accessible Solid Angle	> 0.25 deg^2	In-beam calibrators
Pulsar gating	Enable correlator to only record when pulsar is "on"	Improve signal-to-noise ratio of the pulsar

7.4.1. Observing Frequency

SCI-T-REQ-0500: The SKA Phase 1 shall have a frequency range of at least 1 to 3 GHz.

Pulsars are steep spectrum sources, with a typical spectral index of –1.6, so that lower frequencies tend to improve the signal-to-noise ratio. However, at lower frequencies, the angular resolution is decreased, and the magnitude of propagation effects (both interstellar and ionospheric) is increased. Trading off these effects, in general, the optimum observing frequency for pulsar astrometry is 1–3 GHz, though the optimum value for a specific pulsar will vary from pulsar to pulsar. Experience has shown that the limit to precision astrometry is not signal-to-noise ratio but control of systematics. Higher frequencies (4 to 8 GHz) allow propagation effects to be minimized, particularly improving ionospheric calibration, and these could be exploited for pulsar astrometry, if higher frequency capability is enabled as part of the extension to SKA Phase 2.

7.4.2. Maximum baseline

SCI-T-REQ-0510: The SKA Phase 1 shall provide a maximum baseline of at least 100 km.

This requirement is consistent with that of Section 1.4.4 and SCI-A-0050. We discuss it here as a motivation for that assumption.

The maximum baseline requirement is derived directly from the required positional accuracy, which is given by the quantity $\theta/(2\times\mathrm{SNR})$. Here, θ is the angular resolution and SNR is the signal-to-noise ratio. Using the standard expression for the angular resolution, $\theta = \lambda/b$, for an observing wavelength λ and maximum baseline b, one obtains the required positional accuracy, at least for a fraction of the wavelengths required. Higher positional accuracies may be obtained for some objects, particularly if extremely high signal-to-noise ratios can be achieved. An extension to longer baselines would be useful for providing higher positional accuracy, or the same positional accuracy over a larger wavelength range.

7.4.3. Instantaneous Accessible Solid Angle

SCI-T-REQ-0520: The SKA Phase 1 shall have an instantaneously accessible solid angle greater than 0.25 deg^2.

The astrometric accuracy that can be obtained by phase referencing is strongly dependent on the separation between the target and reference source. In order to minimize the separation between the phase reference calibrator and the target pulsar, typical pulsar astrometry techniques use an "in-beam calibration" approach. In this approach, there is a primary (nodding) calibrator, which is typically linked to the ICRF, and one or more weaker, compact sources within the primary beam of the antenna ("in-beam calibrator") that are used as secondary position references. The location of the pulsar is determined by a "bootstrap" procedure of linking the position of the "in-beam" calibrator to the primary calibrator and the target pulsar to the in-beam calibrator. After initial calibration on a primary (nodding) phase reference source, residual calibration errors arise primarily from the unmodeled ionosphere between target and reference source. Using a secondary calibrator in the telescope primary beam can reduce these errors. Such a secondary in-beam calibrator can be much fainter than the primary calibrator. We expect that sources as faint as 0.5 mJy could be used as in-beam calibrators at 2.5 GHz. Source counts suggest that an "accessible area" > 0.25 deg^2 will allow for multiple in-beam calibrators. Note that the full "accessible area" is not necessarily imaged, only small regions around the target pulsar and the in-beam calibrator(s).

7.4.4. Pulsar gating

SCI-T-REQ-0530: The SKA Phase 1 correlator shall allow for pulse phase-resolved observations, at a minimum to include forming as many as 100 phase bins across the pulse and producing the visibilities for a user-specified subset (to include the full set) of these.

Because the signal from a pulsar is not always "on," it is possible to increase the signal-to-noise during pulsar astrometric observations by correlating the signal only when it is "on," a technique known as "pulsar gating." The exact amount of signal-to-noise ratio increase depends on the pulsar duty cycle and can be expressed as $\mathrm{sqrt}(W_e/(P - W_e))$ where P is the pulse period and W_e is the effective pulse width. However, simple "on" and "off" gates will reduce the signal-to-noise ratio of the in-beam calibrators as well, so multiple-gates or "binning" is preferred. More generally, this mode allows the "off" pulse phase bins to be retained for detecting the in-beam calibrators as well as allow studies of off-pulse emission and/or pulsar wind nebulae.

7.5. Data Products

Total intensity images and positions, at specified epochs and relative to the then-current realization of the ICRF, at a specified frequency within the SKA Phase 1 operational frequency range as well as information about the geometric model used in the correlation.

Bibliography

Brisken, W. F., Benson, J. M., Goss, W. M., & Thorsett, S. E. 2002, "Very Long Baseline Array Measurement of Nine Pulsar Parallaxes," Astrophys. J., 571, 906

Chatterjee, S., Brisken, W. F., Vlemmings, W. H. T., Goss, W. M., Lazio, T. J. W., Cordes, J. M., Thorsett, S. E., Fomalont, E. B., Lyne, A. G., & Kramer, M. 2009, "Precision Astrometry with the Very Long Baseline Array: Parallaxes and Proper Motions for 14 Pulsars," Astrophys. J., 698, 250

Chatterjee, S., Cordes, J. M., Vlemmings, W. H. T., Arzoumanian, Z., Goss, W. M., & Lazio, T. J. W. 2004, "Pulsar Parallaxes at 5 GHz with the Very Long Baseline Array," Astrophys. J., 604, 339

Cordes, J. M., Kramer, M., Lazio, T. J. W., Stappers, B. W., Backer, D. C., & Johnston, S. 2004, "Pulsars as Tools for Fundamental Physics & Astrophysics," New Astron. Rev., 48, 1413

Cordes, J.M., & Lazio, T.J.W. 2002, "NE2001.I. A New Model for the Galactic Distribution of Free Electrons and its Fluctuations," astro-ph/0207156

Damour, T. 2006, "Was Einstein 100% Right?" AIP Conference Proceedings, 861, 135

Deller, A. T., Bailes, M., & Tingay, S.J. 2009, "Implications of a VLBI Distance to the Double Pulsar J0737-3039A/B," Science, 323, 1327

Hobbs, G., Lorimer, D. R., Lyne, A. G., & Kramer, M. 2005. "A statistical study of 233 pulsar proper motions," MNRAS, 360, 974

Kaplan, D. L., van Kerkwijk, M. H., & Anderson, J. 2007, "The Distance to the Isolated Neutron Star RX J0720.4-3125," Astrophys. J., 660, 1428

Kramer, M., Stairs, I. H., Manchester, R. N., McLaughlin, M. A., Lyne, A. G., Ferdman, R. D., Burgay, M., Lorimer, D. R., Possenti, A., D'Amico, N., Sarkissian, J. M., Hobbs, G. B., Reynolds, J. E., Freire, P. C. C., & Camilo, F. 2006, "Tests of General Relativity from Timing the Double Pulsar," Science, 314, 97

Kramer, M., Backer, D. C., Cordes, J. M., Lazio, T. J. W., Stappers, B. W., & Johnston, S. 2004, "Strong-field Tests of Gravity Using Pulsars and Black Holes," New Astron. Rev., 48, 993

Ma, C., Arias, E. F., Eubanks, T. M., Fey, A. L., Gontier, A.-M., Jacobs, C. S., Sovers, O. J., Archinal, B. A., & Charlot, P. 1998, "The International Celestial Reference Frame as Realized by Very Long Baseline Interferometry," Astron. J., 116, 516

Shklovskii, I.S. 1970, "Possible Causes of the Secular Increase in Pulsar Periods," Soviet Astron., 13, 562

van Straten, W., Bailes, M., Britton, M., Kulkarni, S. R., Anderson, S. B., Manchester, R. N., & Sarkissian, J. 2001, "A test of general relativity from the three-dimensional orbital geometry of a binary pulsar," Nature, 412, 158

Verbiest, J. P. W., Bailes, M., van Straten, W., Hobbs, G. B., Edwards, R. T.; Manchester, R. N., Bhat, N. D. R., Sarkissian, J. M., Jacoby, B. A., & Kulkarni, S. R. 2008, ApJ, 679, 675

Winkler, P. F., & Petre, R. 2007, "Direct Measurement of Neutron Star Recoil in the Oxygen-rich Supernova Remnant Puppis A," Astrophys. J., 670, 635

8. Galaxy Evolution in the Nearby Universe: H I Observations

Principal Authors: T. Oosterloo, E. de Blok

This Design Reference Mission component is motivated primarily by the Key Science Project "Galaxy Evolution, Large Scale Structure, and Dark Energy" (Rawlings et al. 2004) and has the specific goal of probing the gas content and flows into and out of galaxies across a wide range of morphologies.

This chapter is part of the Design Reference Mission because it provides requirements on the spectral resolution, array configuration, and sensitivity.

8.1. Motivation

The SKA will be able to directly trace the gradual transformation from primordial neutral hydrogen (H I) gas into galaxies over cosmic time. However, direct detailed observations of the sub-kpc–scale physical processes that cause this transformation, taking place both inside and around these distant galaxies, will probably stay beyond our reach—even with the full SKA—for a large span of cosmic time due to limited resolution and sensitivity. Only in the nearby Universe can such a comprehensive survey of the "Galactic Ecosystem" can be conducted—where a detailed study of the flow of gas into galaxies, its physical conditions, its transformation into stars, and how in turn, the gas is affected by feedback from these stars can be performed. The H I kinematics constrain the distribution of dark matter, angular momentum, the shape of the halo potential, the disk gravitational potential, and, ultimately, how the dark and visible matter together determine and regulate the evolution of galaxies. These local galaxies are the "fossil records" of the distant, high-redshift galaxies. The study of nearby galaxies thus provides the foundations on which studies of higher redshift galaxies are built.

There are two main aspects that can be addressed:

1. The interface between galaxies and the intergalactic medium (IGM): What are the properties of the low column density environments of galaxies? What is the importance of cold gas accretion; what are the properties of the accreting gas; what is the physics of gas accretion?
2. The detailed gas physics of star formation in galaxies: how does star formation depend on the sub-kpc properties of the interstellar medium (ISM); what, in turn, is the effect of star formation in the ISM?

8.1.1. Galaxies and the IGM

In recent years it has become clear that galaxies do not dominate the Universal baryon budget, but are merely the brightest pearls of an underlying cosmic web. Gaseous filaments extending between the massive galaxies are a prediction of all models of structure formation (e.g., Davé et al. 1999). These models predict that most of the baryons at low redshift are in a warm-hot intergalactic medium (WHIM; T = 10^5–10^7 K), while 25% are in the 10^4 K diffuse IGM, with only 25% condensed in galaxies and their gaseous halos. Due to the moderately high temperature in the IGM (10^4 K), most of the gas in the cosmic web is highly ionized.

The accretion onto galaxies of gas from this reservoir is thought to be one of the main mechanisms by which galaxies acquire their gas over cosmic time and the evolution of star formation is thought to be set largely by the evolution of this gaseous accretion. In the inner regions of spirals, time scales for consumption of all gas by star formation are smaller than a Hubble time. This gas can, in principle, be replenished by accreting gas-rich companion galaxies, but the slope of the H I mass function is not steep enough for small companions to supply larger galaxies with a substantial amount of gas for a sufficiently long time. Consequently, spirals have to accrete directly from the IGM. It is therefore critical to detect the faint gaseous environments of galaxies, to study their properties, to investigate the physics of the accretion, and to directly observe the relevance of the accretion for galaxy properties. Given the sensitivities and spatial resolutions required, these observations can only be conducted in the nearby Universe.

Observational evidence for cold gas accretion already exists. Cold gas in the halo region of our Milky Way was discovered several decades ago (the high velocity clouds, Wakker & van Woerden 1997) and has recently also been established for a small number of external disk galaxies (Oosterloo et al. 2007, and references therein). A significant fraction of the gas in the H I halos detected must be infalling from intergalactic space. For example, many H I complexes are counter-rotating with respect to the disk, so cannot have originated in it. In addition, to explain the many massive H I complexes seen far above the disk would require an unrealistically large number of supernovae. Recent models suggest gas flows that are driven from the disk into the halo ("galactic fountains") also play an important role in gas accretion from the IGM. Thermal instabilities in the warm gaseous halo, and the associated cooling, which are triggered by the interaction of the galactic fountain with the warm halo may be an important channel for supplying a galaxy with new gas. It is crucial to understand the physics of this process.

8.1.2. The Detailed Gas Physics of Star Formation

Understanding the processes that drive star formation in galaxies is one of the most challenging astrophysical topics, both observationally and theoretically. Of particular interest are studies of how stars form out of the ISM on scales comparable to the Jeans mass and Jeans length of neutral atomic clouds, and how, in turn, these stars shape the structure and physical properties of their ambient ISM. Of key importance in any such studies are high-resolution observations of the different tracers of the ISM (e.g., H I and CO observations) and the stellar population (e.g., broad band imaging, Hα imaging). Although arcsecond resolutions are achieved routinely using ground-based optical telescopes, observations of similar resolutions at radio wavelengths, targeting the different phases of the ISM, are lacking. To date, the lack of sufficiently high resolution and sensitivity observations at radio wavelengths is the limiting factor of all studies on these small, critical scales. High-resolution observations of nearby galaxies allow scales of order 100 pc to be probed, a range which has hitherto been inaccessible except in a few galaxies (mainly dwarfs in the Local Group). It is at these scales where the "global" and "local" star formation processes and conditions intersect. At these scales, energy is injected into the ISM through stellar winds and supernovae, driving turbulence. These are also the scales on which atomic clouds at the Jeans mass collapse to form giant molecular clouds and hence stars. Other important observables will be the fine-scale structure of the ISM. A resolution of tens of pc represents a critical scale as it samples the typical sizes of individual giant molecular and atomic clouds that are the precursors of star formation. Also, observations at this resolution will enable us to directly study the feedback and energy input from individual supernovae due to massive stars. With the high resolution described here, it may be possible to isolate absorption spectra (seen against bright background continuum sources) from the surrounding emission. Doing so opens the possibility to determine directly the H I spin temperature, something that has only been possible in Local Group galaxies.

8.2. Observational Summary

These observations would follow in the spirit of the VLA THINGS survey (Walter et al. 2008), the WSRT HALOGAS survey (Heald et al. 2011), and the planned MeerKAT H I Observations of Nearby Galactic Objects: Observing Southern Emitters (MHONGOOSE) project. Specifically, a large number of galaxies, with a wide range of morphologies and in diverse environments, would be selected for targeted, deep observations.

This survey would be different than other surveys described in the Design Reference Mission. Rather than a uniform integration time per field, as one might use in an all-hemisphere survey, these observations would target known galaxies at approximately known distances, for which different integration times per galaxy would be appropriate. Moreover, as this survey would consist of a relatively small number of fields (~ 100), we have adopted a different integration time assumption than for the typical survey. We assume that a typical field would have an integration time of *30 hr*.

8.3. Scientific Requirements

Table 8-1 summarizes the scientific requirements. Motivation for and discussion of each scientific requirement follows. Throughout, we discuss high and low linear resolution requirements within a galaxy jointly, consistent with the notion that one would like to track gas flows into and within galaxies and potentially within the same galaxy.

Table 8-1. H I Cosmology Scientific Requirements

Parameter	Value
Linear resolution	300 pc
Redshift / distance	0–0.02 / 60 Mpc
H I column density	5×10^{20} cm^{-2} (high linear resolution, ~ 300 pc or better) 10^{18} cm^{-2} (low linear resolution, ~ 1 kpc)
Velocity resolution	0.5 km s^{-1}
Area of regard	500 kpc at a

8.3.1. Linear Resolution

SCI-S-REQ-0600: The SKA Phase 1 shall provide a linear resolution of 300 pc at a redshift of 0.02 or distance of 60 Mpc.

The objective of these observations is to track the transition from "local" star formation processes and conditions to "global" processes and conditions. The linear resolution requirement is set by two complementary considerations. First, existing work on THINGS nearby galaxies has shown that sub-kpc resolution is required to track the distribution of the various gaseous components of the disk (e.g., Bigiel et al. 2008). Second, telescopes at other wavelengths, most notably ALMA, which will be used to study the molecular component of galactic disks, will have a linear resolution of order 10–100 pc at distances of order 10 Mpc (e.g., Meier & Turner 2009; Turner 2009a,b; Wilson 2009). The specified linear resolution allows galaxies at larger distances to be studied, but still provides comparable resolution to ALMA at smaller distances (e.g., 50 pc at 10 Mpc).

8.3.2. Redshift

SCI-S-REQ-0610: The SKA Phase 1 shall be able to access the H I line over the redshift range of 0 to 0.02.

This requirement is coupled to the linear resolution requirement and the column density requirement. The objective of these observations is to track the transition from "local" star formation processes and conditions to "global" processes and conditions. Ideally, one would like to probe this transition to as large a distance or redshift as possible, as the interplay between global disk conditions and local star formation might evolve with redshift. However, studying galaxies at larger distances or higher redshifts makes increasing demands upon other aspects of the SKA Phase 1 system, most notably the length of the interferometric baselines requirement (in order to continue to comply with the required linear resolution) and the sensitivity (in order to continue to comply with the required H I column density). The specified value represents an effort to optimize between the competing objectives, requirements, and assumptions. We specify both a redshift and a distance because in the local Universe peculiar velocities may impact redshift-dependent distance estimates.

8.3.3. H I column density

SCI-S-REQ-0620: The SKA Phase 1 shall be able to reach an H I column density of 5×10^{20} cm^{-2} at its highest linear resolution within galaxies and 10^{18} cm^{-2} at low linear resolution characteristics of galactic scales.

In order to track the flow of gas from the IGM and the outskirts of galaxies into the star forming regions requires the capability to probe a wide range of H I column densities. The larger of the two requirements is that which is required to track the distribution of gas on the scales of spiral arms and molecular clouds (i.e., 300 pc, SCI-S-REQ-0600, §8.3.1). The smaller of the two requirements is that which is required to probe the galaxy-IGM interface, particularly as the gas is no longer capable of self-shielding itself from the intergalactic ultraviolet ionizing radiation field. Typical linear scales for this latter requirement are of order 1–10 kpc.

8.3.4. Velocity Resolution

SCI-S-REQ-0630: The SKA Phase 1 shall provide a velocity resolution of at least 0.5 km s^{-1}.

Gas-rich galaxies display a wide range of morphologies, including low mass, gas-rich dwarfs. In order to study the gas content and motions in and within the full range of galaxies, a velocity resolution of at least 0.5 km s^{-1} is required. Such a high velocity resolution allows the H I profiles of even dwarf galaxies to be resolved, e.g., the ALFALFA survey finds multiple galaxies with H I velocity widths of less than 20 km s^{-1} (Giovanelli et al. 2007) and the *warm* neutral medium within a galaxy to be resolved (Walter et al. 2008). Notably, the velocity resolution of the THINGS observations was limited by the VLA correlator, rather than by the scientific objectives of that survey.

8.3.5. Area of Regard

SCI-S-REQ-0670: The SKA Phase 1 shall provide the capability to image an area of 500 kpc diameter at a redshift of 0.02 or distance of 60 Mpc, with the goal of providing the capability to image an area of 1 Mpc diameter at a distance of 10 Mpc.

The objective of these observations is to track the transition from "local" star formation processes and conditions to "global" processes and conditions, as part of understanding how galaxies acquire their gas and convert it to stars. This objective is most naturally achieved if the area imaged is sufficiently large to encompass both a galaxy and its immediate environment. As a characteristic scale, we specify an area with a diameter of 500 kpc at the largest distance (redshift = 0.02/distance = 60 Mpc), which could encompass either a galaxy and its satellites or an inflowing filament. As a goal, we specify an area with a diameter of 1 Mpc at a distance of 10 Mpc, which would be sufficient to image a major galaxy (e.g., Milky Way Galaxy, Andromeda Galaxy) or a group of galaxies (e.g., Local Group).

8.4. Technical Requirements

Table 8-2 summarizes the technical requirements derived from the scientific requirements. Discussion of each technical requirement follows. As with the discussion of the scientific requirements, the high and low resolution requirements are considered jointly.

Table 8-2. H I Cosmology Technical Requirements

Parameter	Value	Comment
Frequency range	1390–1420 MHz	Redshift range
Baselines	50 km	Linear resolution
Spectral resolution	2 kHz	Velocity resolution
Brightness Temperature Sensitivity	200 K for 50 km baselines 0.3 K for 1.5 km baselines	H I column density and linear resolution
Field of View	0.5º FWHM (goal: 5.7º FWHM)	Area of regard

8.4.1. Frequency Range

SCI-T-REQ-0600: The SKA Phase 1 shall provide a frequency coverage of at least 1390 to 1420 MHz.

The frequency range required follows directly from the redshift coverage requirement. The rest frequency of the H I line is 1420 MHz. The lower frequency end is determined by the requirement to reach a specified redshift [i.e., 1420 MHz/(1 + z)]. A redshift of 0.02 corresponds to a lower frequency of 1390 MHz.

8.4.2. Baselines

SCI-T-REQ-0610: The SKA Phase 1 shall provide a maximum baseline of at least 50 km.

The maximum baseline extent follows directly from the stated linear resolution requirement. A linear extent of 300 pc at a distance of about 65 Mpc subtends approximately 1". At a frequency of 1400 MHz, corresponding to the approximate mid-range of the required frequency coverage, an angular resolution of 1" requires interferometric baselines of approximately 45 km. Accordingly, we specify 50 km as the requirement.

8.4.3. Spectral Resolution

SCI-T-REQ-0620: The SKA Phase 1 shall provide a spectral resolution of at least 2 kHz, over the maximal range of frequencies within the SKA Phase 1 goal as possible.

The frequency resolution follows directly from the stated velocity resolution requirement. The frequency resolution, at a frequency ν, corresponding to a velocity resolution Δv is given by $\Delta\nu = \nu(\Delta v/c)$, where c is the speed of light. At a nominal frequency of 1420 MHz, the required frequency resolution is 2 kHz.

8.4.4. Brightness Temperature Sensitivity

SCI-T-REQ-0630: The SKA Phase 1 shall provide a brightness temperature sensitivity of at least 200 K on 50 km baselines and at least 0.3 K on 1.5 km baselines.

Studying H I in emission requires surface brightness sensitivity, which reflects both total collecting area and how it is distributed within the (synthetic) aperture. For these reasons, we specify a brightness temperature sensitivity. For reference, in the optically thin gas case, which almost always applies for H I gas, the H I column density and brightness temperature are related as $N_{HI} \propto \int T_B(v)\, dv$, and the integral is performed over the emission line's extent in velocity v. As noted above, because it may be desired to study gas flows into and within the same galaxy, brightness temperature sensitivity requirements are specified jointly for high resolution (50 km baselines) and low resolution (1.5 km baselines).

8.4.5. Field of View

SCI-T-REQ-0640: The SKA Phase 1 shall provide a field of view of at least 0.5° (FWHM) over the required frequency range, with the goal of providing a field of view of at least 5.7° (FWHM) over the required frequency range.

The field of view follows directly from the stated area of regard requirement at the specified distances. The field of view corresponding to an area of diameter R at a distance D is given by $\Theta = R/D$. For the specified area of regard, the required field of view is 0.5° (FWHM), with a goal of 5.7° (FWHM).

8.5. Data Products

Total intensity image cubes of specified galaxies or groups of galaxies, over the entire field of view, covering 1390–1420 MHz, at 1" and 0.5 km s^{-1} velocity resolution.

Bibliography

Bigiel, F., Leroy, A., Walter, F., Brinks, E., de Blok, W. J. G., Madore, B., & Thornley, M. D. 2008, "The Star Formation Law in Nearby Galaxies on Sub-Kpc Scales," Astron. J., 136, 2846

Davé, R. Hernquist, L., Katz, N., & Weinberg, D. H. 1999, "The Low-Redshift Lyα Forest in Cold Dark Matter Cosmologies," Astrophys. J., 511, 521

Giovanelli, R., Haynes, M. P., Kent, B. R., et al. 2007, "The Arecibo Legacy Fast ALFA Survey. III. H I Source Catalog of the Northern Virgo Cluster Region," Astron. J., 133, 2569

Heald, G., Józsa, G., Serra, P., Zschaechner, L., Rand, R., Fraternali, F., Oosterloo, T., Walterbos, R., Jütte, E., & Gentile, G. 2011, "The Westerbork Hydrogen Accretion in LOcal GAlaxieS (HALOGAS) survey. I. Survey description and pilot observations," Astron. & Astrophys., 526, A118

Meier, D., & Turner, J. 2009, "The GMC Scale Chemical Anatomy of Nearby Galaxies," in ALMA Design Reference Science Plan, v. 2.2; http://www.eso.org/sci/facilities/alma/science/drsp/

Oosterloo, T., Fraternali, F., & Sancisi, R. 2007, "The Cold Gaseous Halo of NGC 891," Astron. J., 134, 1019

Rawlings, S., Abdalla, F. B., Bridle, S. L., Blake, C. A., Baugh, C. M., Greenhill, L. J., & van der Hulst, J. M. 2004, "Galaxy Evolution, Cosmology and Dark Energy with the Square Kilometre Array," in Science with the Square Kilometre Array, eds. C. Carilli & S. Rawlings, New Astronomy Reviews, Vol. 48, (Elsevier: Amsterdam) p. 1013

Turner, J. 2009b, "The Molecular ISM in Low Surface Brightness Galaxies," in ALMA Design Reference Science Plan, v. 2.2; http://www.eso.org/sci/facilities/alma/science/drsp/

Turner, J. 2009a, "Study of Gas Masses and Star Formation Efficiencies in Nearby Galaxies," in ALMA Design Reference Science Plan, v. 2.2; http://www.eso.org/sci/facilities/alma/science/drsp/

Walter, F., Brinks, E., de Blok, W. J. G., et al. 2008, "THINGS: The H I Nearby Galaxy Survey," Astron. J., 136, 2563

Wakker, B. P., & van Woerden, H. 1997, "High-Velocity Clouds," Ann. Rev. Astron. & Astrophys., 35, 217

Wilson, C. 2009, "Structure of the ISM in irregular galaxies," in ALMA Design Reference Science Plan, v. 2.2; http://www.eso.org/sci/facilities/alma/science/drsp/

9. Additional Science Capabilities of Phase 1

As described in §1.3, the intent of the Design Reference Mission is to specify the most demanding technical requirements, as derived from the science goals and requirements for the telescope. One of the motivations for doing so is that the most demanding technical requirements are the ones most likely to influence the cost. In this section, we discuss the broader science capabilities and the astronomical, physical, and astrobiological questions that will be enabled, if the SKA Phase 1 meets the technical requirements specified in previous chapters. No priority should be inferred from the order of presentation of the science components or of the ordering of scientific or technical requirements within each component.

Cosmic Magnetic Fields: Understanding the origin and evolution of cosmic magnetism is one of the Key Science Programs for the SKA Phase 2 (Gaensler et al. 2004; Beck & Gaensler 2004; Feretti & Johnston-Hollitt 2004; Hoare 2004), with the goal of following the evolution of magnetized structures from redshifts $z \approx 5$ to the present and developing a detailed model of the magnetic field geometry of the intergalactic medium and of the overall Universe. Compatibility with SKA Phase 2 (Chapter 10) will mean that SKA Phase 1 will be able to perform initial studies of cosmic magnetic fields, building the foundation for the SKA Phase 2 experiments through an all-sky survey of rotation measures (RMs). With SKA Phase 2, the aim is to accumulate a sufficiently large sample of RMs to determine the overall magnetic power spectrum of the Universe. A vital stepping stone towards this goal is to delineate the magnetic field of our own Milky Way, both to properly account for foreground Faraday rotation, and to derive a complete three-dimensional field geometry for a typical galaxy, against which dynamo and other models for cosmic magnetic field generation can be tested. Broadly speaking, Faraday rotations measured through the Milky Way are composed of two RM contributions: a large-scale, coherent, magnetic field, tied to the overall structure of the spiral arms, disk and halo; and a small-scale, fluctuating field which traces individual regions such as supernova remnants (SNRs) and H II regions, as well as diffuse turbulence in the ionized interstellar medium (ISM). The effective angular resolution with which a grid of background RMs can probe the Galaxy's magnetic field is determined by the need to be able to separate large-scale and small-scale fields. Further, capability at higher frequencies, as part of the expansion to SKA Phase 2, will enable sources having larger rotation measures or internal Faraday dispersion to be probed (Arshakian & Beck 2011).

Diffuse Radio Emission from the Intracluster Medium: In the hierarchical structure formation scenario, the mergers of clusters of galaxies are an important contributor to the formation of large-scale structure. Analogous to the generation of intergalactic shocks, the merging of clusters can amplify magnetic fields and accelerate particles, producing diffuse synchrotron radio emission from clusters (Feretti et al. 2004). This radio emission can be used to study the structure formation process or to probe the magnetic field distribution within the cluster (Feretti & Johnston-Hollitt 2004). The radio halos and relics resulting from mergers of clusters have already been detected from existing facilities (e.g., VLA, GMRT) and are expected to be detected with LOFAR. Consequently, it should be possible to study these with SKA Phase 1, to fainter radio luminosities. The requirements for cluster radio emission studies are similar to those for studying intergalactic shocks, and the wide frequency coverage and relatively centrally condensed configuration remain important aspects of the SKA Phase 1. Also essential will be that the polarization performance of SKA Phase 1 meet the requirements for SKA Phase 2 (Chapter 10).

Proto-Planetary Disks: The imaging of proto-planetary disks is recognized as part of the Key Science Program for SKA Phase 3, and may be accessible to SKA Phase 2 (Wilner 2004; Lazio et al. 2004). Experience with the EVLA and eMERLIN will be invaluable in assessing the extent to which SKA Phase 1 can contribute to the study of proto-planetary disks, but it is likely that a higher frequency capabilities for SKA Phase 1, as part of an expansion to SKA Phase 2, would be invaluable.

Cosmology with the SKA Phase 1: SKA Phase 2 is intended to have a high survey speed, both for spectral line surveys such as an H I survey for baryon acoustic oscillations and continuum surveys such as for weak lensing (Blake et al. 2004). While it was thought initially that SKA Phase 1 would not have sufficient survey speed to enable these surveys, but recent assessments may be showing that the SKA Phase 1 will be able to make a significant improvement in the determination of cosmological parameters. Moreover, a relatively new technique known as "intensity mapping" has been developed. In this method, individual galaxies are not resolved, which is acceptable given that the length scales that need to be probed are far larger than the size of an individual galaxy. For SKA Phase 1, the desired frequency range for H I intensity mapping as well as the required spectral (~ 1 MHz) and angular resolutions (few arcminutes) are well within the requirements specified elsewhere in this document. In this respect, the relatively centrally condensed array distribution is useful in order to have adequate sensitivity at arcminute resolution.

Changes in Fundamental Constants: Some models for a Grand Unified Theory (GUT) predict that fundamental constants, or combinations of fundamental constants (e.g., the fine structure constant), might vary with cosmic time, a notion that dates back at least to Dirac's speculations about variations in the Newtonian gravitational constant. Observations of spectral lines at optical wavelengths have led to suggestions that some constants might change with cosmic time. Observations of radio spectral lines would likely obtain much higher spectral resolution, for higher precision localization of the line centroid, and would be unaffected by dust obscuration (Curran et al. 2004). The key lines at radio wavelengths would be from H I and the OH radical. These are within the SKA Phase 1 operational frequency range, and the required spectral resolution is comparable to that required for H I observations of nearby galaxies. Thus, to the sensitivity limit of SKA Phase 1, it would be able to search for changes in fundamental constants.

Intergalactic Shocks: As baryons fall into dark matter halos during structure formation, strong shocks in the intergalactic medium are expected to result (Keshet et al. 2004; Wilcots 2004). Magnetic field amplification and particle acceleration are likely to generate synchrotron emission, which could then be used to trace the structure formation process. Initial estimates were that the synchrotron emission from shocks might be within reach of current facilities (e.g., LOFAR). If LOFAR is able to detect this signal, then the greater sensitivity of the SKA Phase 1 will enable it to probe structure formation at higher significance than can LOFAR; if the signal is not detected with LOFAR, the greater sensitivity of the SKA Phase 1 will enable it to detect the signal or improve the constraints significantly. Further, synchrotron emission is broadband, and that expected from intergalactic shocks is expected to extend well above LOFAR's operational frequency range, so that the wide frequency range of SKA Phase 1, as compared to LOFAR, the GMRT, SKAMP, and the EVLA, is an important advantage. The predicted signal is a continuum signal on fairly large angular scales (requiring fairly short baselines). In this respect, the relatively centrally condensed configuration of SKA Phase 1 is also useful in attempting to detect or constrain synchrotron emission from intergalactic shocks.

Low Luminosity Active Galactic Nuclei: The vast majority of radio sources are low luminosity active galactic nuclei (AGN) and star forming galaxies. Understanding the overall energy budget of galaxies (the balance of fusion versus accretion) and its evolution over cosmic time requires that these populations be identified and separated (Falcke et al. 2004; Jarvis & Rawlings 2004; Jackson 2004). The EVLA and MeerKAT are both expected to produce deep continuum images of the sky, likely to the sub-microJansky level, and with its greater sensitivity and longer baselines, the SKA Phase 1 should be able to probe to even lower flux density levels. One open question is the extent to which natural confusion, determined by the diameters of faint radio sources, becomes an issue for the SKA Phase 1.

High-Redshift Galaxies: At the highest redshifts, the maser and continuum emissions from galaxies are shifted out of the frequencies normally considered to be the operating regime for ALMA and to much lower frequencies, accessible to the SKA Phase 1 (Blain et al. 2004). For instance, thermal free-free

emission is a direct measure of the ionizing luminosity of stars in a galaxy, intense star forming galaxies can produce OH megamasers, and tori around accreting supermassive black holes can host H_2O masers. If, at a redshift of 10, there are star-forming galaxies that also host accreting supermassive black holes, the rest-frame thermal emission at 30 GHz (ALMA Band 1) would be shifted to 2.7 GHz, any OH megamaser emission would be shifted to 0.15 GHz, and any H_2O maser emission would appear at 2 GHz. While the luminosities of galaxies at these redshifts are not known—if they are discovered—the operational frequency range of SKA Phase 1 would be able to access highly-redshifted galactic emissions such as these. Further, the spectral resolution required for detecting highly-redshifted maser emission is well within the requirements specified elsewhere in this document.

Stellar and Sub-Stellar Radio Emission: Stars across the Hertzsprung-Russell diagram, and even sub-stellar objects are known to emit at radio wavelengths, by a variety of emission mechanisms including gyro-synchrotron, synchrotron, and the electron cyclotron maser instability (White 2004). Not only does this radio emission constrain the properties of stellar magnetic fields, the study of other stars may inform our understanding of the Sun, the nearest star, with implications for understanding its impact on Earth and our civilization. Existing and previous radio observatories (e.g., Clark Lake Radio Observatory, VLA) have already conducted a number of significant studies of stellar and sub-stellar radio emission. The greater sensitivity of the SKA Phase 1 should enable it to probe to larger distances, fainter emissions, or both. However, higher frequency capabilities (e.g., 5–8 GHz) for SKA Phase 1, as part of an expansion to SKA Phase 2, would enable a greater range of studies, both of more classes of objects and a broader range in emission mechanisms.

The Interstellar Medium: The interstellar medium (ISM) both is the raw material from which stars form and a source of additional signal as radio waves propagate through it. The requirements for the study of the neutral ISM (Dickey et al. 2004; see also Brinks 2004) are satisfied by the discussions elsewhere in this document on H I observations. Polarization signatures from the ionized ISM are contained within the study of cosmic magnetic fields (Gaensler et al. 2004), which will be possible to the sensitivity and survey speed capabilities of SKA Phase 1 by virtue of its compatibility with SKA Phase 2 (Chapter 10). Radio waves propagating through the ISM from compact sources are also scattered, which can be used to probe the source characteristics, namely constraining the source diameter, and the properties of the ISM itself (Lazio et al. 2004). Many of the radio-wave scattering studies have used pulsars as the background sources, and the requirements for pulsar searching and timing specified elsewhere in this document would also allow such observations to be conducted. Studies of angular broadening require milliarcsecond resolution for most lines of sight through the Galaxy and would have to wait for SKA Phase 2; though there are a few significantly scattered lines of sight, particularly toward the inner Galaxy, which could be accessed with the angular resolution provided by SKA Phase 1.

Extragalactic Water Masers: These can be used as a geometrical distance measure and probe of the inner environment of the "central engine" of an active galactic nucleus (Greenhill 2004). SKA Phase 1 will not have sufficient extended baselines for conducting geometrical distance measurements, and, with the frequency coverage described in SKA Memo 130, could detect water masers only at redshifts $z > 6$, of which none are known currently. However, higher frequency coverage of SKA Phase 1 to 10 GHz, as part of the expansion to SKA Phase 2, could allow it to search for water masers at lower redshifts ($z \sim 2$), which might become targets for future observations with SKA Phase 2.

Strong Gravitational Lensing: Although a robust prediction from General Relativity, Einstein thought that gravitational lenses would never been observed given the requirements on the alignment between foreground and background sources. Today, however, many gravitational lenses, including those producing multiple images have been detected, and they have become a powerful tool for probing the matter distribution in galaxies and clusters of galaxies as well as cosmology (Koopmans et al. 2004). Observations of lenses in the radio do not suffer dust obscuration, and consequently can provide more

robust constraints on the derived mass models. The angular resolution of the SKA Phase 1 is marginal (0.2" at 20 cm) with respect to the desired angular resolution (0.1"). Nonetheless, SKA Phase 1 would still be quite capable of conducting followup observations of lenses or of conducting a pilot survey in anticipation of SKA Phase 2.

Clusters and Cosmology with the Sunyaev-Zel'dovich Effect: The Sunyaev-Zel'dovich (SZ) effect is a distortion of the cosmic microwave background (CMB) caused by the plasma within clusters of galaxies. It is a powerful tool both for cosmological studies and for structure formation. Because of the thermal spectrum of the CMB, observations at higher frequencies are favored. SKA Phase 3, operating at frequencies of 20 GHz and above, would be able to determine source counts and constrain spectral distortions in the CMB resulting from energy injections at various cosmological epochs (Burigana et al. 2004). SKA Phase 1 will be able to conduct deep source counts near 1 GHz, but a detailed examination would have to be conducted to assess the effects of extrapolating these source counts to higher frequencies (e.g., Murphy et al. 2010); it is beyond the scope of this document to consider those implications. A higher frequency capability of SKA Phase 1, as part of the expansion to SKA Phase 2, would mitigate the uncertainties related to the extrapolation of source counts in frequency.

Relativistic Jets: Jets are recognized to be an important means for extracting angular momentum from accretion disks and imparting energy to surrounding media for sources ranging from young stellar objects to supermassive black holes. Jets from compact objects can produce extremely relativistic outflows and those from supermassive black holes produce some of the largest galactic structures in the Universe, but significant uncertainties remain regarding their launching and collimation mechanisms (Bicknell et al. 2004; Falcke et al. 2004; Fender 2004). Recently, jets produced by the tidal disruption of stars passing too close to supermassive black holes have also been identified and recognized as an important means of studying the launching of jets (e.g., Bower 2011; Miller & Gultekin 2011; van Velzen et al. 2011; Zauderer et al. 2011). Radio wavelength observations, particularly when combined with X- and γ-ray observations, provide important constraints on the evolution of the accretion disk and the launching mechanism. Further, because of the smaller masses involved, studies of X-ray binary systems provide a model for understanding the (much longer time scale) processes occurring around supermassive black holes. The SKA Phase 1, by itself, will not provide the parsec-scale or AU-scale resolution needed to study the inner regions of the jets for supermassive black holes or X-ray binaries, respectively. However, the SKA Phase 1, particularly the central region, could be an important addition to a global very long baseline interferometric (VLBI) network to conduct such observations. Moreover, the SKA Phase 1's broadband frequency coverage will be useful in tracking the time evolution of jet emission. In this respect, higher frequency capabilities for SKA Phase 1, as part of the expansion to SKA Phase 2, would be valuable.

First Accreting Black Holes: The discovery of many quasars at redshifts $z > 6$ indicates that supermassive black holes are able to form on rapid time scales in the early Universe. Finding even higher redshift accreting (supermassive) black holes would provide increasing stringent constraints on their formation and growth mechanisms. Radio emission from the first black holes would be a clear indication of accretion, and the resultant jets could be an important feedback process for the formation for the first galaxies, though it is not yet clear if the jet emission will not be frustrated or the sources self-absorbed at SKA Phase 1 frequencies. Falcke et al. (2004) outline a strategy for finding the highest redshift accreting black holes. The SKA Phase 1, by itself, will not provide the parsec-scale resolution required in their strategy, but the SKA Phase 1, particularly the central region, could be an important addition to a global VLBI network to conduct such observations. The SKA Phase 1 could conduct finding surveys for candidates—compact, non-variable, sub-milliJansky sources—which could also be combined with deep optical observations to identify high redshift objects.

Gas in Galactic Nuclear Environments: AGN are fueled by gas inflow, and their immediate environments often contain complex structures (disks or tori). Radio wavelength observations provide

probes of these inflows and structures that are not subject to obscuration (Morganti et al. 2004). The SKA Phase 1 will be able to probe certain aspects of gas inflow or in the environment, some of which is described elsewhere in this document (Chapter 3). Some of the radio wavelength diagnostics, e.g., the 22 GHz H_2O line, will only be accessible at very high redshift or in SKA Phase 3, however.

Star Formation: One of fundamental processes in astronomy, understanding star formation has implications from the first stars to life elsewhere in the Galaxy. Observations at radio wavelengths are an important component of studies of star formation because they are not subject to dust obscuration within the natal environments of stars. Both the continuum and spectral-line imaging capabilities of the SKA Phase 1 will be important for improving our understanding of star formation, particularly when combined with observations with ALMA (Hoare 2004; Johnson 2004). The SKA Phase 1 will not have the AU-scale resolution that would be helpful in probing the innermost regions around young stars. In this respect, a higher frequency capability for SKA Phase 1, as part of an expansion to SKA Phase 2, would be valuable and would enable the study of more spectral lines.

Late Stages of Stellar Evolution: Low-mass stars return a significant fraction of their mass to the interstellar medium as the raw material for future generations of stars, and these late stages may be important for understanding dust production in early galaxies. As with star formation, radio wavelength observations are valuable because they are not subject to dust obscuration. Marvel (2004) summarizes a number of molecular lines that are accessible within the SKA Phase 1's operational frequency range. The spectral resolution required for other SKA experiments should be sufficient to access these lines as well. The SKA Phase 1 will not have the AU- or sub-AU scale resolution required to image the distributions of masers (e.g., OH) in the environments of evolved stars, but its central region could be an important addition to a global VLBI network to conduct such observations. Higher frequency capabilities for SKA Phase 1, as part of an expansion to SKA Phase 2, would be valuable to enable the study of additional spectral lines and obtain higher angular resolution.

Supernovae, Gamma-Ray Bursts, and Transient Radio Sources: When high-mass stars end their lives, they often do so catastrophically, producing explosions that can be observed across the visible Universe. They also seed the surrounding medium with metals that can be incorporated into future generations of stars and planets. Radio emission is typically generated when the blast wave from a supernova or γ-ray burst interacts with the surrounding medium, and radio wavelength studies provide information about the circum-stellar medium of the progenitor (Weiler et al. 2004). Radio supernovae and γ-ray burst studies are already routine with existing facilities (e.g., EVLA). The higher sensitivity of the SKA Phase 1 will enable it to search for weaker emission, potentially including radio emission from Type Ia supernovae. Radio emission from supernovae and γ-ray bursts is an exemplar of an expanding incoherent explosion that becomes optically thin at longer wavelengths as it expands. In this respect, higher frequency capabilities for SKA Phase 1, as part of an expansion to SKA Phase 2, would be invaluable for probing earlier times after the initial explosion.

Ultra-High Energy Cosmic Rays and Neutrinos: Particles with energies comparable to and exceeding the Greisen-Zatsepin-Kuzmin (GZK) limit of 5×10^{19} eV have been detected (e.g., Abbasi et al. 2008), indicating that cosmic accelerators capable of accelerating particles to these energies must exist. Further, although charged particles are subject to the GZK suppression, neutrinos would not be and, if detected, would provide evidence for the limits to cosmic acceleration. When ultra-high energy cosmic rays (UHECRs) strike the Earth's atmosphere or energetic neutrinos strike the lunar regolith, they produce radio pulses via the Cherenkov and Askaryan effects, respectively (Falcke et al. 2004). One of the advantages of searching for energetic particles via these mechanisms is that the Earth's atmosphere and a fraction of the Moon's volume are being used as the detector, and, in both cases, the equivalent detector volume is much larger than typical particle detection experiments. The spectrum for UHECRs peaks at low frequencies, indicating that the low-frequency component of SKA Phase 1 would be most relevant for detecting them. Most likely, these observations would require cross-correlating all of the dipoles in a localized region to form an image above the array. The radio pulses

are extremely short in duration (~ 10 ns), but a trigger (likely in software) and associated data capture hardware would be required. The optimum frequency for the detection of radio pulses from ultra-high energy neutrinos is not known, but is likely to be in the range 200–1000 MHz. Searches for such radio pulses could be conducted in a manner similar to pulsar searching by phasing sub-arrays to cover the limb of the Moon, though the expected signal is not periodic and the range of dispersion measures that must be considered (from the Earth's ionosphere) is much smaller than that from the interstellar medium. It is likely that the SKA Phase 1 design could accommodate searching for radio pulses from both UHECRs and ultra-high energy neutrinos, though a modest amount of additional hardware for data capture may be necessary.

Solar System Science: Both continuum and molecular line emission can be detected at radio wavelengths from solar system objects ranging from comets to the giant planets (Butler et al. 2004). Radio wavelengths can be used to probe the sub-surface of a body, and ground-based observations often provide an important complement to spacecraft-based observations. Solar system observations would require two additional software capabilities, notably the ability to track objects not moving at the sidereal rate and the ability to image in the near field (for objects closer than about 1 AU at 30 cm wavelength). Higher frequency capabilities for SKA Phase 1, as part of an expansion to SKA Phase 2, would be valuable, in two respects. First, the thermal emission from solar system bodies becomes stronger at shorter wavelengths. Second, coverage of the spacecraft downlink band (in the X band, near 8.4 GHz) would enable spacecraft tracking and telemetry reception (Jones 2004).

International Celestial Reference Frame: The International Celestial Reference Frame (ICRF) is the frame to which all astronomical observations are referenced and is currently realized through a series of radio-loud quasars (Ma et al. 1998). The SKA Phase 1, particularly the central region, could be an important addition to global VLBI observations for improving or maintaining the ICRF, particularly if its frequency coverage is extended to higher frequencies as part of the extension to Phase 2. Over the lifespan of the SKA, it is possible that the reference frame will be defined by optical sources, as part of the observations of the GAIA spacecraft. Even so, maintaining a radio reference frame will be important to link radio wavelength observations with observations at other wavebands.

Extrasolar Planets: All of the solar system's giant planets and the Earth emit coherent radio emission via the electron cyclotron maser instability, though only Jupiter's radiation can be detected from the ground due to the Earth's ionospheric cutoff. Even Jupiter's emission cuts off near 40 MHz, below the formal SKA Phase 1 lower operational frequency limit. However, if there are extrasolar planets (presumably giant planets) that also generate electron cyclotron maser emission and their cutoff frequencies are above the 70 MHz (or 50 MHz) lower operational frequency limit, then SKA Phase 1 could search for them, and study any detected.

Searches for Extraterrestrial Intelligence: The traditional signal model for transmissions from extraterrestrial civilizations is that of a directed beacon, a narrowband signal transmitted with the express purpose of being able to be detected by another civilization. The focus on this signal model is because current telescopes do not have the sensitivity to detect "leakage" or unintended emissions (Tarter 2004). The reduced sensitivity of SKA Phase 1 relative to SKA Phase 2 mean that this situation may not change. Searches for this signal model have focused on extremely narrowband signals (e.g., 1 Hz), as a narrowband signal require less total power, relative to a broadband signal, to be detectable, all other factors being equal. Formally, a spectral resolution of 1 Hz is outside of the current SKA Phase 1 requirements (notionally 2 kHz near 1 GHz, Chapter 8). However, the pulsar search modes may enable access, with additional processing, to obtain these spectral resolutions. Further, motivated by the use of spread-spectrum signals in our own civilization, there is increasing interest in conducting searches for such signals. The spectral resolution of SKA Phase 1 would be sufficient to enable such searches.

9.1. Data Products

In what follows, we summarize data products from observations that are contained within the envelope of the SKA Phase 1 design. These should be seen as illustrative of the kind of data products that will be required but may not be comprehensive.

Cosmic Magnetic Fields: Positions and RMs for all polarized sources detected within an individual observation or survey.

Diffuse Radio Emission from the Intracluster Medium: Full polarization (Stokes I, Q, U, and V) image cube at 1" resolution (TBC) and 1 MHz spectral resolution (TBC) at a set of sub-bands within the accessible SKA Phase 1 frequency range.

Changes in Fundamental Constants: Total intensity spectra with 1 km s^{-1} velocity resolution. These observations could likely be conducted in the context of H I surveys.

Galaxy Cluster Observations (magnetic fields, shocks, galaxy evolution): Full polarization (Stokes I, Q, U, and V) images, of specified galaxies or clusters of galaxies, over a region nominal 10' in diameter at 3" resolution for a nominal central frequency of 1.5 GHz (or comparable resolution scaled to other frequencies) with at least 500 MHz of bandwidth at a nominal central frequency of 1.5 GHz (or comparable fractional bandwidth scaled to other frequencies).

Spectral Line Image Cubes (deep H I fields, masers, …): Full polarization (Stokes I, Q, U, and V) images, obtained at a user-specified cadence, at a user-specified position in the sky, at a user-specified central frequency within the SKA Phase 1 accessible range, at a user-specified spectral resolution to the maximum provided by the SKA Phase 1, at a user-specified angular resolution, up to the maximum provided by the SKA Phase 1, over a region at least 100 synthesized beams in diameter to a user-specified sensitivity, up to the maximum provided by the SKA Phase 1.

Continuum Images (stellar and sub-stellar radio emission, individual galaxies in continuum, transient followup, gravitational lensing, …): Full polarization (Stokes I, Q, U, and V) images, obtained at a user-specified cadence, at a user-specified position in the sky, at a user-specified central frequency within the SKA Phase 1 accessible range, at a user-specified angular resolution, up to the maximum provided by the SKA Phase 1, over a region at least 100 synthesized beams in diameter to a user-specified sensitivity, up to the maximum provided by the SKA Phase 1.

Very Long Baseline Interferometric (VLBI) Observations (interstellar medium, masers, relativistic jets, stellar evolution, …): Full polarization (Stokes I, Q, U, and V) baseband data, in the then-standard format for VLBI processing, for a user-specified position in the sky, at a user-specified central frequency within the SKA Phase 1 accessible range. These baseband data should be provided for one or multiple subsets of the SKA Phase 1 receptors, with a maximum number of receptors being those in the so-called "inner region."

Dynamic Spectra (interstellar medium): Full polarization (Stokes I, Q, U, and V) phased array data streams, for one or multiple user-specified positions on the sky, at a user-specified central frequency within the SKA Phase 1 accessible range, using a user-specified sub-set of the SKA Phase 1 receptors, up to the maximum provided by the SKA Phase 1.

Cosmology from continuum surveys: Full polarization (Stokes I, Q, U, and V) images, centered at 1.4 GHz, covering the entire accessible sky (TBC), at 0.5" resolution (TBC) obtaining a 1 μJy point-source sensitivity.

Cosmology from H I intensity mapping: Total intensity image cube of a specified region, nominally 1000 deg^2, at 1' resolution and 10 km s^{-1} velocity resolution over a nominal frequency range 350–1000 MHz.

Ultra-High Energy Cosmic Rays and Neutrinos: The implementation of certain aspects of this science may require additional hardware, beyond the standard SKA Phase 1 processing system.

Solar System Science: The implementation of certain aspects of this science may require additional hardware, beyond the standard SKA Phase 1 processing system.

Searches for Extraterrestrial Intelligence: The implementation of certain aspects of this science may require additional hardware, beyond the standard SKA Phase 1 processing system.

Bibliography

Abbasi, R. U., Abu-Zayyad, T., Allen, M., et al. 2008, "First Observation of the Greisen-Zatsepin-Kuzmin Suppression," PhRvL, 100, 101101

Arshakian, T. G., & Beck, R. 2011, "Optimum frequency band for radio polarisation observations," Mon. Not. R. Astron. Soc., in press; arXiv:1101.2631

Beck, R., & Gaensler, B. M. 2004, "Observations of Magnetic Fields in the Milky Way and in Nearby Galaxies with a Square Kilometre Array," New Astron. Rev., 48, 1289

Bicknell, G. V., Jones, D. L., & Lister, M. 2004, "Relativistic Jets," New Astron. Rev., 48, 1151

Blain, A. W., Carilli, C., & Darling, J. 2004, "Searching for High-Redshift Centimeter-Wave Continuum, Line, and Maser Emission Using the Square Kilometer Array," New Astron. Rev., 48, 1247

Blake, C. A., Abdalla, F. B., Bridle, S. L., & Rawlings, S. 2004, "Cosmology with the SKA," New Astron. Rev., 48, 1063

Bower, G. C. 2011, "Constraining the Rate of Relativistic Jets from Tidal Disruptions Using Radio Surveys," ApJ, 732, L12

Brinks, E. 2004, "The ISM in Nearby Galaxies," New Astron. Rev., 48, 1305

Burigana, C., De Zotti, G., & Feretti, L. 2004, "Sunyaev-Zeldovich Effects, Free-Free Emission, and Imprints on the Cosmic Microwave Background," New Astron. Rev., 48, 1107

Butler, B. J., Campbell, D. B, de Pater, I., & Gary, D. E. 2004, "Solar System Science with SKA," New Astron. Rev., 48, 1511

Curran, S. J., Kanekar, N., & Darling, J. K. 2004, "Measuring Changes in the Fundamental Constants with Redshifted Radio Absorption Lines," New Astron. Rev., 48, 1095

Dickey, J. M., McClure-Griffiths, N. M., & Lockman, F. J. 2004, "SKA Studies of Atomic Gas in the Interstellar Medium of the Milky Way," New Astron. Rev., 48, 1311

Falcke, H., Koerding, E., & Nagar, N. M. 2004, "Compact Radio Cores: From the First Black Holes to the Last," New Astron. Rev., 48, 1157

Falcke, H., Gorham, P, & Protheroe, R. J. 2004, "Prospects for Radio Detection of Ultra-High Energy Cosmic Rays and Neutrinos," New Astron. Rev., 48, 1487

Fender, R. 2004, "Using SKA to Observe Relativistic Jets from X-ray Binary Systems," New Astron. Rev., 48, 1399

Feretti, L., Burigana, C., & Ensslin, T. 2004, "Diffuse Radio Emission from the Intracluster Medium," New Astron. Rev., 48, 1137

Feretti, L., & Johnston-Hollitt, M. 2004, "Magnetic Fields in Clusters of Galaxies," New Astron. Rev., 48, 1145

Gaensler, B. M., Beck, R., & Feretti, L. 2004, "The Origin and Evolution of Cosmic Magnetism," New Astron. Rev., 48, 1003

Greenhill, L. J. 2004, "Extragalactic Water Masers, Geometric Estimation of H0, and Characterization of Dark Energy," New Astron. Rev., 48, 1079

Hoare, M. G. 2004, "Star Formation at High Angular Resolution," New Astron. Rev., 48, 1327

Jackson, C. A. 2004, "Deep Radio Continuum Studies with the SKA: Evolution of Radio AGN Populations," New Astron. Rev., 48, 1187

Jarvis, M. J., & Rawlings, S. 2004, "The Accretion History of the Universe with the SKA," New Astron. Rev., 48, 1173

Johnson, K. E. 2004, "Star Formation, Massive Stars, and Super Star Clusters in Nearby Galaxies," New Astron. Rev., 48, 1337

Jones, D. L. 2004, "Spacecraft Tracking with the SKA," New Astron. Rev., 48, 1537

Keshet, U., Waxman, E., & Loeb, A. 2004, "Searching for Intergalactic Shocks with the Square Kilometre Array," New Astron. Rev., 48, 1119

Koopmans, L.V. E., Browne, I. W. A., & Jackson, N. J. 2004, "Strong Gravitational Lensing with the SKA," New Astron. Rev., 48, 1085

Lazio, T. J. W., Cordes, J. M., de Bruyn, A. G., & Macquart, J.-P. 2004, "The Microarcsecond Sky and Cosmic Turbulence," New Astron. Rev., 48, 1439

Lazio, T. J. W., Tarter, J. C., & Wilner, D. J. 2004, "The Cradle of Life," New Astron. Rev. 48, 985

Ma, C., Arias, E. F., Eubanks, T. M., et al. 1998, "The International Celestial Reference Frame as Realized by Very Long Baseline Interferometry," Astron. J., 116, 516

Marvel, K. 2004, "Late Stages of Stellar Evolution," New Astron. Rev., 48, 1349

Miller, J. M., & Gultekin, K. 2011, "X-ray and Radio Constraints on the Mass of the Black Hole in Swift J164449.3+573451," ApJ, in press; arXiv:1106.2502

Morganti, R., Greenhill, L. J., Peck, A. B., Jones, D. L., & Henkel, C. 2004, "Disks, Tori, and Cocoons: Emission and Absorption Diagnostics of AGN Environments," New Astron. Rev., 48, 1195

Murphy, T., Sadler, E. M., Ekers, R. D., et al. 2010, "The Australia Telescope 20 GHz Survey: the source catalogue," MNRAS, 402, 2403

Tarter, J. C. 2004, "Astrobiology and SETI," New Astron. Rev., 48, 1543

van Velzen, S., Koerding, E., & Falcke, H. 2011, "Radio jets from stellar tidal disruptions," MNRAS, in press; arXiv:1104.410

Weiler, K. W., Van Dyk, S. D., Sramek, R. A., & Panagia, N. 2004, "Radio Emission from Supernovae and Gamma-Ray Bursters and the Need for the SKA," New Astron. Rev., 48, 1377

White, S. M. 2004, "The Solar-Stellar Connection," New Astron. Rev., 48, 1319

Wilcots, E. 2004, "SKA Observations of the Cosmic Web," New Astron. Rev., 48, 1281

Wilner, D. J. 2004, "Imaging Protoplanetary Disks with a Square Kilometer Array," New Astron. Rev., 48, 1363

Zauderer, B. A., Berger, E., Soderberg, A. M., et al. 2011, "The Birth of a Relativistic Outflow in the Unusual γ-ray Transient Swift J164449.3+573451," arXiv:1106.3568

10. Additional Telescope Considerations: Phase 1 to Phase 2

Principal Authors: M. Huynh, J. Lazio, L. Harvey-Smith

10.1. Motivation

The Science Working Group has identified the two key science goals of SKA Phase 1 as i) Probing the Dark Ages and the Epoch of Reionization with neutral hydrogen, and ii) Strong Field Tests of Gravity Using Pulsars and Black Holes. The design of SKA Phase 1 must not preclude the full SKA science case, however. In other words, key aspects of the design have to be SKA Phase 2 compliant so that the other core science drivers of the SKA will be enabled upon completion of the full SKA.

The main difference between SKA Phase 1 and Phase 2 is the collecting area (factor of ten) and longer baselines (probably thousands of km, compared to 100 km). In the following sections we discuss other Phase 2 science requirements that must be enabled in Phase 1 to make it as forward compatible as possible.

10.2. Frequency Coverage

The frequency coverage required of the two SKA Phase 1 key science goals is 70 MHz to 3 GHz. Coverage to higher frequency as part of the extension to SKA Phase 2 enables a number of larger SKA science goals.

Higher frequencies are useful in searching for signatures of complex organic molecules around protoplanetary disks, which falls into the key science goal of studying the Cradle of Life. Table 7.1 lists some key organic molecules and the frequency of their spectral line emission. There is no firm upper limit, but ALMA will search for signatures from organic molecules at much higher frequencies. We adopt 10 GHz as a nominal upper frequency bound, consistent with the current preliminary specifications (Schilizzi et al. 2007), but an even higher frequency (up to 15 GHz) would be valuable.

Table 10-1. Examples of Detected Transitions of Complex Organic Species

Species	Transition	Frequency (MHz)	Reference
Formamide $HCONH_2$	3_{12}-3_{13}(= 4 – 4)	9237.03	Hollis et al. (2006b)
Acetamide CH_3CONH_2	2_{20}-2_{11} A	9254.42	Hollis et al. (2006b)
Acetaldehyde CH_3CHO	1_{10}-1_{11}E...	1849.63	Hollis et al. (2006a)
	1_{11}-2_{02}A…	8243.46	
Cyanoformaldehyde CNCHO	5_{15}-6_{06}	2078.068	Remijan et al. (2008)
	7_{07}-6_{16}	8574.116	
Acetamide CH_3CONH_2	1_{01}-1_{11} E	13388.7	Hollis et al. (2006b)
	4_{31}-4_{22} A	14210.35	

The higher frequency coverage is also needed to search for, and time, pulsars in the galactic plane. Sgr A*, the supermassive black hole in the galactic center, is expected to be orbited by hundreds, if not thousands, of pulsars (Cordes & Lazio 1997; Pfahl & Loeb 2004). Pulsar signals passing close to Sgr A* could provide tests of the black hole spacetime, which is motivated by the SKA key science project "Strong Field Tests of Gravity Using Pulsars and Black Holes". Pulsars in close orbit to Sgr A* suffer from as much as thousands of seconds of pulse broadening at GHz frequencies due to hyperstrong scattering in the direction of the galactic center. Scattering effects, notably pulse broadening, has a strong frequency dependence, $\tau_d \propto \nu^x$ with $x \approx -4.4$, so observations at higher frequencies are needed in order to minimize the effects. Frequency coverage to 10 GHz allows a significant fraction of the pulsar population to be probed (Figure 9.2 from DRM v1.0). Millisecond pulsars studies towards Sgr A* would require frequencies > 10 GHz.

Higher frequency coverage would allow studies of cosmic magnetism in sources with larger rotation measures or large internal Faraday dispersion (Arshakian & Beck 2011).

Coverage to 10 GHz requires a dish surface accuracy to 1 mm rms.

10.3. Polarization Purity

Several Phase 2 science goals require a high level of polarization purity. Studies of cosmic magnetism, whether with a deep field to trace the changes in magnetic field properties with redshift or a shallower wide field observation of an all-hemisphere rotation measure grid, require Q, U, and V purity, after calibration, of at least −25 dB, (i.e., 0.5%). The effects of polarization on pulsar timing are an active area of study, but it is thought that polarization purity of 40 dB (0.01%) is needed for 100 ns timing accuracy (Cordes et al. 2004). The purity required of the cosmic magnetism projects is over the full field of view, to allow a survey, whereas that for pulsars need only be maintained on or near the pointing axis.

The feeds, receivers, and digital processing system must be able to achieve this polarization purity so that they do not have to be replaced.

10.4. Dynamic Range

The collecting area of the full SKA will allow surveys of unprecedented sensitivity, but these surveys will be limited by dynamic range.

The dynamic range for a continuum deep field is mainly limited by the brightest source in the field. Source counts suggest the brightest source 1 to 7 Jy for a 10 $\deg^2$ field (1.4 GHz). Appropriate choice of field of view, combined with correlator field of view shaping (Lonsdale et al., 2004) or similar techniques, may reduce the strongest source in the field of view to approximately 0.1 Jy. Detecting luminous infrared galaxies (LIRGs) at redshift 7 will require a sensitivity of 4 nJy (1σ). Hence, studies of star formation at high redshift with a continuum deep field require a dynamic range of 74 dB in imaging.

Spectral dynamic range must be considered for deep HI surveys. There could be many galaxies within the data cube and hence signal-to-noise ratios of at least 7 (8 dB) are probably required to identify emission line features. Spectral dynamic range has two contributions, one due to the electronics and one due to the imaging dynamic range. The electronics contribution comes from the filters, or bandpass (Perley 1989). For example, the dynamic range limit from a 1000-antenna array with an rms phase error of 1 degree would be approximately 47 dB. The imaging dynamic range can be estimated from radio sources counts: we expect, on average, one source with a flux density of order 1 Jy or stronger within the field of view, and want to detect a 5×10^9 $M_\odot$ galaxy at $z \sim 2$ (need 1.4 μJy rms). Hence, the resulting imaging dynamic range requirement is 59 dB. The total dynamic range requirement for HI survey is then 59 + 8 = 67 dB.

10.5. Advanced Instrumentation Programme

The Advanced Instrumentation Programme (AIP) is investigating technologies, such as Phased Array Feeds (PAFs), Dense Aperture Arrays, and high frequency feeds, for the full SKA. The design of SKA Phase 1 should allow for the possible inclusion of these technologies. For example, the dishes must be able to accommodate multiple receivers, including the PAFs.

Bibliography

Arshakian, T. G., & Beck, R. 2011, "Optimum frequency band for radio polarisation observations," Mon. Not. R. Astron. Soc., in press; arXiv:1101.2631

Cordes, J. M., & Lazio, T. J. W. 1997, "Finding Radio Pulsars in and beyond the Galactic Center," Astrophys. J., 475, 557

Cordes, J. M., Kramer, M., Lazio, T. J. W., Stappers, B. W., Backer, D. C., & Johnston, S. 2004,"Pulsars as Tools for Fundamental Physics & Astrophysics," New Astron. Rev., 48, 1413

Hollis, J. M., Lovas, F. J., Remijan, A. J., Jewell, P. R., Ilyushin, V. V., & Kleiner, I. 2006b,"Methyltriacetylene (CH3C6H) toward TMC-1: The Largest Detected Symmetric Top," Astrophys. J., 643,L25

Hollis, J. M., Remijan, A. J., Jewell, P. R., & Lovas, F. J. 2006a, "Cyclopropenone (c-H2C3O): A New Interstellar Ring Molecule," Astrophys. J., 642, 933

Lonsdale, C. J., Doeleman, S. S., & Oberoi, D. 2004, "Efficient Imaging Strategies For Next-Generation Radio Arrays," Experimental Astron., 17, 345

Perley, R. A. 1989, in *Synthesis Imaging in Radio Astronomy*, eds. R. A. Perley, F. R. Schwab, &A. H. Bridle (ASP: San Francisco) p. 287

Remijan, A. J., Hollis, J. M., Lovas, F. J., Stork, W. D., Jewell, P. R., & Meier, D. S. 2008, "Detection of Interstellar Cyanoformaldehyde (CNCHO)," Astrophys. J., 675, L85

Schilizzi, R. T., et al. 2007, "Preliminary Specifications for the Square Kilometre Array," SKA Memorandum 100; http://www.skatelescope.org/PDF/memos/100MemoSchilizzi.pdf

11. Overall Telescope Characteristics

Table 11-1 distills the discussion in the preceding chapters to a set of overall telescope characteristics and technical requirements. Shown are various telescope characteristics, requirements imposed by the observations implied by the science components, the science component itself that sets the requirement, and the overall science case motivation for each.

Table 11-1. Technical Requirements Traceability Matrix for Phase 1 of the SKA

Parameter	Value	DRM Component	Science Case
Upper Operational Frequency	3 GHz	Pulsar Timing (§6.4.3) Pulsar Survey (§5.4.2)	Strong-field Gravity
Lower Operational Frequency	0.07 GHz (0.05 GHz goal)	H I Emission from the EoR (§2.4.1) H I Absorption in the EoR (§4.4.1)	Probing the Dark Ages
Sensitivity	2000 m^2 K^{-1}	Epoch of Reionization (§2.4.5)	Probing the Dark Ages
	1000 m^2 K^{-1}	Pulsar Timing (§6.4.1) Pulsar Survey (§5.4.1)	Strong-field Gravity
Survey Speed	> 10^6 m^4 K^{-2} deg^2	H I Absorption Survey (§3.4.3)	Galaxy Evolution
Maximum Baseline	> 100 km	Pulsar Astrometry (§7.4.2)	Strong-field Gravity
Frequency Resolution	0.1 kHz	H I Absorption in the EoR (§4.4.2)	Probing the Dark Ages
	2 kHz	Galaxy Evolution in the Local Universe (§8.4.3)	Galaxy Evolution
Temporal Resolution	50 μs	Pulsar Survey (§5.4.4)	Strong-field Gravity
Instantaneous Accessible Solid Angle	0.25 deg^2	Pulsar Astrometry (§7.4.3)	Strong-field Gravity
Field of View	0.5° (FWHM) (5.7° [FWHM] goal)	Galaxy Evolution in the Local Universe (§8.4.5)	Galaxy Evolution
		Pulsar Survey (§5.4.5)	Strong-field Gravity
Configuration	high filling factor	Galaxy Evolution in the Local Universe (§8.4.4)	Galaxy Evolution
Polarization	–40 dB	Pulsar Timing (§6.4.5)	Strong-field Gravity
	Full	H I Emission from the EoR (§2.4.4)	Probing the Dark Ages
Frequency Agility	near simultaneous access to multiple frequencies	Pulsar Timing (§6.4.4)	Strong-field Gravity
Non-Imaging Data Products	phased array output	Pulsar Survey (§5.4.6)	Strong-field Gravity
	phased array output	Pulsar Timing (§6.4.2)	Strong-field Gravity
Pulsar Gating	100 pulse phase bins	Pulsar Astrometry (§7.4.4)	Strong-field Gravity
Cadence	Pulse times of arrival acquired at least once per two weeks	Pulsar Timing (§6.4.7)	Strong-field Gravity